THE UNIVERSITY *of* EDINBURGH

Mechanisms of disease pathogenesis in Spinal Muscular Atrophy

Chantal Adriana Mutsaers

A thesis submitted for the degree of Doctor of Philosophy

The University of Edinburgh

2013

Declaration

I declare that this thesis was composed entirely by myself and the work on which it is based is my own, unless clearly stated in the text.

Chantal Adriana Mutsaers

Acknowledgements

First of all I would like to thank my supervisor Tom Gillingwater for always being supportive and motivational and having great ideas. I really enjoyed working in his lab. I would also like to thank my second supervisor Tom Wishart for always having the time to help me, especially at the start of my PhD and for getting me coffee and chocolates.

I would like to thank all the current and past members of the Gillingwater lab. Especially Laura Comley, for teaching me dissections at the start of my PhD and for always being helpful. Derek Thomson for always helping out and having answers to all my questions (also non-science-related ones). I would also like to thank Simon Parson for always being genuinely interested and having good ideas. I would like to thank Paul Skehel for his help with the *in vitro* experiments and Douglas Lamont for his help with the proteomic analyses.

I would like to thank everyone from the anatomy department for making teaching an enjoyable and interesting experience.

I would like to thanks the SMA trust for financially supporting my PhD project.

I would like to thank Yvonne and Scott for making my time in HRB enjoyable and interesting. Scott for always having interesting stories. Yvonne for always making

time to help or for a chat when needed. I am happy that we became good friends and I am sure that our friendship will last.

A very special thanks to my flatmates Sarah and Lukas. Sarah, for proofreading this thesis but foremost for becoming a very good friend and for always having time to listen to my stories. And Lukas for making me coffee in the morning.

I would also like to thank my friends from home for visiting me and having a great time exploring Edinburgh and Scotland. A special thank you to Judith, for making time for our weekly skype chats and still being a very close friend even with the distance between us.

I would like to thank Brice for just being you and making me wake up with a smile on my face.

And last but not least I would like to thank my parents and sister for always being very supportive and making time to come over to visit me.

Abstract

Low levels of survival motor neuron (SMN) protein cause the autosomal recessive neurodegenerative disease spinal muscular atrophy (SMA), through mechanisms that are poorly defined. SMN protein is ubiquitously expressed, however the major pathological hallmarks of SMA are focused on the neuromuscular system, including a loss of lower motor neurons in the ventral horn of the spinal cord and atrophy of skeletal muscle. At present there is no cure for SMA. Most research to date has focused on examining how low levels of SMN lead to pathological changes in motor neurons, therefore the contribution of other tissues, for example muscle, remains unclear. In this thesis I have used proteomic techniques to identify intrinsic molecular changes in muscle of SMA mice that contribute to neuromuscular pathology in SMA. I demonstrate significant disruption to the molecular composition of skeletal muscle in pre-symptomatic SMA mice, in the absence of any detectable degenerative changes in lower motor neurons and with a molecular profile distinct from that of denervated muscle. Functional cluster analysis of proteomics data and phospho-histone H2AX labelling of DNA damage revealed increased activity of cell death pathways in SMA muscle. In addition robust up-regulation of VDAC2 and down-regulation of parvalbumin was confirmed in two mouse models of SMA as well as in patient muscle biopsies. Thus intrinsic pathology of skeletal muscle is an important event in SMA. I then used proteomics to identify individual proteins in skeletal muscle of SMA that report directly on disease status. Two proteins, GRP75 and calreticulin, showed increased expression levels over time in different muscles as well as in skin samples, a more accessible tissue for biopsies in patients. Preliminary results suggest that GRP75 and calreticulin can be detected and measured in SMA

patient muscle biopsies. These results show that proteomics provides a powerful platform for biomarker identification in SMA, revealing GRP75 and calreticulin as peripherally accessible potential protein biomarkers capable of reporting on disease progression in muscle as well as in skin samples. Finally I identified a role for ubiquitin-dependent pathways in regulating neuromuscular pathology in SMA. Levels of ubiquitin-like modifier activating enzyme 1 (UBA1) were reduced in spinal cord and skeletal muscle tissue of SMA mice. Dysregulation of UBA1 and subsequently the ubiquitination pathways led to the accumulation of β-catenin. I show here that pharmacological inhibition of β-catenin robustly ameliorates neuromuscular pathology in animal models of SMA. Interestingly, downstream disruption of β-catenin was restricted to the neuromuscular system in SMA mice. Pharmacological inhibition of β-catenin failed to prevent systemic pathology in organs. Thus disruption of ubiquitin homeostasis, with downstream consequences for β-catenin signalling, contributes to the pathogenesis of SMA, thereby highlighting novel therapeutic targets for this disease.

Table of contents

Abbreviations

ACh	Acetylcholine
AChR	Acetylcholine receptor
aCSF	Artificial cerebrospinal fluid
ALS	Amyotrophic lateral sclerosis
ASO	Antisense oligonucleotide
BCA	Bicinchoninic acid (assay)
BTX	Bungarotoxin
CNS	Central nervous system
DeSyn	Delayed synapsing
DMSO	Dimethyl sulfoxide
FaSyn	Fast synapsing
FDB	Flexor digitorum brevis
FITC	Fluorescein isothiocyanate
GRP75	Stress-protein 70
HDACi	Histone deacytelase inhibitor
IPI	International protein index
IPA	Ingenuity pathway analysis
iTRAQ	isobaric Tags for Relative and Absolute Quantitation
KO	*Smn*$^{-/-}$*;SMN2* mouse
LAL	Levator auris longus
LC-MS	Liquid chromatography–mass spectrometry
Mgf	Mascot generic file
MND	Motor neuron disease

MuSK	Muscle-specific receptor tyrosine kinase
NMJ	Neuromuscular junction
P	Postnatal (i.e. P5 = postnatal day 5)
PAGE	Polyacrylamide gel electrophoresis
PBS	Phosphate buffered saline
PCR	Polymerase chain reaction
PFA	Paraformaldehyde
qRT-PCR	quantitative Reverse Transcription polymerase chain reaction
RIPA	Radio-immunoprecipitation assay
RRBP1	Ribosome-binding protein 1
SAHA	Suberoylanilide hydroxamic acid
SDS	Sodium dodecyl sulfate
SMA	Spinal muscular atrophy
Smn/SMN/SMN	Murine/human survival motor neuron *gene/*protein
snoRNP	Nucleolar ribonucleoproteins
snRNP	Small nuclear ribonucleoproteins
TCPB	T-complex protein 1 subunit beta
TRITC	Tetramethylrhodamineisothiocyanate
TSA	Trichostatin A
TVA	Transversus abdominis
UBA1	Ubiquitin-like modifier activating enzyme 1
UCL-l1	ubiquitin carboxyl-terminal esterase L1
VDAC2	Voltage-dependent anion-selective channel protein 2
WT	Wild-type

Chapter 1

Introduction

1.1 Autosomal recessive spinal muscular atrophy

Motor neuron disease (MND) is a group of progressive diseases that result from the degeneration and death of the large motor neurones in the brain and spinal cord. This leads to muscle weakness and ultimately paralysis, and in severe cases is fatal within a few years after diagnosis (Rezania and Roos 2013). Autosomal recessive proximal spinal muscular atrophy (SMA), first described by Werdnig and Hoffman in the late 19th century, is a childhood form of motor neuron disease. It is the most common genetic cause of infant death in the western world, with an incidence of one in 6000-10000 and with a carrier frequency of one in 50 (Pearn 1978; Feldkotter *et al.* 2002).

1.1.1 Clinical manifestations

There are three forms of childhood onset SMA based on the age of onset and the maximum motor milestone the patients achieve. Type I SMA (also known as Werdnig-Hoffmann disease) is the most severe and common type and is characterized by infantile hypotonia during the first 6-12 months of life (Pearn 1978; Markowitz *et al.* 2004). These patients never achieve the ability to sit unaided and most patients die within two years, because their intercostal muscles (found in the chest wall) are strongly affected, resulting in severe breathing problems and

increased risk of infection. With respiratory support patients can survive for more than two years (Lunn and Wang 2008).

Type II SMA patients are able to sit unaided but fail to walk independently. The onset for this type is usually between 6-18 months. These patients often develop kyphoscoliosis, which is an abnormal curvature of the spine in both the coronal as well as the sagittal plane (Talbot 1999; Lunn and Wang 2008).

Type III SMA (also known as Kugelberg-Welander disease) patients develop weakness after 18 months of age. Most patients achieve all major motor milestones, such as independent walking. However some might need a wheelchair in childhood, whereas others continue to walk until adulthood. Type III patients often develop scoliosis (Lunn and Wang 2008).

In addition to these childhood onset forms of SMA there is also a type IV SMA. Patients with this form develop weakness in their twenties or thirties and their motor impairment is mild. They can live a relatively normal life (Zerres *et al.* 1995).

1.1.2 Genetics

Spinal muscular atrophy is caused by mutations in the survival motor neuron gene (*SMN* gene) resulting in loss of motor neurons from the ventral horn of the spinal cord. Linkage analysis studies have mapped the three childhood forms of SMA to chromosome 5q11.1-13.3 (Brzustowicz *et al.* 1990; Melki *et al.* 1990). In 1995 the *SMN* gene was identified as the disease-causing gene by probing a human fetal brain

cDNA library with genomic DNA from the candidate region (Lefebvre *et al.* 1995). In addition, this group found that the *SMN* gene is duplicated within the 5q13 region (Lefebvre *et al.* 1995). In the human genome there is one telomeric copy (known as *SMN1* gene) and several centromeric copies (known as *SMN2* gene). The *SMN2* gene differs from the *SMN1* gene by five nucleotides (Lefebvre *et al.* 1995). In SMA patients both copies of the *SMN1* gene are deleted or disrupted, however patients retain at least one of the *SMN2* gene copies. In more than 95 % of cases, the patients have a homozygous deletion of the *SMN1* gene. A small part manifests small intragenic mutations or undergoes gene conversions from *SMN1* to *SMN2*. *De novo* mutations occur in 2 % of the patients, because 5q11.1-13.3 is an unstable region (Melki *et al.* 1994; Prior 2007).

The number of *SMN2* copies varies among individuals and in SMA patients there is a clear correlation between *SMN2* copy number and disease severity. Studies have shown that between 80-95 % of type I SMA patients have one or two copies of the *SMN2* gene. In type II SMA patients, 96 % have three copies of the *SMN2* gene and in 96 % of type III SMA patients there are three or four copies (Feldkotter *et al.* 2002; Mailman *et al.* 2002; Arkblad *et al.* 2009).

One of the nucleotide differences between the *SMN1* and the *SMN2* gene is a C-to-T transition in an exonic splicing enhancer (ESE) located in exon7 of *SMN2* (Lorson et al. 1999). This causes differential processing of the *SMN1* and *SMN2* pre-mRNAs, leading to exclusion of exon7 from the *SMN2* messenger RNA (mRNA) transcripts and results in the production of a non-functional and rapidly degrading version of the

SMN protein that is normally produced by the *SMN1* gene (Lorson and Androphy 2000). However, in 10 % of the *SMN2* mRNA transcripts exon7 is not spliced out and is subsequently translated into the normal full-length SMN protein (Lefebvre *et al.* 1995). This results in low levels of SMN protein in SMA patients.

1.1.3 Role of SMN protein

SMN protein is ubiquitously expressed, with particularly high levels in the central nervous system and in the liver. This reflects the fact that it plays a role in a fundamental activity required by all cells. In humans, SMN is a 294 amino acid long protein of about 38 kDA and is encoded by eight exons (Lefebvre *et al.* 1995). SMN is found in both the cytoplasm and in the nucleus of cells (Gubitz *et al.* 2004). In the nucleus, SMN protein is highly enriched within bodies called gems (Liu and Dreyfuss 1996). Gems are closely associated with Cajal bodies, which are known to contain high levels of factors that are involved in transcription and processing of many types of nuclear RNAs, for example small nuclear ribonucleoproteins (snRNPs), nucleolar ribonucleoproteins (snoRNPs) and RNA polymerases (Ogg and Lamond 2002; Gall 2003). However, they are distinct nuclear structures. In the gems SMN forms a complex with a group of proteins called gemins. These include gemins 2 – 7 (for references see review (Gubitz *et al.* 2004)), which have also been found in the cytoplasm. The SMN complex interacts with several proteins that are involved in diverse aspects of RNA processing, including Sm proteins and Sm-like proteins of the snRNPs, which are essential components in the splicing machinery (Liu *et al.* 1997). These observations led to the hypothesis that SMN plays an important role in many aspects of cellular RNA metabolism.

However, studies have suggested a different, specific role for SMN in the motor neurons, since these are the cells that are primarily affected in SMA. In a neuronal cell culture SMN protein was identified in growth cones and filopodia-like structures, suggesting a role for SMN in neurite outgrowth (Fan and Simard 2002). Growth cones are dynamic structures that respond to intra- and extra-cellular cues to guide neurites towards their appropriate targets during neuronal development (Berman *et al.* 1993). SMN protein has also been linked in the transport of axonal messenger RNAs along axons (Rossoll *et al.* 2003), for example β-actin mRNA, which is involved in motor axon pathfinding and outgrowth during development (Rossoll *et al.* 2003). In addition, studies in a zebrafish model of SMA show aberrant motor axon outgrowth and pathfinding defects (McWhorter *et al.* 2003; Beattie *et al.* 2007). This additional function of SMN protein specific to motor neurons might explain the selective vulnerability of spinal cord motor neurons and in particular the distal axonal parts and the neuromuscular synapse.

1.2 Neuromuscular system

1.2.1 The neuromuscular junction

Lower motor neurons are located in the ventral horn of the spinal cord. Their axons leave the spinal cord via ventral roots and travel long distances through peripheral nerves to their target muscles. At the point of contact with the muscle a specialized synapse is formed, called the neuromuscular junction (NMJ). Once an axon reaches a muscle it branches numerous times intramuscularly to innervate between tens and hundreds of muscle fibers (Sanes and Lichtman 1999). A motor neuron along with

the muscle fibers it innervates is called a motor unit. The cells that make up the neuromuscular junction are the skeletal muscle fiber, motor nerve terminal and terminal Schwann cells. More recently a fourth cell type known as a 'capping' cell, has been identified (Sanes and Lichtman 1999; Court *et al.* 2008).

1.2.2 Motor neuron pathfinding

The distal tip of a developing axon contains a growth cone, which is a dynamic structure that responds to multiple sources of spatial information to guide the axon to its target (Lowery and Van Vactor 2009). The growth cone travels by adhering to adhesive molecules that are presented on neighbouring cell surfaces (Maness and Schachner 2007) or assembled into a dense extracellular matrix (Evans *et al.* 2007). These molecules can also activate intracellular signalling pathways by binding to receptors on the growth cone. The morphology of growth cones is defined by the underlying structure of the cytoskeleton. While the axon is dominated by parallel-aligned microtubules, the growth cone mainly consists of actin filaments (Schaar and McConnell 2005). When a growth cone makes first contact with its target (e.g. a muscle fiber), it appears as a bulbous enlargement (called bouton) with very few vesicles. Subsequently, the number of vesicles increases and the cytoskeletal elements that are characteristic of axons disappear. Active zones are formed where vesicles become clustered and where neurotransmitter release will take place (Sanes and Lichtman 1999). When a motor axon is stimulated, an action potential depolarizes the presynaptic membrane, which results in an influx of Ca^{2+} into the synaptic terminal, which causes the vesicles to fuse with the membrane and subsequently releases the neurotransmitter, acetylcholine (ACh). ACh acts on the

nicotinic cholinergic receptors that are clustered on the muscle fiber, the so-called postsynaptic endplate (Sanes and Lichtman 1999).

1.2.3 Development of muscle

Skeletal muscle represents nearly half of the total body mass and is therefore the most abundant tissue in the body. The skeletal muscles induce coordinated body movements through their attachment to the skeleton (Grefte *et al.* 2007).

During embryonic development skeletal muscle precursor cells arise from mesodermal progenitor cells (Yusuf and Brand-Saberi 2012). However, not all muscle precursor cells have the same site of origin within the mesoderm. For example, a significant bulk of trunk muscles are derived from the paraxial mesoderm, flanking both sides of the neural tube and notochord (Christ and Ordahl 1995). The paraxial mesoderm splits into clusters of cells, called somites, starting at the rostral end and continuing caudally. Dorsal somites expressing the transcription factors Pax3 and Pax7 form the dermomyotome. Once the dermomyotome is formed, muscle progenitor cells delaminate from it and migrate to the limb buds (Gros *et al.* 2004), through the action of the membrane receptor c-Met and Pax3 (Dietrich *et al.* 1999). These delaminated cells then down-regulate Pax3 and become myoblasts. The myogenic regulatory factors, Myf5, Mrf4 and MyoD are important regulators for the differentiation of myoblasts into myocytes (Rudnicki *et al.* 1993; Kassar-Duchossoy *et al.* 2004). Myocytes fuse to form myotubes. This process is influenced by many signals from other tissues, for example sonic hedgehog (SHH) and Wnt proteins (Cossu *et al.* 1996; Borycki and Emerson 2000). Once the myotubes are formed they begin to transcribe acetylcholine receptor (AChR) subunit genes (α, β, γ and δ;

(Sanes and Lichtman 2001)) to form an embryonic form of the receptor ($\alpha_2\beta\gamma\delta$). Initially the AChRs are present at a low level throughout the myotube surface. At the same time as the myotube forms, motor axons reach the myotube and once they contact the myotube, a synapse is formed and synaptic transmission commences. This leads to a highly concentrated area of AChRs at the point where the nerve contacts the muscle fiber, the postsynaptic endplate.

Satellite cells are the muscle stem cells located between the sarcolemma and the basal lamina of muscle fibers and represent the major reproductive population in skeletal muscle. Postnatal muscle growth is driven by the proliferation and differentiation of these satellite cells (Hayhurst *et al.* 2012).

1.2.4 Formation and maintenance of the neuromuscular junction

The NMJ undergoes dramatic changes in structure and function in the first few postnatal weeks (Sanes and Lichtman 1999). At birth, muscle fibers are innervated by multiple motor axons in mice. All inputs compete for innervation with 'losing' axons withdrawing and the 'winning' axon reinnervating. This takes place in the first two weeks after birth through a process called synapse elimination (Lichtman and Colman 2000). During the process of synapse elimination the shape of the synapse changes. At first the postsynaptic endplate is a uniform plaque of AChRs, but after axonal inputs retract, spots of low AChR density appear as perforation within the plaque. Changes continue until the postsynaptic endplate acquires a pretzel-like form (Balice-Gordon and Lichtman 1993; Sanes and Lichtman 2001). Together with the changes in shape, the postsynaptic endplate also undergoes molecular alterations.

The AChRs change from an embryonic to an adult form. The embryonic receptor contains a gamma subunit that is replaced by an epsilon subunit (forming the adult receptor; $\alpha_2\beta\varepsilon\delta$) during the first postnatal week (Martinou and Merlie 1991; Sanes *et al.* 1991).

Other genes that are important for the formation and maintenance of the NMJ are muscle-specific receptor tyrosine kinase (MuSK), motor neuron derived agrin, Dok-7, rapsyn and Lrp4 (DeChiara *et al.* 1996; Kim *et al.* 2008). MuSK is a protein that has been shown to colocalize with the AChR at the NMJ (Valenzuela *et al.* 1995). In MuSk null mice the muscle fibers were formed as normal and normal levels of AChR expression were observed, however the clustering of AChR was disrupted and no NMJs were formed (DeChiara *et al.* 1996). This suggests that MuSK is important for the initial formation of postsynaptic AChR clustering (Lin *et al.* 2001). Dok-7 and rapsyn were both closely linked to MuSk and identified to be important for clustering of AChRs and maintaining structural integrity of the endplate (Gautam *et al.* 1995; Okada *et al.* 2006). Interestingly, formation of the postsynaptic endplate started prior to axon arrival. Agrin, which is a glycoprotein synthesized by the motor neuron and released at the NMJ, acts through MuSK to promote apposition of nerve terminals to these nerve independent AChR clusters and also to induce new postsynaptic sites (Lin *et al.* 2001). Agrin is also required for the growth and maintenance of the synapses. MuSK and agrin do not physically interact. Lrp4 was identified as a coreceptor of MuSK that can directly interact with agrin (Kim *et al.* 2008). Taken together, the formation and the maintenance of the NMJ are dependent on the interaction of a wide variety of different genes.

1.3 Neuromuscular pathology in SMA

Since the molecular genetics for SMA are known, it has been possible to generate transgenic animals that recapitulate the disease allowing us to study neuromuscular pathology. When the *SMN* gene is homozygously disrupted in all cell types this results in early embryonic lethality (Frugier *et al.* 2000). Therefore, the most commonly used models are mouse models in which the endogenous *SMN* gene is disrupted (note that only humans have the *SMN2* gene (Lefebvre *et al.* 1995)), but human *SMN2* transgenes are inserted to express low levels of SMN protein. One severe mouse model of SMA was made by Monani *et al.* in 2000 ($Smn^{-/-}$;*SMN2*, hereafter referred to as severe SMA mice). These mice die by postnatal day 5/6 (Monani *et al.* 2000). A less severe phenotype has been observed in mice when an additional copy of the *SMN2* gene without exon7, called the delta7 transgene, is inserted ((Le *et al.* 2005); $Smn^{-/-}$;*SMN2;SMNdelta7*, hereafter referred to as delta7 SMA mice). These mice live for ~ 2 weeks. Another mouse model known as the Taiwanese SMA mice have two copies of the *SMN2* gene on one allele and these mice survive for ~ 12 days ($Smn^{-/-}$;$SMN2^{tg/+}$; (Hsieh-Li *et al.* 2000; Riessland *et al.* 2010).

Several studies in these different mouse models of SMA have shown early morphological abnormalities at the NMJ, occurring before axonal degeneration and motor neuron death (Murray *et al.* 2008; Kong *et al.* 2009; Dachs *et al.* 2011). The number of lumbar motor neurons was not significantly reduced in newborn SMA mice and was only moderately reduced at late stages of disease, whereas NMJ

defects were observed during this time (Dachs *et al.* 2011). In SMA, NMJ abnormalities include both presynaptic and postsynaptic defects. A major hallmark is loss of presynaptic motor nerve terminals at the NMJ, leaving the muscle fibers denervated. Accumulation of neurofilament has been shown at the NMJ as well as poor terminal arborisation, immature plaque-like AChRs and embryonic γ-subunit containing forms of the receptor (Kariya *et al.* 2008; Wyatt and Keirstead 2010). In addition to the morphological changes, functional abnormalities were observed. A study showed a ~ 50 % reduction of overall synaptic vesicle density at the NMJ of severe SMA mice (Kong *et al.* 2009). In addition, a selection of molecular components of the presynaptic terminal was down-regulated in normally innervated muscles, including Rab3A and calcitonin gene related peptide (CGRP) (Dachs *et al.* 2011). Rab3A is a GTP-binding protein involved in targeting synaptic vesicles to the active zones and plays a role in neurotransmitter release in the synaptic cleft. This observation is in agreement with another study that has found decreased neurotransmitter release before appearance of extensive denervation (Ruiz *et al.* 2010). Based on the defects found at the NMJs of SMA mice two independent studies have investigated NMJ pathology in humans (Kariya *et al.* 2008; Martinez-Hernandez *et al.* 2013). Kariya *et al.* confirmed consistent structural defects of the NMJ in humans. Pre-terminal axons and nerve terminals in the diaphragm (a sheet of skeletal muscle that extends across the bottom of the rib cage) of type I SMA patients (younger than six months of age) were characterized as having abnormal accumulation of neurofilament. In addition, they found that motor endplates were small and structurally poorly developed when compared to controls (Kariya *et al.* 2008). Interestingly, defects were also observed in development of the diaphragm

and in limb muscles in SMA fetuses (Martinez-Hernandez *et al.* 2013). This study used confocal and electron microscopy to reveal changes in AChR clustering, abnormal pre-terminal accumulation of vesicles and aberrant ultrastructure of nerve terminals prenatally (Martinez-Hernandez *et al.* 2013). In addition, they confirmed results showed by Kariya *et al.* that there is a delay in maturation of postnatal muscle of type I SMA patients. Thus, the NMJ is considered as an early pathological target in SMA.

1.3.1 Selective vulnerability of neuromuscular junctions

Interestingly, NMJs in different muscles show differences in vulnerability due to low levels of SMN. In addition, the same muscles can be differently affected between mouse models of SMA. Systematic studies have been performed to investigate which factors, such as muscle location, motor neuron pools, muscle fiber type or synapsing phenotypes contributed to synapse vulnerability ((Murray *et al.* 2008; Ling *et al.* 2012; Thomson *et al.* 2012). In general, axial muscles are more vulnerable, however both proximal and distal regions contain both resistant and vulnerable muscles in the delta7 SMA mouse (Ling *et al.* 2012). This study found that the vast majority of vulnerable muscles were innervated by motor neurons located in the cervical and thoracic spinal cord segments.

Muscle fiber type (i.e. fast twitch versus slow-twitch muscle fibers) has been proposed to modulate synapse vulnerability in neurodegenerative diseases. In amyotrophic lateral sclerosis (ALS) for example, fast-twitch muscle fibers innervated by fast fatigable motor neurons are more vulnerable (Hegedus *et al.* 2007). However,

two different mouse models of SMA (severe SMA mice and delta7 SMA mice) have shown that there is no correlation between muscle fiber type and NMJ pathology (Murray *et al.* 2008; Ling *et al.* 2012). In addition, no correlation between factors such as motor unit size, total length of intramuscular axonal arbors, motor unit branching patterns, numbers of synaptic glia and intrinsic remodelling capabilities was found in SMA (Thomson *et al.* 2012). However, a possible explanation could be the synapsing phenotype, characterized as fast-synapsing (FaSyn) and delayed-synapsing (DeSyn), according to intrinsically distinct features of focal AChR clustering and the rate at which they acquire the characteristic organization of a mature NMJ. In muscles with a FaSyn phenotype focally organized clusters of AChRs in the absence of nerve contact become aligned to presynaptic nerve and Schwann cells in one day of development, whereas in DeSyn muscles this process takes up to five days and exhibits dispersed microclusters of AChRs. During this developmental time, nerves and Schwann cells fail to align with AChR microclusters, and extensive sprouting is detected (Pun *et al.* 2002). FaSyn muscle may be more vulnerable to SMA-induced synapse loss (Murray *et al.* 2008). However, not all FaSyn muscles were vulnerable. In contrast, all DeSyn muscles were resistant to denervation in SMA mice (Ling *et al.* 2012). NMJ vulnerability in SMA cannot be attributed to a single determinant, but it is likely to be a combination of various risk factors involving both muscle and nerve. More research is therefore needed to reveal detailed molecular mechanisms of selective vulnerability in SMA.

1.4 The contribution of muscle to SMA pathology

The development of muscle and the survival of motor neurons are dependent on signals from and physical contact with one another (Greensmith and Vrbova 1997; Vrbova 2008). In SMA both muscle and nerve undergo clear pathological alterations. Whether changes in muscle are a secondary effect of lower motor neuron degeneration or whether muscle pathology contributes to SMA pathology directly has been a matter of debate. Henderson *et al.* demonstrated a potential role for muscle in 1987 for the first time (Henderson *et al.* 1987). This study showed that muscle extracts from SMA patients contained substances that inhibit normal neurite outgrowth of chick spinal motor neurons *in vitro*. In addition these inhibitory substances were unique to muscles from SMA patients, as these were not observed in control tissue from other diseases. Co-cultures between SMA patient satellite cells (muscle stem cells) and rat spinal cord have shown degeneration after three weeks in culture, characterized by sarcomeric disorganization and large electron-lucent vacuoles (Braun *et al.* 1995; Braun *et al.* 1997). In mixed co-cultures of 50 % cloned satellite cells from SMA patients and 50 % of cloned satellite cells from healthy donors, the degeneration was not observed after innervation (Guettier-Sigrist *et al.* 1998). These studies suggest that survival of motor neurons depends on receiving signals from muscle.

The discovery of SMN protein in muscle, in sarcomeres of *Drosophilia* (Walker *et al.* 2008), supports these results suggestive of a role for muscle in SMA. Similarly, myoblast cultures from type I SMA patients show defects in the formation of

myotubes and aggregation of AChR (Arnold *et al.* 2004). This was confirmed by a recent study showing that satellite cells isolated from severe SMA mice differentiate more rapidly. More interestingly, these cells failed to form myotubes (Hayhurst *et al.* 2012). To determine whether a defect of *SMN* in skeletal muscle might have a role in SMA pathogenesis *in vivo*, Cifuentes-Diaz *et al.* developed a mouse model in which deletion of *SMN* exon7 was restricted to skeletal muscle. The decrease of SMN led to a severe phenotype characterized by an onset of muscle paralysis after three weeks of age and leading to death at a mean age of 33 days. In addition, necrotic muscle fibers, regenerating myocytes and mononuclear cell infiltration were observed (Cifuentes-Diaz *et al.* 2001). It must be noted that in this mouse model they completely knocked out *SMN* in skeletal muscle, which does not represent a model of SMA as there is still low levels of SMN protein in SMA. In comparison, disruption of SMN directed to motor neurons alone, showed abnormal motor behaviour, characterised by abnormal posture of their hind limbs and severe impairment in their ability to right themself when they were positioned on their back. These mice show skeletal muscle denervation and die at a mean age of 25 days (Frugier *et al.* 2000).

The next question to ask is whether restoring SMN protein levels in skeletal muscle rescues the SMA phenotype. Gavrilina *et al.* made two mouse models, one of which restored SMN levels in skeletal muscle under the human skeletal actin (HSA) promoter and the other restored SMN levels in motor neurons only under the prion promoter (PrP). The severe SMA mice were used in this study. This study concluded that replacement of SMN in neurons rescues the SMA phenotype and increases the survival of the mice, whereas replacement of SMN levels in muscle fibers alone has

no effect on the SMA phenotype or the survival of the mice (Gavrilina *et al.* 2008). However, this study cannot exclude that expression of SMN in both neurons and muscles is needed for the rescue, since the PrP promoter was not completely specific for motor neurons and showed low levels of expression in muscle as well. In contrast, a recent study used MyoD and Myf5 promoters to restore SMN levels in muscle precursor cells and myofibers. The restoration of SMN levels in both satellite cells and myofibers completely rescued myofiber growth accompanied by an increase in median survival and motor behaviour, however no improvement was observed in NMJ structure (i.e. neurofilament accumulation and denervation of endplate was observed) (Martinez *et al.* 2012). A study performed by Bosche-Marce *et al.* attempted to rescue the muscle phenotype by overexpressing muscle specific insulin-like growth factor 1 (IGF-1) (Bosch-Marce *et al.* 2011). IGF-1 is a small polypeptidic hormone important during muscle development and muscle regeneration after injury and denervation. This study showed that muscle mass was increased and the survival of the mice was improved by 40 %, however this was not accompanied by a measurable improvement in motor function (Bosch-Marce *et al.* 2011). Take together, these results show that the role of muscle is still not fully understood and needs further investigation. In addition, the experiments that have been performed to date cannot rule out that the changes observed in muscle are simply occurring as a secondary effect of denervation due to pathology in the innervating motor neurons.

1.5 Are other tissues affected in SMA?

The main pathological feature of SMA is a specific loss of lower motor neuron in the ventral horn of the spinal cord. From the studies described earlier there is some evidence that muscle tissue might be a pathological target in SMA. Recent work has identified a range of additional cell and tissue types that show selective vulnerability to low levels of SMN (Hamilton and Gillingwater 2013). Since defects in non-neuronal tissue have been shown to develop in parallel with neuromuscular pathology this could suggest that SMA is a multi-system disorder rather than a purely motor neuron disease.

1.5.1 Heart defects

One of the most commonly observed abnormalities in SMA outside of the neuromuscular system are congenital heart defects. In a study with a type I SMA patient cohort, three out of four patients were observed with major cardiac septal defects (Rudnik-Schoneborn *et al.* 2008). Electrocardiography (ECG) studies in a mouse model of SMA (*Smn*$^{-/-}$*;SMN2;SMNdelta7*; (Le *et al.* 2005)) revealed severe bradycardia characterized by progressive heart block and impaired ventricular conduction throughout development (Heier *et al.* 2010). Interestingly heart failure, like septum thinning, started at different time point between different mouse models. In the severe SMA mice (*Smn*$^{-/-}$*;SMN2*; (Monani *et al.* 2000)) this was observed in embryonic stages and between postnatal day two and postnatal day five in the delta7 SMA mice (Shababi *et al.* 2010). This indicates an important role for SMN in cardiac development and maintenance.

1.5.2 Vascular defects

Vascular defects, such as digital necrosis and capillary bed defects, have been observed in both patients and animal models of SMA. These defects became apparent when survival was prolonged in patients with the aid of invasive ventilation or in mice after drug treatment (Foust *et al.* 2010; Rudnik-Schoneborn *et al.* 2010; Valori *et al.* 2010). Two studies showed that capillary defects did not proceed NMJ pathology, but rather developed in parallel. It is possible that there is an essential role of SMN deficiency in these tissues and that defects are not developing exclusively secondary to neuromuscular pathology (Somers *et al.* 2012; Schreml *et al.* 2013).

1.5.3 Metabolic abnormalities

Metabolic abnormalities have been found in SMA mouse models. Glucose metabolism defects have been observed as a result of loss of the insulin producing β-cells and a corresponding increase in the number of the glucagon producing α-cells in the pancreas (Bowerman *et al.* 2012). Muscle has a key role here as well, as it is a central player in glucose metabolism via its role in insulin-dependent glucose uptake. In addition, low levels of SMN have recently been shown to have an effect on the liver (Hua *et al.* 2011). SMA mice had decreased hepatic insulin-like growth factor binding protein, acid labile subunit (Igfals) expression, which led to a reduction in circulating insulin-like growth factor 1 (IGF1). IGF1 is a neurotrophic factor and is important for normal postnatal growth (Wu *et al.* 2009). Interestingly, IGF1 levels were rescued by restoring SMN levels systemically (Hua *et al.* 2011).

1.6 Therapies for SMA

At present there is no cure for SMA. Most therapeutic approaches are based on attempts to increase the amount of SMN protein produced by *SMN2* genes with small molecule drugs or gene therapy approaches (Bebee *et al.* 2012). SMN protein levels can be increased by a variety of approaches, including increasing inclusion of exon7 in the *SMN2* transcript, increasing *SMN2* transcription, or increasing the stability of SMN protein generated by *SMN2* (Chang *et al.* 2001; Sumner *et al.* 2003; Avila *et al.* 2007; Sumner *et al.* 2009; Tiziano *et al.* 2010; Farooq *et al.* 2011; Mentis *et al.* 2011). Additional therapies include reintroduction of *SMN* using viral gene therapy, genetic induction of *SMN* and reintroducing healthy cells to replace the loss of motor neurons. These approaches have been tested *in vitro,* in mouse models of SMA and some have already been tested in clinical trials (Brahe *et al.* 2005; Brichta *et al.* 2006; Mercuri *et al.* 2007; Swoboda *et al.* 2010; Tiziano *et al.* 2010; Abbara *et al.* 2011; Darbar *et al.* 2011; Kissel *et al.* 2011). However, there is no FDA-approved treatment for SMA at present. Table 1.1 shows a list of therapies that have been tested for SMA treatment *in vitro*, in animal models and in patients up to date.

1.6.1 SMN2 gene activating treatment

One of the first drugs tested as an SMA therapeutic was hydroxyurea (HU), which is a ribonucleotide reductase inhibitor. HU showed increased levels of full length SMN mRNA in lymphoblastoid cells from SMA patients by promoting inclusion of exon 7 during *SMN2* transcription (Grzeschik *et al.* 2005). In adult severe SMA carrier mice (*Smn*$^{+/-}$*;SMN2*, (Monani *et al.* 2000)) HU increased the expression of human SMN2

protein in spinal cord after a single intra-peritoneal injection (Mattis *et al.* 2008). HU has also been taken to clinical trials, where it has been proven to be safe, and can be administered orally and has a high bioavailability in children, however it failed to improve outcome measures such as motor function, strength, lung function, or levels of full length SMN mRNA (Wang *et al.* 2001; Chen *et al.* 2010).

Another class of drugs that have shown to be effective in SMA function are histone deacytelase inhibitors (HDACi) (Andreassi *et al.* 2004; Hahnen *et al.* 2006; Riessland *et al.* 2006; Avila *et al.* 2007; Narver *et al.* 2008; Tsai *et al.* 2008; Garbes *et al.* 2009; Riessland *et al.* 2010). Histones are basic proteins and their positive charge allows them to associate with DNA to form condense chromatin. Histones undergo post-translational modifications, including acetylation, phosphorylation, methylation, ubiquitination and ADP-ribosylation (Strahl and Allis 2000), which regulates the conformation of chromatin and partially controls the access of the transcriptional machinery to DNA. Acetylation of specific Lysine residues in the amino termini of the core histones, plays a fundamental role in transcriptional regulation (Grunstein 1997; Struhl 1998). Levels of acetylation of histones result from the balance of the enzymes histone acetyltransferases (HATs) and histone deacetylases (HDACs) (Struhl 1998). Transcriptional activity is associated with increased levels of acetylation, whereas decreased levels of acetylation are associated with repression. There are four classes of histone deacetylases based on their homology to yeast deacetylase proteins: Class I-III and HDAC11 (de Ruijter *et al.* 2003). HDAC inhibitors have been shown to increase SMN levels by driving endogenous *SMN2* promoter activity. Most HDACi that are effective in increasing

SMN levels target both class I and II HDACs (Evans *et al.* 2011). One important side effect of HDACi is that these drugs are not gene-specific and therefore might have detrimental off-target effects.

1.6.2 Stabilization of SMNdelta7 transcript

Another approach to treat SMA is to stabilize the SMN transcript without exon 7 (SMNdelta7). SMNdelta7 has a shorter half-life compared to full length SMN. However, it has been shown to be more stable when it forms heterotypic complexes with full length SMN (Burnett *et al.* 2009). A class of antibiotics, known as aminoglycosides, has been shown to increase SMNdelta7 stability. Aminoglycosides have the ability to suppress efficient recognition of stop codons. When the first stop codon of SMNdelta7 exon eight is not recognized this will allow the translational machinery to elongate the protein with five amino acids. Studies have shown that this protein is more stable, can promote neurite outgrowth and can increase the assembly of the spliceosome (a macromolecule complex containing snRNPs) *in vitro* (Mattis et al. 2008). An increased level of SMN protein in fibroblasts from SMA patients, a significant elongation of lifespan and an increased number of cells in the ventral horn of the spinal cord in delta7 SMA mice have been observed (Heier and DiDonato 2009; Mattis *et al.* 2009).

1.6.3 SMN2 alternative splicing modulation

Another potential treatment is to enhance alternative splicing to restore the expression of the full length SMN protein. Several drugs have been shown to be effective, including tetracycline and quinazoline (Thurmond *et al.* 2008; Hastings *et*

al. 2009; Butchbach *et al.* 2010). Alternative splicing has also been increased by using antisense oligonucleotides (ASOs). These are single stranded RNA molecules that are complementary to a certain mRNA sequence to block access to a specific site. An antisense oligonucleotide directed toward the intron seven/exon eight junction in the SMN2 pre-mRNA reduces the recognition of the exon eight 3′ splice site. As a consequence, the splice site pairing competition between exons seven and eight was altered to favour exon7 inclusions and led to a 2-fold increase of SMN2 exon7 inclusion *in vitro* (Lim and Hertel 2001). Several studies have shown that injections of ASOs intra-cerebralventricularly (ICV) to deliver the ASO into the cerebrospinal fluid (CSF) increased exon7 inclusion and subsequently increased SMN levels in brain and spinal cord (Williams *et al.* 2009; Hua *et al.* 2010; Hua *et al.* 2011; Passini *et al.* 2011), resulting in improved motor function and modest extended survival. Interestingly, when the ASOs were delivered systemically via a subcutaneous injection, exon7 inclusion and SMN levels were also increased in heart and liver, leading to a more robust rescue in Taiwanese SMA mice (Hua *et al.* 2011). This again suggests that SMN has an important function, not only in motor neurons but also in peripheral tissues.

1.6.4 Neuroprotective agents

Neuroprotective agents could be an effective intervention to delay or limit motor neuron loss and disease progression in SMA (Rose *et al.* 2009). This treatment might be beneficial especially for patients with a milder form of SMA (Swoboda *et al.* 2007). An example of such an agent is riluzole, which acts on voltage-dependent sodium channels to limit the release of the neurotransmitter glutamate. In this way it

reduces exitotoxicity (Haddad *et al.* 2003). In addition, it has been shown to exhibit neurotrophic activity and it enhances expression of brain-derived neurotrophic factor (BDNF) (Katoh-Semba *et al.* 2002). Riluzole dependent blockage of sodium channels result in a reduction of ATP release followed by depletion of ecto-adenosine, which is thought to increase BDNF synthesis. Increased levels of BDNF have been shown to promote neuronal survival, guide axonal pathfinding, and participate in activity dependent synaptic plasticity (Katoh-Semba *et al.* 2002). A study in a mouse model of mild SMA showed that with riluzole treatment from postnatal day 21 the neuromuscular junction organization was improved (i.e. there was less neurofilament accumulation) and the median survival was increased (Haddad *et al.* 2003).

1.6.5 Gene therapy

The first gene therapy attempt to enhance SMN protein levels in motor neurons was done by an intra-muscular injection with a lentiviral vector encoding the full length SMN protein (Azzouz *et al.* 2004). The theory behind this study was that intra-muscular injection would result in infection of the presynaptic termini of motor neurons and subsequent retrograde axonal transport of the viral vector to the motor neuron cell soma. The treated mice showed a reduction in motor neuron death, however the effect on survival was modest (Azzouz *et al.* 2004). Subsequent approaches used systemic delivery via the temporal facial vein using a self-complementary adeno-associated vector serotype 9 (scAAV9). Three individual studies showed that this approach rescued characteristic SMA phenotypes such as muscle atrophy, immobility and weight loss. In addition the therapy substantially

improved survival of the SMA mice (Foust *et al.* 2010; Valori *et al.* 2010; Dominguez *et al.* 2011). Foust *et al.* also showed that the scAAV9 vector traverses the blood-brain barrier in a nonhuman primate, which supports the possibility of translating this treatment to humans (Foust *et al.* 2010). An alternative to system delivery is to deliver the vector directly into the CNS (Passini *et al.* 2010). This showed improvement of motor behaviour, body weight and overall survival, although the mice still died prematurely. This suggests that rescue of tissue, other than the motor neurons, is needed for complete rescue of the mice.

1.6.6 Stem cell therapy

Neural stem cell therapy was first shown to be effective in a mouse model of ALS. These mice showed a modified disease progression via neurogenesis and also via growth factor release (Corti *et al.* 2007). The beneficial effect was not only mediated by cell replacement but also by the neuroprotective effect of factors released by the donor cells. The first attempt of stem cell therapy in a mouse model of SMA used primary murine neural stem cells (Corti *et al.* 2008). The same group also showed that embryonic stem cell-derived neural stem cells can differentiate into motor neurons *in vitro*, and when transplanted into the cerebrospinal fluid can migrate along the spinal cord (Corti *et al.* 2010). Approximately 15% of these cells engrafted in the spinal cord where most exhibited astrocyte like characteristics and to a lesser extent motor neuron characteristics. Surprisingly, this still revealed an increase in survival, body weight and an improvement in muscle morphology (Corti *et al.* 2010).

Table 1.1 SMA treatments tested *in vitro*, in animal models and in patients

Treatment	Target	Effects			Reference
		In vitro	*In vivo*	In patients (clinical trial)	
SMN2 gene activation					
HDAC inhibitors					
Sodium butyrate	Histone deacetylase inhibition; activate *SMN2* promoter	Increased expression of exon7-containing SMN protein from the *SMN2* gene in Epstein–Barr virus-transformed lymphoid cell lines from type I - III SMA patients	Increased amount of full-length mRNA of the *SMN2* gene. Pregnant type II and III SMA mice received water with sodium butyrate *ad libitum*. This resulted in reduced number of pups born with severe SMA and increased the survival by 39 %	not tested	Chang *et al.* 2001
Sodium phenyl butyrate	Histone deacetylase inhibition; activate *SMN2* promoter	Increased *SMN2* gene expression in SMA patients fibroblast cultures	not tested	Increased SMN expression in peripheral blood leukocytes. Increased muscle strength was observed (Brahe *et al.*). Mercuri *et al.* showed no improvement in motor and lung function	Andreassi *et al*. 2004; Brahe *et al.* 2005; Mercuri *et al*. 2007
Trichostatin A (TSA)	Histone deacetylase inhibition	Increased expression of exon7-containing *SMN2* transcripts in a fibroblast cell line of a type III SMA patient	Treatment from P5 in delta7 SMA mice improved survival (19 %), motor function, muscle fiber size, and spinal motor neuron size. Additional nutritional supplementation improved survival by 170 % even with treatment cessation at 20 days. Sensory neuronal circuitry defects were corrected	not tested	Avila *et al*. 2007; Narver *et al.* 2008; Mentis *et al.* 2011
Valproic acid (VPA)	Histone deacetylase inhibition; activate *SMN2* promoter	Increased exon7-containing *SMN* transcript levels, SMN protein levels, and gem number in type I SMA patient–derived fibroblast cell lines in a dose-dependent fashion	In a mouse model of SMA type III, motor neuron loss was prevented, improvement of motor function and muscle pathology and reduced NMJ defects were observed. Increased SMN protein levels in the spinal cord	*SMN2* mRNA levels were increased in 50 % of the patients (Brichta *et al.*). In type II patients an improvement in motor function test was observed. This was not seen in type III patients (Darbar *et al.*). No improvement in strength or function in ambulant and non- ambulant children was observed (Kissel *et al.* and Swoboda *et al.* 2010)	Sumner *et al.* 2003; Brichta et al. 2006; Tsai *et al.* 2008; Swoboda *et al.* 2010; Darbar *et al.* 2011; Kissel *et al.* 2011

Suberoylanilide hydroxamic acid (SAHA)	Histone deacetylase inhibition	Increased SMN levels in a fibroblast cell line derived from SMA patients	Treatment of pregnant mother mice rescued embryonic lethality of severe SMA pups. In Taiwanese SMA pups SAHA increased the mean survival by 30%. Body weight and motor abilities were increased. SMN2 transcripts, Full-length SMN2 and delta7-SMN2 levels were increased in brain, liver, spinal cord and muscle	not tested	Hahnen *et al.* 2006; Riessland *et al.* 2010
LBH-589	Reduce methylation-dependent *SMN2* silencing	Increased SMN levels in a fibroblast cell lines derived from SMA patients, in human neural stem cells and in murine fibroblasts derived from *SMN2*-transgenic mice. SMN is post-translationally stabilized via reduced ubiquitination as well as enhanced incorporation into the SMN complex	Treatment of 3-month old SMA carrier mice showed increased SMN protein levels	not tested	Garbes *et al.* 2009
M344	Histone deacetylase inhibition	Increased SMN2 protein expression in a fibroblast cell line derived from SMA patients up to 7-fold. Increased total number of gems/nucleus as well as the number of nuclei that contain gems	not tested	not tested	Riessland *et al.* 2006
Hydroxyurea	Ribonucleotide reductase inhibitor	Increased levels of full length *SMN* mRNA	Increased expression of SMN2 protein in spinal cord	No improvement in motor function, strength or lung function. No increased levels of serum full length *SMN* mRNA in SMA patients with type II and III. Neutropenia was observed as a side-effect	Grzeschik *et al.* 2005; Mattis *et al.* 2008; Chen *et al.* 2010
Prolactin	Stat5 pathway	Increased level of *SMN* mRNA and protein levels in a human neuronal cell line and in murine motor neuron MN-1 cells	Significant up-regulation of SMN levels in motor neurons and improvement of motor function in the delta7 SMA mice. They showed a 70% increase in lifespan. All SMA pups responded to the treatment	not tested	Farooq *et al.* 2011

Salbutamol	Exon 7 inclusion	Increased levels of *SMN2* full length transcripts in SMA fibroblasts	not tested	Increased *SMN2* full length transcript levels	Angelozzi *et al.* 2008; Tiziano *et al.* 2010
SMNdelta7 transcript stabilization					
Aminoglycosides					
Geneticin (G418)	Modulate *SMN* translation. Bypasses stop codons in the *SMN* delta7 transcript	Full length SMN protein levels were increased in human and mouse cell lines as well as in patient fibroblasts	Delta7 SMA mice showed increased levels of full length SMN protein in brain and spinal cord and a significant increase in motor function. Drug was found to be toxic after treatment for 9 days	not tested	Heier and Didonato *et al.* 2009
TC007	Modulate *SMN* translation. Bypasses stop codons in the *SMN* delta7 transcript	Increased SMN levels in induced pluripotent stem cell-derived human SMA motor neuron cultures	In delta7 SMA mice the number of motor neurons was increased in spinal cord, motor function was improved and mean survival was increased by 30%	not tested	Mattis *et al.* 2009
Neuroprotection					
Follistatin	Inhibition of the myostatin pathway	not tested	Increased muscle mass, motor function and number of motor neurons in the spinal cord and increased mean survival by 30%. Transgenic expression of follistatin in muscle failed to improve SMA phenotype and survival of delta7 SMA mice	not tested	Rose *et al.* 2009; Sumner *et al*. 2009
Riluzole	Neurotrophic activity and enhances expression of brain-derived neurotrophic factor	not tested	Median survival was increased by 15% and exerted a protective effect against aberrant cytoskeletal organization of motor synaptic terminals but not against loss of proximal axons	Phase I clinical trial to optimize the pharmacokinetics of riluzole	Haddad *et al.* 2003; Abbara *et al.* 2011

SMN alternative splicing					
tetracycline/ PTK-SMA1	*SMN2* splicing modulation	Stimulates exon 7 splicing and increases SMN protein levels in SMA patient and carrier fibroblasts	Stimulates exon 7 splicing and increases SMN protein levels in liver of SMA mice. The compound can not cross the blood-brain barrier	not tested	Hastings *et al.* 2009
quinazoline	*SMN2* splicing modulation	Activating *SMN2* promoter activity and increased levels of SMN protein in SMA patient fibroblasts	Increased SMN levels in the spinal cord, amelioration of the SMA motor phenotype and an increase of the mean survival by 20-30% in delta7 SMA mice	not tested	Thurmond *et al.* 2008; Butchbach *et al.* 2010
Antisense oligonucleotides	*SMN2* preRNA/splice-regulators	A 2-fold increase of *SMN2* exon 7 inclusion	Administered directly into CNS corrects exon 7 splicing. Prevents tail and ear necrosis in SMA type III mice. Increased number of motor neurons in the spinal cord, improvement of motor function and increase in weight. Mean survival increased with 18-26%. Administration sub-cutaneously improved survival up to 248 days	not tested	Lim and Hertel *et al.* 2001; Williams *et al.* 2009; Hua *et al.* 2010; Passini *et al.* 2011; Hua *et al.* 2011
Gene replacement					
lentiviral SMN; scAAV9-SMN; scAAV9-coSMN; scAAV9-SMNop*ti*	SMN1 delivery	Restoration of SMN protein concentration and number of gems in an SMA type I fibroblast cell line	Lentiviral administration by intramuscular injection improved weight gain and motor neuron numbers. Survival was extended by 20-40%. An scAAV8 CNS injection increased survival up to 157 days and improved motor function and NMJ pathology. Systemic delivery with scAAV9 increased survival up to more than 250 days in the delta7 SMA mice. Improved weight, neuromuscular physiology and motor function	not tested	Azzouz *et al.* 2004; Foust *et al.* 2010; Valori *et al.* 2010; Passini 2010; Dominguez *et al.* 2011
Stem cell therapy					
Stem cells	Neurotrophic support		Primary motor neuron stem cells injected into the spinal canal engrafted to the spinal cord, improved motor function and extended survival by 39%. Embryonic stem cell-derived neural stem cells injection in the cerebrospinal fluid showed a 24% increase of mean survival compared to injections of motor neuron stem cells	not tested	Corti *et al.* 2008; Corti *et al.* 2010

1.7 Biomarkers for SMA

Now that there are potential approaches to treat SMA, reliable clinical outcome measures and biomarkers are essential to effectively evaluate these approaches. It is essential for a reliable biomarker to 1) overcome the risk of placebo effect, 2) allow comparison of clinically heterogeneous individuals, 3) help to distinguish between responder and non-responder individuals to a given treatment and 4) facilitate the accuracy and speed of a clinical trial (Tiziano *et al.* 2013). Different motor function (Hammersmith Motor Function Scale or HMFS specifically designed for SMA (Main *et al.* 2003)), quality of life and respiratory measures as well as strength tests have been piloted as outcome measures in these studies (Cook *et al.* 1990; Samaha *et al.* 1994; Main *et al.* 2003; Lewelt *et al.* 2010; Kaufmann *et al.* 2011). However, these measures have raised a number of concerning issues. These tests depend on the motivation and state the patients are in. For example, some tasks might be unbearable for patients. Moreover, some complications related to the disease such as scoliosis, retractions and weight gain could further impair motor functions. Therefore recent studies have been investigating molecular biomarkers, including SMN transcript and protein levels from accessible peripheral tissues such as blood and urine (Crawford *et al.* 2012; Finkel *et al.* 2012). Sensitive techniques are needed to reliably quantify the level of a biomarker. An immunoassay has been developed suitable for SMN protein quantification in peripheral blood mononuclear cells (PBMC) (Kolb *et al.* 2006). However, a reduction in SMN levels was only found in PBMC from type I SMA patients and did not correlate with phenotypic severity. These findings raise the question of whether the technique is sensitive enough or

whether SMN protein levels in PBMC are a good readout of disease severity. In addition, association between clinical phenotype and molecular characteristics in type III SMA patients has been investigated (Tiziano *et al.* 2013). This study did not find a correlation between motor performance and *SMN2* copy number. These findings suggest that there is an urgent and essential need for a reliable biomarker for SMA.

1.8 Pathways involved in SMA independent of SMN

The pathogenesis of SMA has been extensively studied, however detailed disease mechanisms remain to be fully understood. In addition, it has only recently been appreciated that non-neuronal tissues, such as muscle and other organs, are affected in SMA. Treatments to date have not been successful in rescuing the disease, therefore there might be other pathways and regulatory proteins involved in the pathogenesis of SMA.

1.8.1 Plastin-3

The first potential SMN-independent disease modifier identified was plastin-3. Increased levels of plastin-3 protein were discovered in individuals with a homozygous deletion of *SMN1,* who were fully asymptomatic despite carrying the same number of *SMN2* copies as their affected siblings (Oprea *et al.* 2008). Plastin-3 is an actin binding protein and regulates actin filament organization. It colocalizes with SMN in granules throughout motor neuron axons and it shows reduces levels in brain and spinal cords of SMA mice (Bowerman *et al.* 2009). A recent study in the

Taiwanese SMA mice overexpressing plastin-3 showed neuromuscular improvement (Ackermann *et al.* 2013), confirming its protective role in SMA. However, the mechanism behind the protective effect of plastin-3 has yet to be fully investigated.

1.8.2 Myostatin pathway

The myostatin pathway has been proposed to be involved in SMA. Myostatin (MSTN) is a member of the transforming growth factor-beta (TGF-beta) family and it is proposed to be a negative regulator of muscle growth. Several proteins reduce the activity of MSTN, including follistatin. Administration of follistatin to delta7 SMA mice showed an improved lifespan and gross motor functions associated with an increase in muscle mass and the preservation of motor neurons (Rose *et al.* 2009). Interestingly SMN levels were not changed after follistatin treatment. This suggests that follistatin induced rescue by acting on the MSTN pathway and rescued the SMA phenotype in an SMN independent manner. However, this study is contradicted by a study that took a genetic approach and knocked out the *MSTN* gene in delta7 SMA mice (Rindt *et al.* 2012). In this study no improvement of survival or motor function was observed. This might suggest that the inhibition of MSTN may have been suboptimal and furthermore follistatin might have additional targets influencing muscle growth.

1.8.3 Ubiqitination pathway

X-linked infantile spinal muscular atrophy (XL-SMA) is a disease closely linked to SMA. XL-SMA patients present similar clinical characteristics, including hypotonia, areflexia, and multiple congenital contractures associated with loss of cells in the

ventral horn of the spinal cord (Ramser *et al.* 2008). Using mutation screening in six XL-SMA families, mutations were located in the ubiquitin-like modifier-activating enzyme 1 gene (UBA1). UBA1 catalyses the first step in the ubiquitination pathway for proteasome degradation (Rubinsztein 2006). In addition, ubiquitin carboxy-terminal hydrolase L1 (UCHL1), which is also an enzyme in the ubiquitination pathway, is increased in fibroblasts from type I SMA patients (Hsu *et al.* 2010). These studies suggest a role for the ubiqitination pathway in SMA.

1.9 Aims

Based on the current literature the following questions were raised and will be addressed in this thesis

Chapter 3: Is there a direct role for skeletal muscle in the pathogenesis of SMA?

Chapter 4: Can biomarkers be identified in skeletal muscle? Are these potential biomarkers also measurable in more accessible peripheral tissues, such as blood and skin?

Chapter 5: Can new pathways involved in SMA pathogenesis be identified? Does targeting this pathway with a pharmacological compound ameliorate the SMA phenotype in a mouse model of SMA?

Chapter 6: Does a dopamine agonist ameliorate the SMA phenotype in a mouse model of SMA?

Chapter 2

Materials and methods

2.1 Animals and colony maintenance

Smn$^{+/-}$*;SMN2* mice (Jackson labs strain no. 005024) were maintained as heterozygous breeding pairs under standard SPF conditions in animal care facilities in Edinburgh. This breeding scheme gave rise to severe SMA mice (*Smn*$^{-/-}$*;SMN2*) and two different control littermates; heterozygous (*Smn*$^{+/-}$*;SMN2*) and wild-type (*Smn*$^{+/+}$*;SMN2*). Taiwanese SMA mice were maintained as two separate stocks; *Smn*$^{+/-}$ (crossed with wild-type FVB mice to maintain the stock) and *Smn*$^{-/-}$*;SMN2*$^{tg/tg}$. *Smn*$^{+/-}$ and *Smn*$^{-/-}$*;SMN2*$^{tg/tg}$ were crossed to obtain SMA mice (*Smn*$^{-/-}$*;SMN2*$^{tg/wt}$) or control littermates (*Smn*$^{+/-}$*;SMN2*$^{tg/wt}$). The *SMN2* transgene carries two *SMN2* copies. Taiwanese SMA mice treated with SAHA (tissue used in chapter 3) were bred and maintained in micro-isolation chambers in Cologne as previously reported (Riessland *et al.* 2010). C57Bl/6 mice were maintained as breeding colonies in the animal care facilities in Edinburgh under standard SPF conditions.

Mice were housed in individual ventilated cages (IVC) and were fed a standard chow diet. Mice older than postnatal day five (P5) were sacrificed by intra-peritoneal injection of sodium pentobarbital or an overdose of isofluorane. Mice younger than P5 were chilled on ice and decapitated. All animal procedures and breeding were performed in accordance with Home Office guidelines in the UK and according to

guidelines established by the Landesamt fur Natur, Umwelt und Verbraucherschutz NRW in Germany.

2.2 Human tissue

Quadriceps femoris biopsy samples from SMA and control patients were obtained from Fondazione IRCCS Istituto Neurologico "C. Besta" in Milan, Italy and Fondazione Ospedale Maggiore Polclinico Mangiagalli en Regina Elena, IRCCS in Milan, Italy through EuroBioBank (http://www.eurobiobank.org/).

Table 2.1 Biopsy obtained from Fondazione IRCCS Istituto Neurologico "C. Besta" in Milan, Italy.

Code	Sex	Age	Type
6306	Female	3 years	SMA II

Table 2.2 Biopsies obtained from Fondazione Ospedale Maggiore Policlinico Mangiagalli en Regina Elena, IRCCS in Milan, Italy.

Code	Sex	Age	Type
8916	Female	25 years	SMA III
9150	Female	4 years	SMA II
9012	Male	22 years	Control
9110	Male	27 years	Control
9426	Male	17 years	Control
9436	Female	15 years	Control

2.3 Genotyping

DNA was extracted from ear clips (for genotyping stock mice) or from a tail tip (for genotyping experimental mice) and a PCR was performed to genotype the mice. The following primers were used for genotyping mice from the severe SMA colony:

SMN knock out primers (NEO insert)

Forward: CTTGGGTGGAGAGGCTATTC

Reverse: AGGTGAGATGACAGGAGATC

PCR product is 280 base pairs (bp).

SMN wild-type primers

Forward: TTTTCTCCCTCTTCAGAGTGAT

Reverse: CTGTTTCAAGGGAGTTGTGGC

PCR product is 420 bp.

PCR program

Step 1 Separation	94°C	120 sec
Step 2 Denaturation	94°C	30 sec
Step 3 Annealing	61°C	30 sec
Step 4 Polymerization	72°C	45 sec
Step 5 Final	72°C	120 sec

Step 2-4 are repeated 27 times.

For genotyping the Taiwanese SMA mice the following primers were used:

Forward: ATAACACCACCACTCTTACTC

Reverse 1: GTAGCCGTGATGCCATTGTCA

Reverse 2: AGCCTGAAGAACGAGATCAGC

SMN1 gene products: A band of 1050 bp and a band of 950 bp for heterozygous mice ($Smn^{+/-};SMN2^{tg/wt}$) and only one band of 950 bp for SMA mice ($Smn^{-/-};SMN2^{tg/wt}$).

PCR program

Step 1 Separation	95°C	180 sec
Step 2 Denaturation	94°C	30 sec
Step 3 Annealing	59°C	30 sec
Step 4 Polymerization	68°C	60 sec
Step 5 Final	68°C	5 min

Step 2-4 are repeated 35 times.

Products were separated by gel electrophoresis and genotype assigned by presence or absence of a band of appropriate size.

2.4 Surgery

Surgery was performed by Laura Comley

Mice were anaesthetised by inhalation of halothane (2% in 1:1 N_2O/O_2) before exposing the sciatic nerve in the thigh. A ~1 mm section of the sciatic nerve was removed to ensure complete transection before suturing the skin and allowing the mouse to recover.

2.5 Muscle, spinal cord and organ preparation

Levator auris longus (LAL, from the dorsal surface of the neck), *flexor digitorum brevis* (FDB; from the plantar surface of the hind-paw) and/or *transversus abdominis* (TVA; from the antero-lateral abdominal wall) were dissected in oxygenated mammalian physiological saline (120 mM NaCl , 5 mM KCl, 2 mM $CaCl_2$, 1 mM $MgCl_2$, 0.4 mM NaH_2PO_4, 23.8 mM $NaHCO_3$, 5.6 mM D-glucose) in a Sylgard-lined dish. Gross dissection was done before fixing the tissue in 0.1 M phosphate buffered saline (PBS) containing 4% paraformaldehyde (Electron Microscopy Services) for 10 min. The tissue was cleaned and further dissected after fixation. For proteomics and/or quantitative fluorescent western blotting experiments, spinal cord, heart, liver, LAL (separated in rostral and caudal band), FDB and/or *gastrocnemius* (from the hind limb) muscles were quickly frozen on dry ice. The muscles were stored in -80°C freezers until enough tissue was collected for analysis.

2.5.1 Synaptosome preparation

Synaptosomes were made from either whole brain or hippocampus only. High Mg^{2+} artificial cerebrospinal fluid (aCSF, 125 mM NaCl, 26 mM $NaHCO_3$, 25 mM glucose, 2.5 mM KCl, 1.25 mM $NaH_2PO_4(\bullet 2H_2O)$, 1mM $CaCl_2$, 4 mM $MgCl_2$) was prepared and cooled in the freezer to the point of becoming slush. The brain was removed and dropped immediately into ice-cold sucrose solution (0.2 M sucrose, 1 mM EDTA and 5 mM Tris-HCL, pH 7.4) or when hippocampal synaptosomes were made dropped into high Mg^{2+} aCSF first, to increase firmness for cutting. Once the tissue was firm enough the brain was cut in the sagittal plane just off the midline. The hippocampus was then scooped out of both hemispheres before being dropping into ice-cold sucrose solution. The tissue was homogenized in 1 ml or 100 µl ice-cold sucrose solution, for whole brain and hippocampus respectively, and then centrifuged in a fixed-angel rotor at 900 g for 10 min. The supernatant (S1, containing the synaptosomes) was collected in a new tube. The pellet (P1) was resuspended in fresh sucrose solution and centrifuged again at 900 g for 10 min. The supernatant (S2) was collected in the same tube as S1 and this was centrifuged again at 20 000 g for 20 min. The supernatant was removed and the pellet, containing the synaptosomes, was stored in the -80 °C freezer until used for further analyses. For isolation of the mitochondria the pellet with the synaptosomes was resuspended in RIPA buffer with 10 % protease inhibitor cocktail and centrifuged at 6000 g for 15 min (Cox and Emili 2006). The pellets formed were the mitochondria.

2.6 Immunohistochemistry

The fixed muscles were washed in a solution of PBS and 4% Triton for 30 min before it was blocked in blocking solution (4% bovine serum albumin and 2% Triton-X in PBS) for 30 min. The muscle dissections were then incubated in primary antibodies anti-2H3 and anti-SV2 to label axonal neurofilament (both 1:100, Developmental studies hybridoma bank), parvalbumin (1:200, Abcam) or phospho-H2AX (1:200, Upstate) on a rocking plate in the cold room overnight. The next day the muscle dissections were washed in PBS for two hours on the rocker at room temperature before being incubated in α-Bungarotoxin (BTX) conjugated to tetramethyl-rhodamin isothiocyanate (TRITC-α-BTX; 5 mg/ml, Molecular Probes) to label post-synaptic acetylcholine receptors or TOPRO-3 (Alexa Fluor 647®; 0.7 mg/ml, Life Technologies) to label nuclei for 10 min. Hereafter the muscle dissections were incubated in goat-anti mouse Dylight-488 (1:200, Thermo Scientific) or donkey-anti goat Cy-3 (1:200, Jackson laboratory) for two hours at room temperature. After washing in PBS for 45 min the muscle preparations were mounted on glass slides in Mowiol® and covered with a cover slip for subsequent imaging.

2.7 Image analysis

Muscle dissections were viewed using a phase contrast microscope (for muscle fiber measurements), a standard epi-fluorescence microscope equipped with a chilled CCD camera (x10 0.3NA, x40 0.6NA lens; Nikon IX71 microscope; Hammamatsu

C4742-95), and/or a laser scanning confocal microscope (Zeiss Axiovert LSM 150, x40 1.3NA, x63 1.4NA oil immersion lenses). TRITC-α-BTX-labelled muscle dissections were imaged using 543 nm excitation and 590 nm emission optics and FITC-labelled muscle dissections were imaged using 488 nm excitation and 520 nm emission optics. For confocal microscopy, 488 nm (green), 543 nm (red) and 633 nm (far-red) laser lines were used for excitation and confocal Z-series were merged using Lasersharp (Biorad). All images were then assembled using Adobe Photoshop. The montage of immunohistochemically labelled LAL muscle was produced in Adobe Photoshop software by layering and combining multiple micrographs covering the entire muscle.

2.8 Quantification of endplates

A minimum of 30 endplates from a minimum of three fields of view per muscle/muscle band was examined. Muscles with poor staining or that were damaged were excluded from quantification. The quantification was done blind. Endplates were examined for basic occupancy counts and for the total number of axonal inputs per endplate. For basic occupancy counts the endplates were categorized as either fully occupied (neurofilament staining overlies the endplate entirely), partially occupied (neurofilament staining overlies the endplate partially) or vacant (no neurofilament staining overlies the endplate).

2.9 H2AX cell count

LALs were examined using the confocal microscope, 63 x magnification. Nuclei were examined in 20 fields of view per muscle. Nuclei were either scored as having no H2AX labelling, moderate accumulation or intense H2AX labelling.

2.10 Muscle fiber diameter measurements

Muscle fiber diameter measurements were taken from phase contrast micrographs of teased muscle fiber preparations. Fifty pictures were taken per muscle. Per muscle fiber three diameter measurements were taken in Image J and these were averaged in excel before statistics were performed. Only isolated fibers with no overlapping fibers obscuring their profile were included in these analyses.

2.11 Protein level quantification

Tissue from mouse (either muscle, spinal cord, skin, blood, heart or liver) and human (muscle biopsy) was homogenized in RIPA buffer (Thermo scientific) and 10% protease inhibitor cocktail (Thermo scientific) using a pestle. The homogenate was left on ice for a few minutes and then vortexed before centrifugation at 14 000 rpm for 30 min. The supernatant was collected. Protein quantification was performed using a Micro BCA protein assay kit (Pierce) according to manufactures instructions.

2.12 Quantitative fluorescent (Li-COR) western blotting

Samples were mixed with 4 x LDS sample buffer (Novex) before being boiled for 2 min at 98 °C. After a brief spin 10 µl of the samples was loaded onto a NuPage 4-12% Bis Tris gradient gel (Invitrogen) in NuPage MES SDS running buffer (Invitrogen). After electrophoresis (180 V for 45 min) the samples were transferred onto a PVDF membrane using an iBlot (Invitrogen, transfer time 8.5 min). The membranes were blocked using Odyssey blocking buffer (Li-COR) for 30 min at room temperature. Hereafter membranes were incubated overnight at 4°C with either, anti-calreticulin (1:1000, Lifespan) anti-β-catenin (1:1000, BD Transduction laboratories), anti-COX IV (1:1000, Mitosciences), anti-cytochrome-C (1:1000, Abcam), anti-E1-ubiquitin activating enzyme (1:1000, Abcam), anti-phospho-H2AX (1:1000, Upstate), anti-histone H2B (1:1000, Active Motif), anti-GEM5C (1:100, obtained from Glenn Morris' laboratory), anti-GRP75 (1:2000, Lifespan), anti-ManSMN12 (1:100, obtained from Glenn Morris' laboratory) anti-parvalbumin (1:500, Abcam), anti-RRBP1 (1:500, Abcam), anti-SMN (1:500, BD transduction laboratories), anti-synaptophysin (1:1000, DAKO), anti-TCPB-beta (1:1000, Abcam), anti-β-III-tubulin (1: 5000, Abcam), anti-β-V-tubulin (1:500, Abcam), anti-ubiquitin (1:500, Millipore), anti-UCH-l1 (1:2000, Novus Biologicals), anti-VDAC2 (1:1000, Abcam) in 5 ml Odyssey blocking buffer (Li-cor) with 1 % TWEEN 20 (Promega). After washing in 1 x PBS for 30 min, the membranes were incubated for two hours at room temperature with either goat anti-rabbit, goat anti-mouse or donkey anti-goat (all Odyssey IRDye 680 or 800 dependent on required combinations, 1:1600) in 5 ml Odyssey blocking buffer with 1 % TWEEN 20. After washing for 30 min with 1 x

PBS the membranes were imaged using an Odyssey Infrared Imaging System (Li-COR Biosciences). Scan resolution of the instrument ranges from 21-339 μm and the membranes were imaged at 169 μm. Laser intensity levels were changed according to the brightness of the band of interest. Fluorescent intensity of each individual band was measured using the software provided with the Li-COR or with ImageStudioLite (free Li-Cor software). Where possible, western blot membranes were scanned twice and two independent sets of measurements were taken from it to minimise user variability and to provide a more accurate result.

2.13 Real-time PCR

To extract total RNA, the pellet with the synaptosomes was resuspended in tri-reagent before chloroform was added to separate the different layers. The top aqueous layer was collected and isopropanol was added to extract RNA. After centrifugation for 15 min at 14000 rpm at 4 °C supernatant was removed and RNA was resuspended in 0.1 % DEPC water. Samples were checked for DNA contamination and concentration was determined using a nanodrop spectrophotometer (Thermo Scientific). qRT–PCR was carried out using a Sybr-Green '1 step qRT – PCR kit' (Invitrogen) on a Model 7700 instrument (Applied Biosystems). The following primer sets were used:

Beta actin primer set 1 forward – CATTGCTGACAGGATGCAGAAGG

reverse – TGCTGGAAGGTGGACAGTGAGG

Primers designed to a sequence on exon five.

Amplifies a product of 138 bp.

Beta actin primer set 2 forward – ATGTTGAAGGTCTCAAACATGAT

reverse - ACCACACCTTCTACAATGAGCTG

Primers designed to a sequence on the end of exon three and the start of exon four. Amplifies a product of 127 bp.

2.14 *In vitro* experiments

2.14.1 Cells

NSC-34 cells and hippocampal neurons from embryonic day 17 old rat were kindly provided and plated out by Paul Skehel. The NSC-34 cells were cultured in DMEM media complemented with 10% fetal calf serum and the primary hippocampal neurons were cultured in BME serum free medium complemented with 1.6% of a 32.5% glucose solution, 1% Sodium Pyruvate 100 nM solution, 1% N2 supplement and 5% B27 supplement respectively.

2.14.1.1 UBEI-41 treatment

UBEI-41 (Biogenova) is a cell-permeable ubiquitin E1 inhibitor and was kept at -20 °C. The cells were harvested and plated in a 12-wells plate (approximately 1.6 x 10^5 cells per well) and kept in 500 µl of their normal culture media. The cells were treated with either 10 µM or 50 µM of UBEI-41. Control cells were treated with dimethyl sulfoxide (DMSO; Sigma) alone. The cells were left for 1, 2, or 16 hours before the cells were harvested, by lysing the cells in RIPA buffer with 10 % protease inhibitor cocktail.

2.14.1.2 UCH-L1 inhibitor treatment

UCH-L1 inhibitor (Millipore) was kept as a stock concentration of 25 mM at -20°C. Cells were plated in a 12-wells plate (approximately 1.6x10^5 cells per well) and kept in their normal culture media. Cells were treated with either 1 μM, 5 μM, 10 μM or 25 μM of the drug and left for 0.5, 1, 2, 3, or 6 hours in a total volume of 500 μl. Control cells were treated with the equivalent volume of DMSO only.

2.15 *In vivo* drug treatment

Mice were given a subcutaneous (only severe SMA mice) or intra-peritoneal injection daily from the day of birth (P1) until P4 for the severe mice and P9/P10 for the Taiwanese SMA mice. For the survival study mice were injected until they died, or looked too unhealthy and were subsequently killed. The mice were either injected with 10 mg/kg Trichostatin A (TSA; InvivoGen), 100 mg/kg, 50 mg/kg or 10 mg/kg Quercetin (Sigma) or 10 mg/kg NPA (Sigma) or an equivalent volume of DMSO alone.

For SAHA experiments, litters of Taiwanese SMA mice were dosed twice daily from birth with either 25 mg/kg SAHA dissolved in DMSO, or an equivalent volume of DMSO alone, via oral application with a feeding needle. These injections were carried out in Cologne in Brunhilde Wirth's laboratory and afterwards tissue was sent to Edinburgh.

2.16 Physical test and general health assessment

All mice (SMA and control) were weighted and checked for general health every day during the time of drug treatment. Mice that looked very unhealthy (i.e. were not moving or felt cold) or had lost 10 % of their body weight per day over two consecutive days were killed. Every three days the righting reflex test was performed in order to assess neuromuscular function. In this test the pups were placed on their back on a flat surface and were timed for the amount of time it took them to reposition themselves dorsal side up. If the pups did not achieve this within 1 min it was noted as a failed attempt.

2.17 *Ex vivo* vulnerability essay

Whole brain synaptosomes from SMA and control mice were resuspended in 1 ml Krebs buffer (118.5 mM NaCl, 4.7 mM KCl, 1.18 mM $MgSO_4$, 10 mM glucose, 1 mM Na_2HPO_4, 20 mM hepes, pH 7.4). $CaCl_2$ was added to make a 1.3 mM solution. The samples were put on a rocking plate in an incubator at 37 °C. At different time points a 200 µl aliquot was taken from the samples for analysis. The aliquot taken at time point zero (TO) was used as a control. Hereafter aliquots were collected at 30 min (T0.5), 1h (T1), 2h (T2), 3h (T3), 4h (T4), 5h (T5) and 6h (T6). The aliquots were centrifuged at 20 000 g for eight min. The supernatant was collected (Krebs buffer) and the pellet was resuspended in 50 µl RIPA buffer with protease inhibitors. The sample was vortexed for 15 sec before centrifuged again at 20 000 g for eight

min. The supernatant (synaptosol) was taken of the pellet (membranes and organel-bound proteins) and stored separately until all samples were collected.

2.18 Proteomic techniques

2.18.1 iTRAQ proteomics

Protein extracts were sent to Douglas Lamont at the 'Fingerprint' Proteomics facility in the university of Dundee, where the mass spectrometry with the necessary preparations was performed.

Protein was extracted in an MEBC buffer (50 mM Tris, 100 mM NaCl, 5 mM NaEDTA, 5 mM NaEGTA, 40 mM β-glycerophosphate, 100 mM sodium fluoride (NaF), 100 mM sodium orthovanadate, 0.25 % NP-40, 1 Roche 'complete' protease inhibitor tablet, pH 7.4) before acetone precipitation and labelling for iTRAQ analysis. Synaptic hippocampal samples (N=9 mice per genotype) were precipitated with -20 °C chilled acetone (1:4, v/v) and stored at -20 °C overnight. The precipitates were spun at 4 °C for 10 min then washed with an acetone:water mixture (4:1,v/v) twice prior to air-drying. The pellets were then resuspended in an iTRAQ sample buffer (25 µl of 500 mM TEAB, 1 µl of denaturant (2% SDS) and 2 µl of reducing agent (TCEP)). The samples were allowed to incubate for 1 hour at 60 °C prior to protein estimation in triplicate (3 × 1 µl) by Micro BCA assay. Aliquots of each sample equivalent to 100 µg were made up to 28 µl using the iTRAQ sample buffer minus denaturant. To each sample, 1 µl of 84 mM indole-3-acetic acid (IAA) was added, and the samples were mixed and spun prior to incubation at room temperature in the dark for 30 min. To each sample, 10 µl of a 1 µg/µl solution of trypsin

(sequencing grade, Roche) in water was added and the samples incubated overnight on a shaking platform at 30 °C. To each vial of iTRAQ reagent, 70 µl of ethanol was added, mixed and spun prior to transfer to each sample vial. The pH value was checked for each sample to ensure pH was 8.0 prior to incubation for 1 hour at room temperature. One hundred microliters of water were added to each sample to quench the reaction prior to pooling of the four iTRAQ-labelled samples and subsequent drying by vacuum centrifugation. Samples were run in duplicate using the 4-plex system (114 &116 were extracts from *Smn*$^{-/-}$*;SMN2* and 115 & 117 were extracts from *Smn*$^{+/+}$*;SMN2*). The pooled iTRAQ sample was re-suspended in 25 % acetonitrile/ 0.1 % formic acid (50 ml) prior to loading through a home-made SCX ziptip using a 10 % slurry of Poros HS (10 ml) in a methanol:water mixture (50:50). The SCX ziptip was equilibrated with 25 % acetonitrile/ 0.1 % formic acid (3 × 25 ml) prior to loading of the pooled iTRAQ sample. After sample loading, the SCX ziptip was washed with 25 % acetonitrile in 0.1 % formic acid (3 × 25 ml). The bound iTRAQ peptides were eluted from the SCX ziptip using increasing millimolar concentrations of sodium chloride (5, 10, 20, 50, 100,150, 200, 150, 300, 400, 800) in 25 % acetonitrile/ 0.1 % formic acid (2 × 25 ml). A final elution of the SCX ziptip with 200 mM NH_4OH in 50 % propanol was used to remove most of the hydrophobic peptides. Each fraction from the SCX ziptip was then dried by vacuum centrifugation and stored until analysed by nano liquid chromatography-mass spectrometry/mass spectrometry (nLC-MS/MS). Prior to the analysis, each dried SCX fraction was re-suspended in 35 µl of 1 % formic acid and 10 µl aliquots were injected onto an Agilent 6520 Q-TOF using an Agilent 1200 series nanoLC system with microfluidic interface. Raw data files were converted to mascot generic file

(mgf) by MassHunter workstation software prior to merging of the files with Mascot Daemon and subsequent database (international protein index; IPI Mouse) searching with the Mascot search engine (Matrix Science, Version 2.2).

2.18.2 Label-free proteomics

Protein was extracted in MEBC Buffer (50 mM TRIS, 100 mM NaCl, 5 mM NaEDTA, 5 mM NaEGTA, 40 mM β-glycerophosphate, 100 mM sodium fluoride (NaF), 100 mM sodium orthovanadate, 0.25 % NP-40, 1 Roche 'complete' protease inhibitor tablet, pH 7.4). Protein concentration was determined by BCA assay according to manufacturers instructions on solubilized muscle (WT-Rostral P1 was compared to KO-Rostral P1 and WT-Rostral P5 was compared KO-Rostral P5).

Protein extracts were sent to Douglas Lamont at the 'Fingerprint' Proteomics facility in the university of Dundee, where the mass spectrometry with the necessary preparations was performed.

Ten µg aliquots of each muscle type were reduced with 10 mM DTT and alkylated with 50 mM iodoacetamide prior to digestion with trypsin (Roche, sequencing grade) overnight at 30 °C. Technical replicates (3 x 2.5 µg) of each digested muscle type were injected onto a nLC-MS/MS system (Ultimate 3000 (Dionex) coupled to a LTQ Orbitrap XL (Thermo Scientific). The peptides from each digest were separated over a 65 min linear gradient from 5-35 % acetonitrile in 0.1 % formic acid. The LTQ Orbitrap XL was configured with a TOP 5 methodology comprising a 60 K resolution FT-MS full scan followed by IT-MS/MS scans for the 5 most intense peptide ions.

The raw data files were sent back to me for analysis. Progenesis LC-MS (version 4.0) software was used for label free differential analysis and subsequent identification and quantitation of relative ion abundance ratios, both up-regulated and down-regulated. Individual peptide sequences generated by the proteomics analysis were submitted to the IPI database (chapter 3) or Swiss-Prot (chapter 4) for protein identification. As an indication of identification certainty, the false discovery rate for peptide matches above identity threshold was 9.39 % for P1 data and 3.34 % for P5 data.

2.19 *In silico* protein network analyses

Ingenuity Pathways Analysis (IPA) application (Ingenuity Systems, version 1.0) was used. IPA dynamically generates networks of gene, protein, small molecule, drug, and disease associations on the basis of "hand-curated" data held in a proprietary database. More than 90 % of the information in this database is "expert-curated" and is drawn from the full text of peer-reviewed journals. Less than 10 % of interactions have been identified by techniques such as natural language processing. Networks generated by IPA were limited in this study to a maximum of 35 members and are enriched for the input proteins. To enhance the explorative interpretation of data, networks are ranked according to a score calculated via a right tailed Fisher's exact test. This test outputs a value that takes into account the original input proteins of interest and the size of the network generated. The value enables the application to approximate how relevant the network is to the analysis. It should be noted that this score does not indicate the biological relevance or quality of the network but simply

provides a useful indicator with which to start an explorative analysis. Further information on the computational methods implemented in IPA can be obtained from Ingenuity Systems. Available at http://www.ingenuity.com.

2.20 Statistics

When two groups were compared either the parametric unpaired two-tailed *t*-test or the non-parametric Mann Whitney test was used ($P<0.05$). For comparisons between more than two groups a one-way ANOVA with Tukey's multiple comparison test or the non-parametric Kruskal-Wallis test with Dunn's post test was used. All tests were performed in Prism software.

Chapter 3

Muscle pathology in mouse models of SMA

3.1 Introduction

Whilst most research to date has focused on examining how low levels of SMN lead to pathological changes in motor neurons, the contribution of muscle to the pathogenesis of SMA remains unclear. Although pathological changes in muscle, including evidence of increased levels of apoptosis, are a well-established hallmark of SMA (Fidzianska *et al.* 1990; Tews and Goebel 1997; Guettier-Sigrist *et al.* 2002; Stathas *et al.* 2008; Dachs *et al.* 2011), it has generally been assumed that changes in muscle occur simply as a secondary consequence of the degeneration of innervating lower motor neurons, rendering muscle fibers denervated. Studies have shown that restoring SMN protein levels in neurons can significantly ameliorate disease progression in SMA animal models (Chan *et al.* 2003; Gavrilina *et al.* 2008). However, these studies cannot rule out an additional contribution resulting from restoration of SMN levels in muscle, raising the possibility that intrinsic responses to low levels of SMN in skeletal muscle may also contribute directly to SMA pathogenesis (Braun *et al.* 1995; Greensmith and Vrbova 1997; Cifuentes-Diaz *et al.* 2001; Chan *et al.* 2003; Arnold *et al.* 2004; Shafey *et al.* 2005; Rajendra *et al.* 2007; Vrbova 2008; Martinez-Hernandez *et al.* 2009). Moreover, SMN protein is present in

muscle sarcomeres in both mice and *Drosophila*, alongside other associated SMN complex proteins such as gemins (Rajendra *et al.* 2007; Walker *et al.* 2008). Establishing whether skeletal muscle directly contributes to SMA pathogenesis therefore remains a critical question for understanding SMA pathogenesis as well as for the successful targeting of future therapeutic strategies.

Previous attempts to address this question have been hampered, at least in part, by the fact that it has proven difficult to distinguish secondary pathological changes, induced as a consequence of denervation due to functional and structural deficits in lower motor neurons, from changes intrinsic to muscle. Moreover, *in vitro* studies of isolated muscle fibers from SMA patients (Anderson *et al.* 2003; Arnold *et al.* 2004; Martinez-Hernandez *et al.* 2009) are similarly defined by the fact that they are, as a direct result of the experimental protocol, devoid of lower motor neuron innervation and therefore denervated.

In this chapter, I have utilised a skeletal muscle preparation from an established mouse model of SMA (*Smn*$^{-/-}$*;SMN2*; hereafter referred to as the severe SMA mouse model (Monani *et al.* 2000)) where it is possible to examine molecular changes occurring in skeletal muscle *in vivo*, in the absence of any detectable denervation-inducing changes in corresponding lower motor neurons. I used this preparation to reveal modifications in the molecular composition of skeletal muscle in SMA mice at a pre-symptomatic age, with a molecular profile distinct from that of denervated muscle. The findings were confirmed in a milder mouse model of SMA and also in muscle biopsies from SMA patients. Finally, I demonstrate that molecular pathology

of skeletal muscle in SMA mice can be ameliorated by treatment with the FDA-approved histone deacetylase inhibitor, SAHA.

3.2 Results

3.2.1 Characterisation of the caudal and rostral band of levator auris longus muscle

Recent papers have shown that the rate of neuromuscular junction (NMJ) degeneration differs considerably between muscles in SMA (Ling *et al.* 2012; Thomson *et al.* 2012). Muscles (or distinct bands of muscles) such as *levator auris longus caudal* (caudal band of LAL), *abductor auris longus* (AAL) and *transversus abdominus* (TA) show approximately 60% denervation at late symptomatic time-points (postnatal day 5; P5) in the severe SMA mouse model compared to littermate controls (Thomson *et al.* 2012). In contrast, other muscles such as *levator auris longus rostral* (rostral band of LAL) and *extensor digitorum longus* (EDL) show 100% innervated endplates at the same time point (Thomson *et al.* 2012).

To identify molecular changes occurring in muscle specifically as a result of low levels of SMN and with the absence of denervation due to degeneration of innervating lower motor neurons, the rostral band of LAL was used in this study. This muscle is located at the back of the neck of the mouse between the ears and is easily accessible by micro dissection (Murray *et al.* 2010). The rostral band of LAL is one of the two bands of the homogeneous fast-twitch *levator auris longus* (LAL) muscle. The two distinct bands (rostral and caudal) have separate pools of motor neurons innervating them. The motor neurons innervating the caudal band of LAL are susceptible to SMA pathology in the severe SMA mouse model, whereas those innervating the rostral band of LAL are resistant (Murray *et al.* 2008). Importantly,

previous studies have demonstrated that motor neurons innervating the rostral band of LAL develop normally in the pre-symptomatic period (P1-P2; (Murray *et al.* 2010)), with both genetic and electrophysiological studies indicating an absence of lower motor neuron pathology or neuromuscular junction dysfunction in the rostral band of LAL from early-symptomatic SMA mice (Baumer *et al.* 2009; Ruiz *et al.* 2010). The caudal and rostral band of LAL show intrinsically distinct features of focal Acetylcholine receptor (AChR) assembly in adult mice after paralysis (Pun *et al.* 2002; Murray *et al.* 2008). Murray *et al.* showed that after paralysing the LAL in a wild-type mouse for 1 month with repeated subcutaneous injections of Botulinum toxin (BotA), there were very few motor nerve terminals showing signs of collateral sprouting in the caudal band of the muscle. In contrast, more than 20% of endplates in the rostral band of LAL showed clear evidence of terminal collateral sprouting and the formation of ectopic AChR microclusters. These results reveal that the caudal band of LAL shows a fast synapsing (Fasyn) phenotype, whereas the rostral band shows a delayed synapsing (DeSyn) phenotype.

To confirm the Fasyn and Desyn phenotype of the caudal and rostal band of LAL respectively, the AChR clustering in these bands were examined during development. At embryonic day 16.5 (E16.5) FaSyn muscles show focally organized clusters of AChRs assembling in the absence of nerve and the clusters rapidly become aligned to presynaptic nerve and Schwann cells. In contrast, DeSyn muscles exhibit dispersed microclusters of AChRs. During this developmental time, nerves and Schwann cells fail to align with AChR microclusters, and extensive sprouting is detected (Pun *et al.* 2002). Therefore, wild-type mice were taken at E16.5. The LAL

was dissected and acetylcholine receptors were labelled using TRITC-conjugated α-Bungarotoxin (α-BTX). The AChR clusters were analysed in both the caudal and the rostral band of LAL, identifying each AChR cluster as one of five distinct degrees of compactness (as described in (Pun *et al.* 2002)) in order to assess their developmental status. Figure 3.1 shows example confocal pictures of the five distinct types of endplates. The descriptions for each group are shown in table 3.1. A compact, mature endplate is given a value 5, whereas a value 1 is given to an endplate that shows dispersed microclusters of AChRs and is the least mature form.

Table 3.1 Compactness values of Acetylcholine receptor clusters

Value	Description
1	prominent labelling along the central half of muscle fiber, multiple central clusters (immature endplate)
2	prominent extra-cluster labelling, central cluster fragmented (immature endplate)
3	detectable extra-cluster labelling, one uninterrupted central cluster (immature endplate)
4	no detectable extra-cluster label, variations in labelling intensity within central synaptic cluster (immature endplate)
5	no detectable extra-cluster label and uniform labelling of central synaptic cluster (mature endplate)

Endplates from 12 LALs (N=6 fetuses) were scored for their developmental status, as shown in figure 3.1. In the caudal band of LAL most endplates appeared as a compact uniform labelled cluster of AChRs (value 4 and 5). By contrast, in the rostral band of LAL a variety of endplate morphologies were observed, with most having extra-cluster labelling, a sign of a not yet mature and compact endplate (value 3). These observations confirm that the caudal band of LAL shows a FaSyn phenotype, whereas the rostral band of LAL shows a DeSyn phenotype.

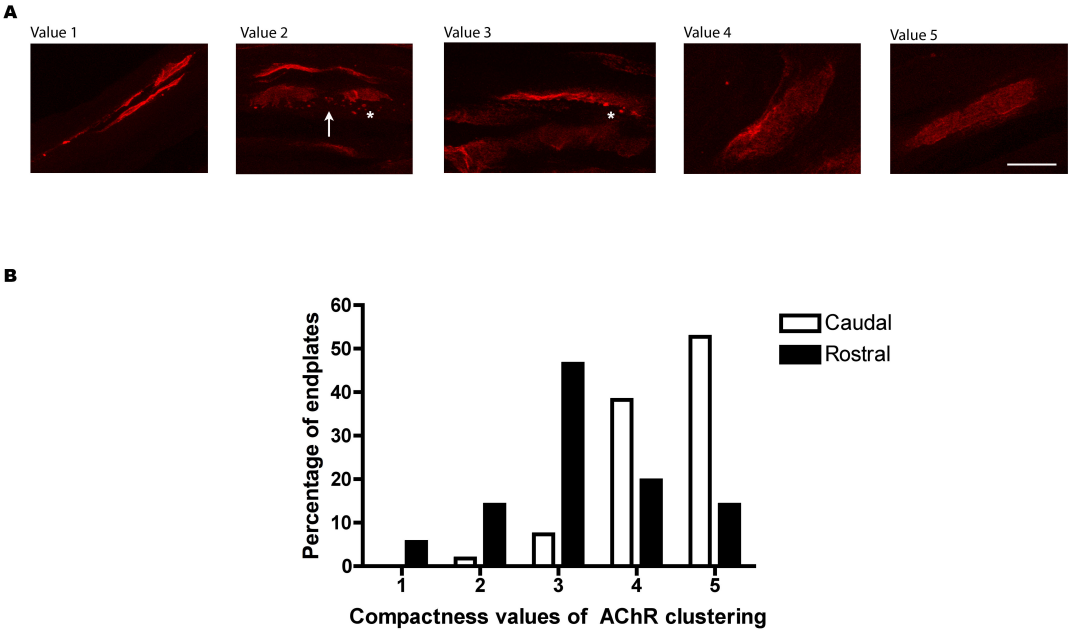

Figure 3.1 Rostral band of LAL shows a Desyn phenotype whereas the caudal band shows a FaSyn phenotype in wild-type mice at E16.5. (A) Confocal micrographs representing compactness of acetylcholine receptor (AChR) clustering (AChR labelled with TRITC-conjugated α-Bungarotoxin). Value 1 endplates have dispersed microclusters of AChRs. Value 2 endplates have fragmented central clusters (indicated by arrow) and show extra-cluster labelling (indicated by asterisk). Value 3 endplates have one uninterrupted central cluster, but have extra-cluster labelling (indicated by asterisk). Value 4 endplates show variations in central cluster labelling, but no detectable extra-cluster labelling. Value 5 endplates represent a mature endplate, showing uniform labelling of one central cluster. **(B)** Graph showing percentage of endplates in each of the categories (value 1-5) for the rostral and caudal bands of 12 LALs from 6 wild-type mice at E16.5. The endplates were analysed and each endplate was identified as one of five distinct degrees of compactness. The majority of endplates in the rostral band of LAL were one central cluster but show prominent extra-cluster labelling (value 3). The caudal band of LAL had mainly value 4/5 endplates, which were a compact central cluster without any extra-cluster labelling.

3.2.2 The rostral band of levator auris longus allows examination of intrinsic changes to skeletal muscle in SMA

To validate the absence of any degenerative pathology in the lower motor neurons innervating the rostral band of LAL, the whole LAL was dissected from P5 severe SMA mice and was immunohistochemically labelled with antibodies against neurofilament protein (green), and AChR were labelled using TRITC-α-BTX (red) (figure 3.2). A higher level of nerve terminal loss (vacant endplates) was observed in the caudal band. Almost 30% of the endplates in the caudal band of LAL were denervated at this late symptomatic time point, whereas in the rostral band of LAL there is almost no denervation (Murray *et al.* 2008). The absence of any degenerative pathology in lower motor neurons innervating the rostral band of LAL in severe SMA mice at a pre-symptomatic age (P1) was validated: >95% of neuromuscular junctions were fully innervated by intact motor axon collaterals in both severe SMA mice and littermate controls and there was no evidence of abnormal neurofilament accumulations in motor nerve terminals in any of the muscles examined (figure 3.3; N=3 mice per genotype; P>0.05, Mann Whitney test).

Similarly, there was no evidence for denervation-induced muscle fiber shrinkage in the rostral band of LAL from severe SMA mice at P1 (figure 3.4A/B; N=3 mice per genotype; P.0.05, unpaired, two-tailed *t*-test). In addition the muscle fibers showed a normal pattern of striations (figure 3.4C). In both genotypes the average muscle fiber diameter was 10 μm. Taken together with the previously published studies, this leads to the conclusion that the rostral band of LAL at P1 represents a muscle preparation from a SMA mouse where no detectable neuronal degeneration or muscle

denervation is present, making it ideal for intrinsic molecular studies of muscle in SMA. As expected, however, there was still a 70-80% reduction in expression levels of SMN protein in the rostral band of LAL from severe SMA mice at P1 compared with littermate controls (figure 3.4A).

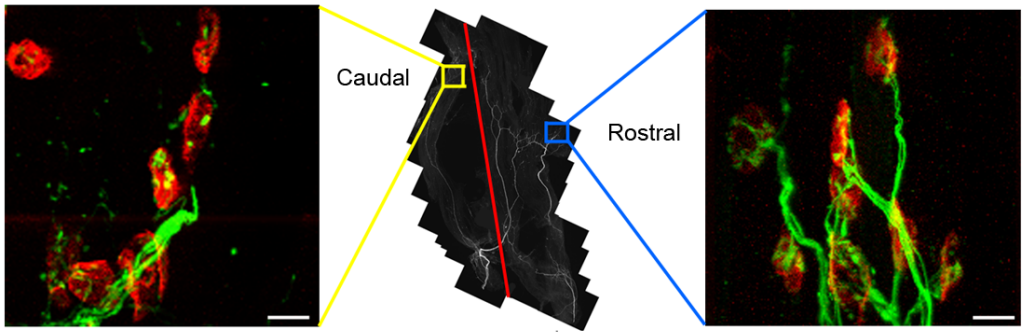

Figure 3.2 Selective vulnerability in synapses in the caudal band of LAL in SMA mice at P5. The middle panel shows a low-magnification overview of the entire muscle innervation pattern of the LAL from an SMA mouse ($Smn^{-/-}$;SMN2). The red line indicates the demarcation point between the rostral band of the muscle (to the right) and the caudal band of the muscle (to the left). The left panel shows an example of a high-power confocal micrograph of the neuromuscular junctions in the caudal band of the muscle at postnatal day 5 (P5) (green; immunohistochemically labelled neurofilament and SV2 synaptic vesicle protein to highlight motor neurons/ red; AChR on skeletal muscle fibers labelled with TRITC-conjugated α-BTX). Note the presence of widespread neuronal pathology evidenced by the loss of neuronal inputs to the endplates. The right panel shows an example of a high-power confocal micrograph of neuromuscular junctions in the rostral band of the muscle at P5. Note the preservation of motor neuron inputs. Scale bar = 20 μm.

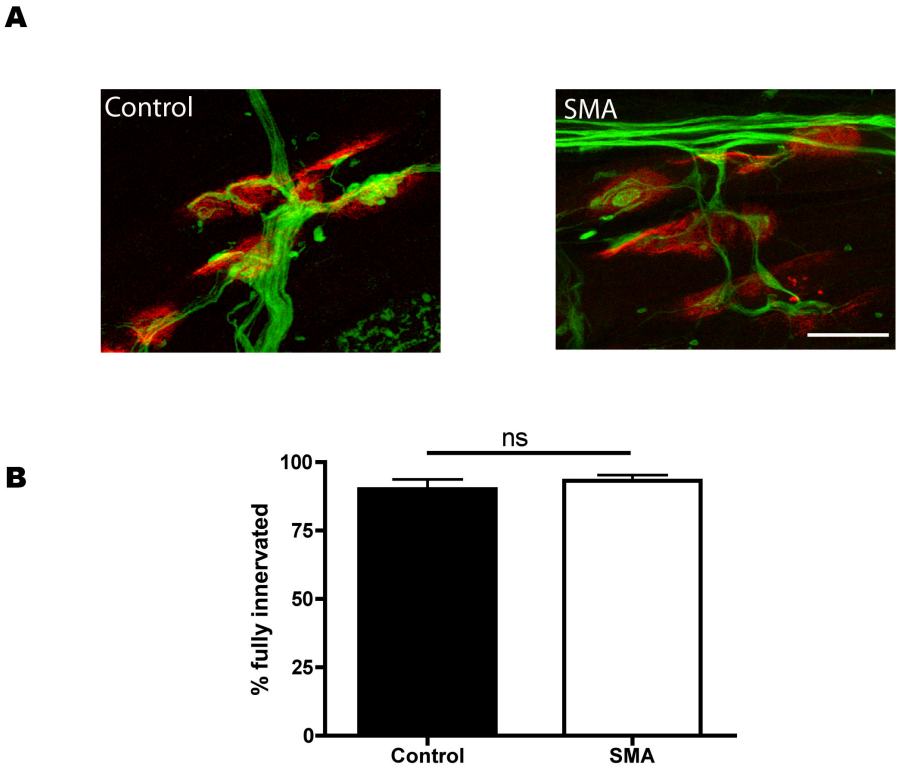

Figure 3.3 The rostral band of LAL at pre-symptomatic time point (P1) in SMA mice provides an experimental model to study SMN-induced changes in the molecular composition of muscle in the absence of neuronal pathology at P1. **(A)** Representative confocal micrographs showing immunohistochemically labelled neuromuscular junctions from the rostral band of LAL in SMA (right panel) and control mice (left panel) at postnatal day 1 (P1). Note the complete absence of any overt neuronal pathology (e.g. vacant endplates or neurofilament accumulations). **(B)** Bar chart (mean ± SEM) showing that there is no difference in the number of innervated endplates (N=3 mice per genotype; P>0.05, Mann Whitney test). Scale bar = 20 μm.

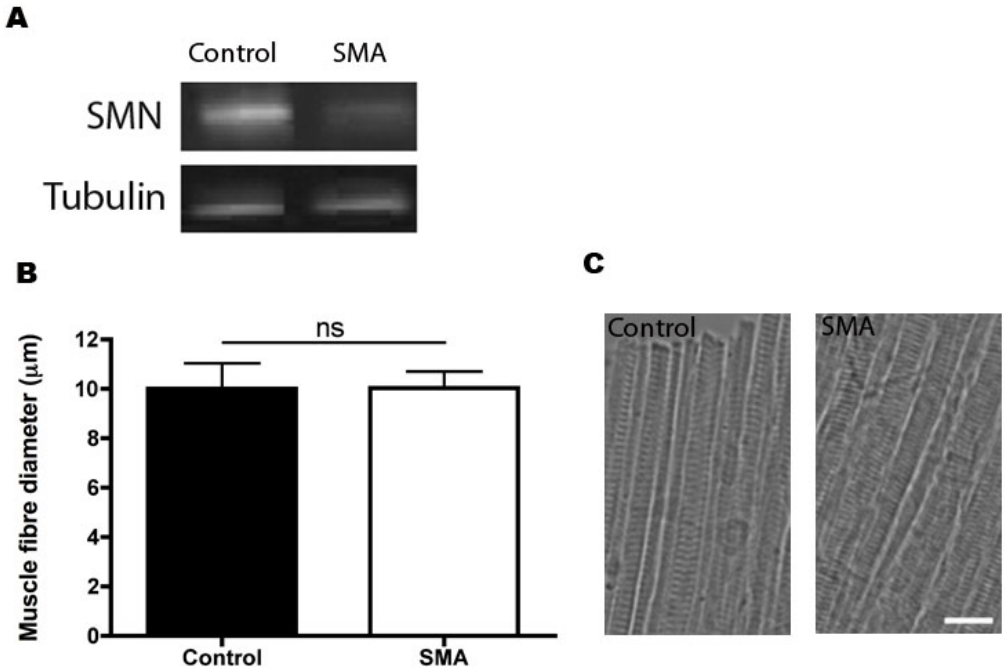

Figure 3.4 There is no muscle fiber shrinkage in the rostral band of LAL from SMA mice at pre-symptomatic time point (P1). (A) Representative western blots showing levels of SMN and beta-V-tubulin (loading control). **(B)** Bar chart (mean ± SEM) showing muscle fiber diameter in the rostral band of LAL from both SMA and control mice at P1. There is no denervation-induced muscle fiber atrophy in the SMA mice (N=3 mice per genotype; P>0.05; unpaired, two-tailed *t*-test). **(C)** Light microscopy micrographs show no shrinkage in muscle fiber size in SMA mice compared to littermate controls. In addition, muscle fibers from SMA mice show a normal pattern of striations. Scale bar = 20 μm.

3.2.3 Label-free proteomics analysis of the rostral band of levator auris longus reveals molecular alterations to skeletal muscle in pre-symptomatic severe SMA mice

A highly sensitive label-free proteomic analysis was used to quantify and compare the molecular composition of the rostral band of LAL in P1 severe SMA mice and littermate controls (WT littermate controls; *Smn*$^{+/+}$*;SMN2*; N=9 mice per genotype; for a detailed description of the mass spectrometry see chapter 2). The raw mass-spectrometry data from SMA and control mice was uploaded to Progenesis label-free software for analysis. From each sample three replicate runs were performed. One control replicate was chosen as a reference dataset, based on a clear and representative feature pattern with minimum distortion. All other runs were then aligned to this reference dataset using the Progenesis software. Alignment was performed to correct for the variable elution of peptides during chromatographic separation. Although Progenesis software automatically aligns data from each experimental run, vectors were also added manually to align peptide ions where needed. After aligning data from each of the runs, data filtering was performed. All ions that were identified with an early (less than 6 minutes) or late retention time (more than 72 minutes) were excluded. The runs were then grouped according to the genotype of the mouse (e.g. into pooled control and SMA datasets) and an ANOVA statistical test was performed to determine whether the means of the two groups were equal.

At this stage further stringent filtering was performed by excluding all 1^+ charged ions on the basis that they were unlikely to represent peptides. Once the list of

candidate peptide ions to identify was created, their MS/MS data was exported to the IPI mouse protein database to allow comparison to known peptides, and subsequently proteins. The output of this search was then re-imported to Progenesis software in order to allow further filtering by excluding peptides that were associated with more than one protein (conflict resolving). Also, peptides that were improperly cleaved by trypsin were excluded (e.g. any peptide that had a Lysine or Arginine mid sequence, or any peptides not ending with a Lysine or Arginine). A filtering protocol was then applied for subsequent stringent positive identification of proteins, with only those proteins identified by two or more unique peptides taken forward for further analysis.

This stringent filtering resulted in a list of 65 out of the 345 identified individual proteins (19%) that were up-regulated >20% in severe SMA mice (table 3.2). Of these, 20 proteins showed a greater than 2-fold increase in expression levels. In addition, 32 out of the 345 identified proteins (9%) were down-regulated >20% in severe SMA mice (table 3.3). The increased expression profiles of many proteins in severe SMA tissue confirmed that the changes observed were active responses to low levels of SMN in muscle, and were not simply occurring as a result of a global decrease in protein synthesis. Initially the proteomics data was validated by quantifying expression levels of one significantly down-regulated protein parvalbumin, (PVALB, hereafter referred to as parvalbumin) in immunohistochemically labelled rostral band of LAL preparations (figure 3.5). The images (figure 3.5A/B) were taken with exactly the same settings on the microscope to ensure comparability (for example exposure time and digital gain). Fluorescence

intensity of parvalbumin staining was measured across four randomly selected areas of each muscle, revealing a ~25% decrease in levels in the SMA mouse compared to littermate controls.

Table 3.2 Proteins up-regulated > 20% with peptide count > 1 in the rostral band of LAL from SMA mice compared with littermate controls at P1

Gene name	Protein name	Accession	Fold	Peptides	Score	Anova (p)*
Vdac2	Voltage-dependent anion-selective channel protein 2	IPI00122547.1	5.12	2	113.2	4.05E-04
Rpl32 60S	ribosomal protein L32	IPI00230623.8	3.33	2	77.7	5.92E-03
Actc1	Putative uncharacterized protein	IPI00654242.1	3.07	6	420.1	1.52E-06
Acta1	Actin	IPI00110827.1	3.01	6	447.1	1.61E-06
Atp5c1	ATP synthase subunit gamma,	IPI00313475.1	2.95	2	116.8	1.59E-04
- 11 kDa protein		IPI00329998.3	2.58	2	117.1	4.67E-06
Alb	Serum albumin	IPI00131695.3	2.51	13	615.8	1.07E-05
Mylpf	Myosin regulatory light chain 2	IPI00224549.3	2.5	6	372.8	5.08E-04
Rpl8 60S	ribosomal protein L8	IPI00137787.3	2.48	2	92.1	9.31E-05
Pgk1	Phosphoglycerate kinase 1	IPI00555069.3	2.36	5	326.2	9.71E-08
Atp5b	ATP synthase subunit beta	IPI00468481.2	2.35	3	271.2	3.17E-05
Dcn	Decorin	IPI00123196.1	2.33	2	51.0	1.41E-04
Apoa1	Apolipoprotein A-I	IPI00121209.1	2.24	2	93.5	2.01E-04
Lgals1	Galectin-1	IPI00229517.5	2.23	3	174.3	5.17E-04
Mdh2	Malate dehydrogenase, mitochondrial	IPI00323592.2	2.21	3	143.5	6.59E-06
Cs	Citrate synthase, mitochondrial	IPI00113141.1	2.17	2	85.1	3.66E-05
Atp5o;	ATP synthase subunit O, mitochondrial	IPI00118986.1	2.08	2	85.4	5.84E-04
Aco2	Aconitate hydratase, mitochondrial	IPI00116074.1	2.05	5	219.6	9.84E-06
Trf	Serotransferrin	IPI00139788.2	2.02	11	645.3	9.07E-05
Afp	Alpha-fetoprotein	IPI00113163.1	2	5	288.8	1.20E-04
Eif4a1	Eukaryotic initiation factor 4A-I	IPI00118676.3	1.98	2	115.4	9.41E-04
Tpt1;Gm14456	Translationally-controlled tumor protein	IPI00129685.2	1.94	2	122.6	2.77E-06
Gm10916	Putative uncharacterized protein	IPI00875087.1	1.93	2	100.5	2.08E-05
Srl	Isoform 1 of Sarcalumenin	IPI00224456.2	1.92	4	201.9	4.45E-04
Cct8	T-complex protein 1 subunit theta	IPI00469268.5	1.91	2	82.3	1.56E-03
Spnb2	Isoform 2 of Spectrin beta chain, brain 1	IPI00121892.9	1.87	3	86.5	6.98E-03
Hnrnpk	Isoform 1 of Heterogeneous nuclear ribonucleoprotein K	IPI00223253.1	1.86	2	77.0	0.09
Myl1	Isoform MLC1 of Myosin light chain 1/3,	IPI00312700.4	1.81	3	143.9	1.34E-04
Hist1h2bf;Hist1h2bj; Hist1h2bl;Hist1h2bn	Histone H2B type 1-F/J/L	IPI00114642.4	1.8	2	134.6	2.52E-04
Rpl6 60S	ribosomal protein L6	IPI00313222.5	1.8	2	62.4	6.34E-04
Spna2	Isoform 2 of Spectrin alpha chain, brain	IPI00753793.2	1.79	3	120.5	7.42E-04
Anxa6	annexin A6 isoform b	IPI00310240.4	1.78	4	289.0	1.20E-04
Nono Isoform 1	Non-POU domain-containing octamer-binding protein	IPI00320016.7	1.71	2	67.2	0.02
Des	Desmin	IPI00130102.4	1.7	2	112.4	7.06E-04
Hspb1	Isoform A of Heat shock protein beta-1	IPI00128522.1	1.69	3	81.8	1.62E-04
Tnnc2	Troponin C, skeletal muscle	IPI00284119.7	1.69	2	125.2	2.80E-03
Myom2	myomesin 2	IPI00115823.2	1.68	3	102.2	5.32E-04
Tpm1	Isoform 1 of Tropomyosin alpha-1 chain	IPI00123316.1	1.65	4	168.4	4.07E-03
Ywhag	14-3-3 protein gamma	IPI00230707.6	1.62	2	100.7	0.02
Csrp3	Cysteine and glycine-rich protein 3	IPI00118153.1	1.62	2	96.4	4.59E-04
Idh2	Isocitrate dehydrogenase [NADP]	IPI00318614.9	1.61	3	211.1	6.00E-05
Pfkm	6-phosphofructokinase, muscle type	IPI00331541.5	1.59	4	148.6	1.92E-04
Nme2	Nucleoside diphosphate kinase B	IPI00127417.1	1.57	5	183.0	3.35E-03
Pygm	Glycogen phosphorylase, muscle form	IPI00225275.5	1.56	3	144.8	9.94E-04
Hnrnpa1	Putative uncharacterized protein	IPI00553777.2	1.55	2	118.3	6.14E-05
Ckm	Creatine kinase M-type	IPI00127596.1	1.53	13	886.2	3.24E-04
Eef1g	Elongation factor 1-gamma	IPI00318841.4	1.53	2	122.1	6.36E-03
Actb	Actin, cytoplasmic 1	IPI00110850.1	1.51	4	302.0	3.12E-04
Hbb-b1	Hemoglobin subunit beta-1	IPI00553333.2	1.5	3	324.0	3.90E-03
Pa2g4	Proliferation-associated protein 2G4	IPI00119305.3	1.47	2	70.1	0.08
Myh8	Myosin-8	IPI00265380.4	1.46	13	750.8	2.74E-04
Vim	Vimentin	IPI00227299.6	1.42	5	207.5	2.42E-03
Hsp90b1	Endoplasmin	IPI00129526.1	1.41	2	158.8	0.02
Hnrnpa3	Isoform 1 of Heterogeneous nuclear ribonucleoprotein A3	IPI00269661.1	1.39	2	105.2	2.63E-03
Fhl1	four and a half LIM domains protein 1 isoform 2	IPI00776352.1	1.36	8	485.9	2.84E-03
Tpm2	Isoform 1 of Tropomyosin beta chain	IPI00123319.1	1.36	4	179.0	0.04
Cryab	Alpha-crystallin B chain	IPI00138274.1	1.33	3	117.6	1.17E-03
Actn2	Alpha-actinin-2	IPI00331664.3	1.3	2	66.4	0.02
Casq2	Calsequestrin-2	IPI00869462.1	1.29	3	197.9	2.61E-03
Hbb-b2	Hemoglobin subunit beta-2	IPI00316491.4	1.27	5	285.0	0.02
Pdia3	Protein disulfide-isomerase A3	IPI00230108.6	1.27	3	116.2	9.86E-03
Hspa8	Heat shock cognate 71 kDa protein	IPI00323357.3	1.25	4	208.1	0.07
Ppid	Peptidyl-prolyl cis-trans isomerase D	IPI00132966.3	1.25	2	82.2	0.02
Cltc	Clathrin heavy chain 1	IPI00169916.11	1.24	4	234.6	1.26E-03
Fscn1	Fascin	IPI00353563.4	1.21	2	85.4	0.11

Table 3.3 Proteins down-regulated > 20% with peptide count > 1 in the rostral band of LAL from SMA mice compared to littermate controls at P1

Gene name	Protein name	Accession	Fold	Peptides	Score	Anova (p)*
P4hb	Putative uncharacterized protein	IPI00122815.3	-2.66	3	111.5	6.29E-05
Pvalb	Parvalbumin alpha	IPI00230766.4	-2.65	2	90.4	3.72E-05
Rcn3	Reticulocalbin-3	IPI00221798.1	-2.28	2	173.7	1.35E-05
Rps7 40S	ribosomal protein S7	IPI00136984.1	-2.15	2	63.7	4.38E-04
Anxa5	Annexin A5	IPI00317309.5	-2.05	2	98.2	8.74E-03
Hist1h1d	Histone H1.3	IPI00331597.6	-2.03	4	168.9	0.03
Vcl	Vinculin	IPI00405227.3	-1.9	2	90.6	1.50E-04
H2afv	Histone H2A	IPI00320149.2	-1.84	2	79.0	7.81E-05
Serpinh1	serpin H1 precursor	IPI00880252.1	-1.72	5	250.8	5.98E-05
Rpl3 60S	ribosomal protein L3	IPI00321170.8	-1.72	2	100.3	1.69E-03
Rpl7a-ps3	Putative uncharacterized protein Gm5044	IPI00265107.4	-1.72	2	61.3	1.91E-03
Cct7	T-complex protein 1 subunit eta	IPI00331174.5	-1.69	2	49.9	0.04
Pkm2 Isoform M1	Pyruvate kinase isozymes M1/M2	IPI00845840.1	-1.66	5	309.1	2.87E-04
Eef2	Elongation factor 2	IPI00466069.3	-1.64	5	251.4	3.58E-04
Hist1h1c	Histone H1.2	IPI00223713.5	-1.64	3	155.1	0.05
Akr1b3	Aldose reductase	IPI00223757.4	-1.59	2	67.1	6.41E-05
Pdlim5	Putative uncharacterized protein	IPI00467374.1	-1.56	3	142.6	2.90E-06
Flna Isoform 1	Filamin-A	IPI00131138.10	-1.5	3	159.7	2.02E-04
Ckap4	Cytoskeleton-associated protein 4	IPI00223047.2	-1.5	3	151.4	8.14E-04
Sept8 Isoform 2	Septin-8	IPI00331497.9	-1.48	2	67.6	1.78E-03
Car3	Carbonic anhydrase 3	IPI00221890.6	-1.46	2	120.7	3.67E-05
Anxa2	Annexin A2	IPI00468203.3	-1.42	6	354.3	6.93E-04
Bin1 Isoform 1	Myc box-dependent-interacting protein 1	IPI00114352.1	-1.41	2	187.0	2.86E-04
Sec23a Protein	transport protein Sec23A	IPI00123349.2	-1.37	2	77.8	1.21E-03
Myom1	Isoform 2 of Myomesin-1	IPI00281109.3	-1.35	4	186.8	6.96E-04
Trim72	Tripartite motif-containing protein 72	IPI00462157.1	-1.34	3	130.3	1.12E-03
Rpl28;Rpl28-ps1 60S	ribosomal protein L28	IPI00222547.6	-1.34	2	59.7	4.53E-03
Fh1 Isoform	Fumarate hydratase, mitochondrial	IPI00129928.2	-1.3	2	94.9	0.04
Gm2574;Gapdh;Gm12033;Gm3272;LOC100042025;Gm10359	Glyceraldehyde-3-phosphate dehydrogenase	IPI00273646.9	-1.23	8	625.5	4.97E-03
Ppia	Peptidyl-prolyl cis-trans isomerase	IPI00554989.3	-1.22	4	170.1	0.02
Gpi1	Glucose-6-phosphate isomerase	IPI00228633.7	-1.2	4	169.7	1.86E-03
Mdh1	Malate dehydrogenase, cytoplasmic	IPI00336324.11	-1.2	2	88.7	9.82E-04

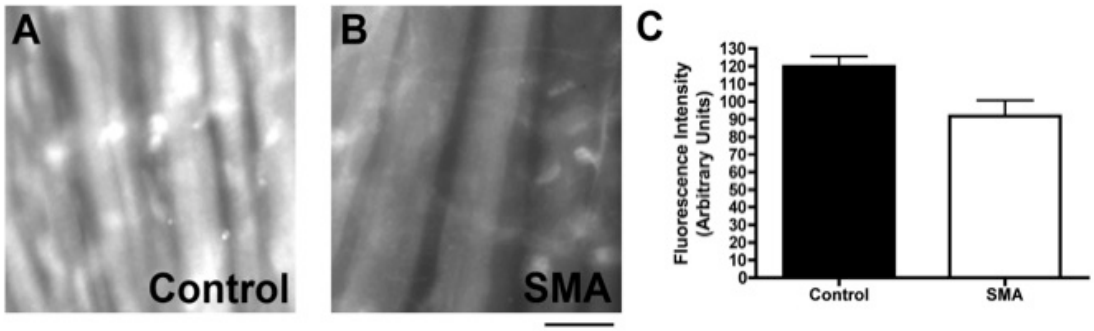

Figure 3.5 Validation of reduced levels of parvalbumin in muscle from an SMA mouse using quantitative immunohistochemistry at P1. (A/B) Representative fluorescence micrographs of the rostral band of LAL muscle preparations from an SMA mouse and **(B)** littermate control **(A)** showing expression levels of parvalbumin. Note that the same microscope settings were used (i.e. exposure time and digital gain). **(C)** Bar chart (mean ± SEM) showing a ~ 25% reduction in parvalbumin levels in the rostral band of LAL of an SMA mouse compared to a littermate control (n=4 measurement areas, N=1 mouse per genotype). Scale bar = 10 µm.

To identify any functional clustering of proteins found to have modified expression levels in the rostral band of LAL of severe SMA mice, a systems level analysis of the proteomics data was performed using Ingenuity Pathway Analysis software. This software incorporates information extracted by experts from the published scientific literature, allowing analysis of candidate proteins with respect to their known roles in biological functions (Wishart *et al.* 2010). 83 out of the 97 proteins identified were listed in this software and therefore available for data mining of the existing published literature to determine potential functional clustering. This analysis revealed that many of the proteins with modified expression profiles in muscle from severe SMA mice are reported to regulate muscle function and pathology (table 3.4). For example, the functional cluster most significantly changed in SMA muscle contained proteins known to contribute to skeletal and muscular disorders: 44 of the proteins changed in severe SMA muscle (53% of the total list) have links to these disorders, 6 of which also directly contribute to myopathies (table 3.4). Similarly, modifications were observed in clusters of proteins contributing to cell death pathways and morphological development (table 3.4). A different analysis at the systems level also highlighted disruption of two protein-interaction networks (identified by known direct or indirect interactions between individual proteins) implicated in development and function of the skeletal and muscular systems (figure 3.6). Green nodes represent proteins up-regulated in severe SMA mice compared to littermate controls, red nodes represent down-regulated proteins, and grey nodes represent proteins in the software-defined interaction network that were not identified by, or were found to be unchanged in, the proteomics dataset. The protein interaction network shown in figure 3.6A represents 27 out of the total of 35 proteins

that were changed in SMA mice. In figure 3.6B 30 out of a total of 35 proteins were changed in this network.

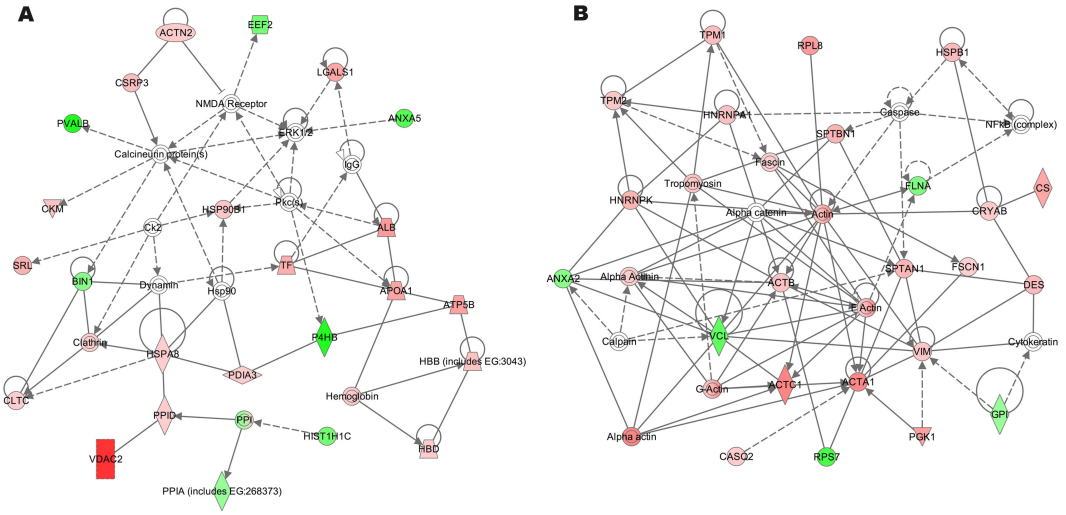

Figure 3.6 Identification of two protein-interaction networks with altered expression in muscle from pre-symptomatic SMA mice (P1). **(A/B)** Ingenuity pathway analysis of the rostral band of LAL proteomics data from SMA and wild-type littermate controls at P1 identified two protein-interaction networks significantly disrupted in SMA muscle. Both interaction networks were reported by the analysis software to be involved in “skeletal and muscular system development and function”. Green nodes represent proteins that are increased in SMA mice, and red nodes represent proteins that are decreased compared to littermate controls. Grey nodes represent proteins in the software-defined interaction network that were not identified by or were found to be unchanged in the proteomics dataset. A normal line represents a direct protein-interaction and a dotted line represents an indirect protein-interaction.

Table 3.4 Systems level analysis of functional pathway changes in the rostral band of LAL muscle in SMA mice at P1

Function Annotation	Number of proteins	Percentage of candidate list	P-value	Proteins
skeletal and muscular disorder	44	53.0	2.31E-08	ACTA1, ACTB, ACTN2, ALB, ANXA2, ANXA5, APOA1, ATP5C1, BIN1, CA3, CASQ2, CKAP4, CLTC, CRYAB, DES, EEF2, EEF1G, FH, FHL1, FLNA, GPI, HNRNPA1, HNRNPA3, HSP90B1, HSPA8, HSPB1, LGALS1, MDH1, MYH8, MYL1, MYOM1, MYOM2, NONO, PDIA3, PFKM, PGK1, PKM2, PPIA, PVALB, RPL3, RPL32, TNNC2, TPM2, VIM
tumorigenesis	41	49.4	5.12E-06	ACTB, ACTC1, AFP, ALB, ANXA2, ANXA5, APOA1, ATP5C1, CA3, CKM, CRYAB, CSRP3, DCN, EIF4A1, FH, FLNA, FSCN1, GPI, HBB, HBD, HNRNPA1, HNRNPK, HSP90B1, HSPA8, HSPB1, LGALS1, MDH1, MYH8, MYLPF, P4HB, PA2G4, PGK1, PKM2, PPIA, SPTBN1, TNNC2, TPM1, TPM2, VDAC2, VIM, YWHAG
cell death	29	34.9	9.60E-04	ACTB, ACTC1, AFP, ALB, APOA1, BIN1, CCT7, CCT8, CRYAB, DCN, FLNA, GPI, HIST1H1C, HNRNPA1, HSPA8, HSPB1, LGALS1, MDH1, NME2, P4HB, PA2G4, PDIA3, PKM2, PPIA, PPID, TF, TPM1, VCL, VDAC2
inflammatory disorder	29	34.9	2.32E-02	ACO2, ACTA1, ACTB, ALB, ANXA5, APOA1, CA3, CLTC, CRYAB, EEF2, EEF1G, GPI, HBD, HNRNPA1, HNRNPA3, HNRNPK, HSP90B1, HSPA8, LGALS1, NONO, P4HB, PDIA3, PGK1, PPID, RPL32, TF, TPM2, VDAC2, VIM
growth of cells	24	28.9	1.18E-04	ACTB, AKR1B1, ALB, ANXA2, ATP5B, BIN1, CA3, CCT7, CRYAB, DCN, DES, EIF4A1, HNRNPA1, HNRNPK, LGALS1, NME2, PA2G4, PDIA3, PGK1, PKM2, SERPINH1, TF, TPM1, TPM2
cardiovascular disorder	24	28.9	2.01E-02	ACTA1, ACTC1, ACTN2, ALB, ANXA2, ANXA5, APOA1, BIN1, CA3, CASQ2, CKAP4, CKM, CRYAB, CS, CSRP3, DES, FHL1, GPI, MYH8, PPIA, SPTBN1, TPM1, VCL, VIM
proliferation of cells	23	27.7	1.10E-02	AFP, AKR1B1, ANXA2, APOA1, BIN1, CLTC, CRYAB, DCN, FHL1, FSCN1, GPI, HNRNPK, HSP90B1, LGALS1, NME2, PA2G4, PGK1, PPIA, SPTAN1, SPTBN1, TF, VIM, YWHAG
connective tissue disorder	21	25.3	1.38E-02	ACTA1, ALB, ANXA5, APOA1, CLTC, CRYAB, EEF2, EEF1G, FLNA, GPI, HNRNPA1, HNRNPA3, HSP90B1, HSPA8, LGALS1, NONO, PDIA3, PGK1, RPL32, TPM2, VIM
developmental disorder	15	18.1	9.47E-04	ACTC1, ALB, APOA1, CA3, CASQ2, CRYAB, CSRP3, DES, FLNA, HBB, MYOM1, SEC23A, TF, TPM1, VCL
progressive motor neuropathy	15	18.1	8.09E-03	ACTB, ANXA2, ANXA5, CA3, CRYAB, FH, HSPB1, MDH1, MYOM1, PDIA3, PDLIM5, PGK1, PVALB, RPL3, VIM
contraction of muscle	14	16.9	6.26E-12	ACTA1, ACTC1, ACTN2, ANXA6, CASQ2, CRYAB, DES, MYL1, MYLPF, MYOM1, MYOM2, TNNC2, TPM1, TPM2
cell movement	13	15.7	5.28E-03	ACTB, ANXA2, APOA1, FLNA, FSCN1, GPI, HSPB1, LGALS1, PA2G4, PPIA, TPM1, VCL, VIM
formation of filaments	10	12.0	1.07E-05	ACTA1, ACTC1, DES, FHL1, GPI, MYOM1, SERPINH1, TPM1, TPM2, VIM
metabolic process of carbohydrate	10	12.0	2.40E-04	AKR1B1, APOA1, CKM, CRYAB, CS, GPI, PFKM, PGK1, PKM2, PYGM
modification of protein	10	12.0	2.73E-02	APOA1, CCT7, CRYAB, HSPA8, LGALS1, P4HB, PDIA3, PPIA, PPID, SPTBN1
developmental process of muscle	9	10.8	5.75E-05	ACTC1, CRYAB, CSRP3, DES, HSP90B1, MYLPF, PKM2, TPM1, VCL
metabolism of protein	9	10.8	1.78E-02	EEF2, EIF4A1, FLNA, HNRNPK, HSPB1, RPL3, RPL6, RPL8, RPL32
binding of normal cells	7	8.4	2.97E-03	ANXA2, ANXA5, APOA1, CKAP4, DCN, PDIA3, VCL
myopathy	6	7.2	3.73E-05	ACTA1, BIN1, CRYAB, DES, FHL1, TPM2
proliferation of connective tissue cells	6	7.2	6.64E-03	DCN, GPI, LGALS1, PA2G4, PGK1, TF
modification of mRNA	5	6.0	1.38E-03	ALB, EIF4A1, HBB, HNRNPA1, NONO
development of cytoskeleton	5	6.0	2.66E-03	ACTB, DES, FLNA, FSCN1, TPM1
degradation of DNA	5	6.0	4.05E-03	ALB, BIN1, CRYAB, HNRNPA1, HSPB1
phosphorylation of protein	5	6.0	3.13E-02	APOA1, LGALS1, PDIA3, PPIA, SPTBN1

3.2.4 Evidence for increased apoptotic cell death in SMA muscle

The finding that 35% of the proteins submitted for functional clustering analysis contribute to cell death pathways (table 3.4) was of particular interest given that apoptotic cell death has previously been reported in SMA muscle (Fidzianska *et al.* 1990; Tews and Goebel 1997; Guettier-Sigrist *et al.* 2002; Stathas *et al.* 2008; Dachs *et al.* 2011). Indeed, several of the protein expression changes identified in the rostral band of LAL of severe SMA mice have previously been implicated in activation of apoptotic and non-apoptotic cell death pathways (e.g. VDAC2) (Yagoda *et al.* 2007; Yamagata *et al.* 2009). I investigated whether markers of cell death were increased in the rostral band of LAL of severe SMA mice using immunohistochemistry. The muscle was labelled for phospho-histone H2AX (H2AX), which is a sensitive marker of DNA damage during the early stages of cell death (Plesca *et al.* 2008; Wen *et al.* 2010). Cell nuclei in the LAL were stained with TOPRO-3. The LALs were examined using a confocal microscope (63 x magnification). Twenty fields of view per muscle (N=3 mice per genotype) were examined and the number of nuclei were scored with H2AX staining. A distinction was made between no H2AX labelling, moderate accumulation and intense H2AX labelling. In severe SMA mice an increased number of cells per mm^2 was observed that showed an accumulation of H2AX protein around the cell nucleus (figure 3.7; *$P<0.05$, unpaired, two tailed *t*-test). This was not observed in the littermate controls. This suggests an elevated level of cell death in muscle from severe SMA mice. Thus, at least some of the protein expression changes identified in the rostral band of LAL of SMA mice (e.g. cell death proteins; see table 3.4) were contributing directly to biological pathways regulating muscle responses to low SMN levels *in vivo*.

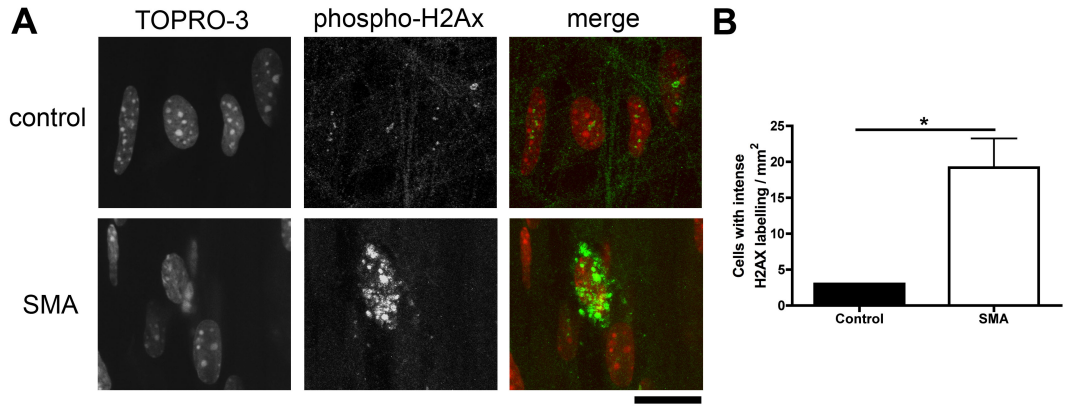

Figure 3.7 Increased levels of cell death in the rostral band of LAL from SMA mice. (A) Representative fluorescence micrographs of the rostral band of LAL from SMA mice (bottom panels) and control littermates (top panels) immunohistochemically labelled with the cell death marker H2AX (green). Nuclei were labelled with TOPRO-3 (red). Almost all muscle nuclei in control mice showed no, or weak, H2AX labelling, whereas strong H2AX labelling was easily identified in SMA muscles. Images were taken with identical settings on the confocal microscope. **(B)** Bar chart (mean ± SEM) showing a significant increase in the number of cells with intense H2AX labelling in the rostral band of LAL of SMA mice compared to littermate control (*P<0.05, unpaired, two tailed *t*-test, N=3 mice per genotype). Scale bar = 10 μm.

3.2.5 Changes in the molecular composition of skeletal muscle in SMA mice are distinct from those elicited following acute or chronic denervation

The proteomics analysis in this chapter was carried out to examine changes in muscle due to low levels of SMN and to exclude changes that are caused by denervation occurring as a result of degeneration of the lower motor neurons. To confirm that the molecular changes observed in this proteomic screen of SMA muscle were different from molecular changes as a result of acute or chronic denervation caused by sub-clinical motor neuron pathology, a literature search was performed on proteomics studies of chronically denervated muscle (>1 week following nerve injury; figure 3.8). I found three papers that showed molecular changes in skeletal muscle due to chronic denervation. In figure 3.8 proteins are highlighted that were identified in my proteomic screen and protein levels were compared to what was found in the literature. The profile of expression changes observed in the rostral band of LAL from severe SMA mice was clearly distinct from those modified following denervation (figure 3.8) (Li *et al.* 2005; Sun *et al.* 2006; Sato *et al.* 2009). For example parvalbumin was decreased in muscle from SMA mice but was increased in muscle from rat after denervation (Sato *et al.* 2009). Beta-enolase and triosephosphate-isomerase-1 were both unchanged in SMA muscle, however they were shown to be changed due to chronic denervation in muscle (figure 3.8).

As the previous molecular studies of denervated muscle were all performed on chronically denervated muscle, I also quantified expression levels of two proteins significantly altered in SMA muscle, voltage-dependent anion-selective channel

protein 2 (hereafter referred to as VDAC2) and parvalbumin in acutely denervated tissue. The sciatic nerve in wild-type mice from one leg was lesioned (a ~1 mm section of nerve was removed to ensure complete transection) and the denervated *flexor digitorum brevis* (FDB) muscles were isolated from the hind-foot 24 hours later and compared to the muscles from the uninjured leg (surgery was performed in collaboration with Laura Comley). Morphological evaluation of neuromuscular junctions confirmed complete denervation in all muscles examined (examined using a fluorescent microscope, no images were taken). However, western blot results show that levels of both VDAC2 and parvalbumin remained unchanged (figure 3.9; N=3 mice, P>0.05; unpaired, two tailed *t*-test), confirming that the changes I found in the proteomics analysis were specific to muscle due to low levels of SMN and distinct from changes due to either chronic or acute denervation.

	SMA	Chronic Denervation		
	Current Study	Li et al. (2005)	Sun et al. (2006)	Sato et al. (2009)
Alpha-crystallin (B chain)	UP	NR	DOWN	DOWN
Creatine kinase (Type M)	UP	DOWN/UP	DOWN	NR
Vdac2	UP	NR	NR	NR
Beta Enolase (Eno3)	NC	DOWN	UP	DOWN
Triosephosphate Isomerase 1	NC	DOWN	NR	UP
Parvalbumin	DOWN	UP	NR	UP

Figure 3.8 Molecular pathology of SMA skeletal muscle is molecularly distinct from changes elicited following chronic denervation. Comparison of expression profiles of individual proteins identified in SMA muscle, with expression changes observed in chronically denervated rodent muscle. Note that the molecular profile of SMA muscle was distinct from that in denervated muscle. NC, no change; NR, not reported; UP, increased expression; DOWN, decreased expression.

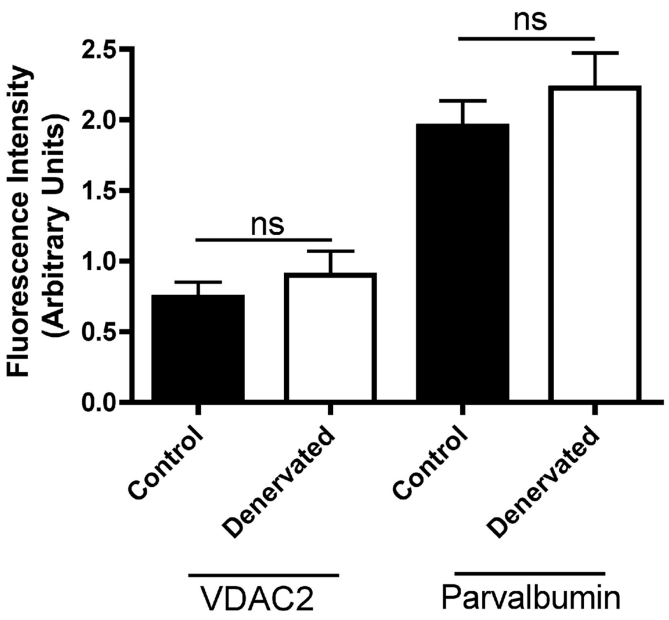

Figure 3.9 Molecular pathology of SMA skeletal muscle is molecularly distinct from changes elicited following acute denervation. Bar chart (mean ± SEM) showing expression levels of VDAC2 and Parvalbumin in mouse FDB muscles without (control) or 24h after (denervated) sciatic nerve lesion. Neither protein showed a significant change in expression in denervated muscle (N=3 mice; P>0.05; unpaired, two tailed *t*-test;). *(Nerve lesions were performed by Laura Comley).*

3.2.6 Molecular pathology of muscle is recapitulated in SMA patients

Having found that intrinsic molecular changes were present in muscle from pre-symptomatic severe SMA mice, I wanted to address the question of whether or not these changes were also present in skeletal muscle from SMA patients. Quantitative fluorescent western blotting was performed on SMA patient *quadriceps femoris* muscle biopsies, to establish expression levels of VDAC2 and parvalbumin (figure 3.10). Biopsies were obtained from type II/III SMA patients (aged between 3 and 25 years old; see table 2.1 and 2.2 for more details on the samples), with genetic diagnosis of SMA confirmed by a homozygous deletion of the *SMN1* gene. Three roughly age-matched control samples (aged between 17 and 27 years old), genetically confirmed to have no mutations in the *SMN1* gene, were used for comparison. First it was confirmed that SMN protein expression levels were indeed significantly decreased in SMA patient samples compared to control samples (figure 3.10A/B). As expected, there is variability in SMN levels observed in the patients, as the patients were diagnosed with either type II or type III SMA. Quantitative western blotting revealed that both VDAC2 and parvalbumin showed similar alterations in expression levels to those previously observed in severe SMA mice: VDAC2 was significantly up-regulated more than three fold in SMA patient muscle (figure 3.10C; *P<0.05; unpaired, two-tailed *t*-test) and parvalbumin was significantly down-regulated more than four fold (figure 3.10D; *P<0.05; unpaired, two-tailed *t*-test).

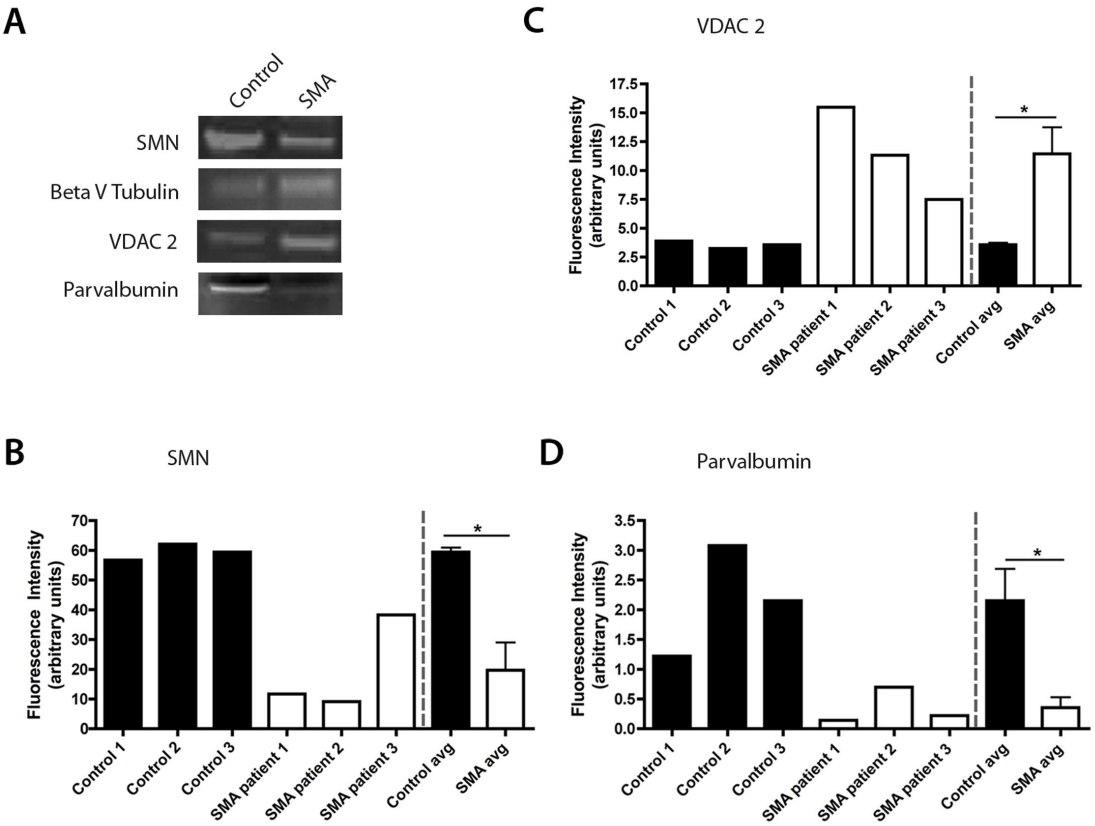

Figure 3.10 Molecular modifications are also present in skeletal muscle from SMA patients. (A) Representative fluorescent western blots on *quadriceps femoris* biopsies from SMA patients (type II or type III; aged between 3 and 25 years old) and non-SMA controls showing levels of SMN, beta-V-tubulin (loading control), VDAC2 and parvalbumin. **(B-D)** Bar charts showing expression levels of SMN, VDAC2 and parvalbumin in SMA patient biopsies compared to controls. Data are shown for individual patients (black and white bars to the left of the hashed line) as well as mean ± SEM for each genotype (right of the line). **(B)** SMN levels were significantly decreased in SMA patients (*P<0.05; unpaired, two-tailed *t*-test), **(C)** VDAC2 levels were significantly increased (*P<0.05; unpaired, two-tailed *t*-test). **(D)** Parvalbumin levels were significantly decreased (*P<0.05; unpaired, two-tailed *t*-test).

3.2.7 Molecular pathology of skeletal muscle is reversed by treatment with the FDA-approved histone deacetylase inhibitor, SAHA

The finding that levels of full-length SMN protein produced by the *SMN2* gene can be modulated by small molecules and drugs has raised the possibility of a therapy for SMA. For example, epigenetic modulation using histone deacetylase inhibitors (HDACi) appears to be successful (Wirth *et al.* 2006), with the HDACi SAHA (also known as Vorinostat or Zolinza) elevating full-length SMN protein levels in SMA mouse models *in vivo*, resulting in a 30 % increase in mean survival and amelioration of muscle fiber size shrinkage (Riessland *et al.* 2010). To examine whether HDAC inhibitors are capable of directly targeting molecular changes in muscle during SMA, expression levels of VDAC2, parvalbumin and the cell death marker H2AX were examined in skeletal muscle from SMA mice treated with SAHA.

For these experiments a milder SMA mouse model was used (Taiwanese SMA mice) with a new breeding protocol ($Smn^{-/-};SMN2^{tg/tg}$ x $Smn^{-/+}$) (Riessland *et al.* 2010) to generate affected SMA mice that survive until 10 days postnatal on a congenic FVB/N genetic background. The slightly longer life-span of this model makes it easier for testing potential therapeutic agents than the more severe SMA mouse model (Riessland *et al.* 2010). First it was confirmed that molecular pathological changes similar to those observed in severe SMA mice were also present in untreated late-symptomatic (P10) Taiwanese SMA mice and in other muscle groups. As expected, SMN protein levels in the *gastrocnemius* muscle were reduced to around 25 % of those in littermate controls (figure 3.11B; ***P< 0.001; ANOVA with Tukey's post hoc test). VDAC2 levels were increased (figure 3.11C; *P< 0.05) and

parvalbumin levels were decreased (figure 3.11D; ***P< 0.001) in Taiwanese SMA mice, and increased cell death was confirmed by an increase in levels of H2AX (figure 3.9E; ***P< 0.001). Importantly, it has previously been demonstrated that neuronal pathology is present in the *gastrocnemius* (muscle from the hind limb of the mouse) of Taiwanese SMA mice at P10 (including denervation of muscle fibers) (Riessland *et al.* 2010). Thus, the molecular changes initially observed in the rostral band of LAL muscle of severe SMA mice at P1 in the absence of neuronal pathology were also present in anatomically distinct muscles susceptible to denervation in SMA.

Taiwanese SMA mice and littermate controls were treated with SAHA from birth via oral administration of 25 mg/kg SAHA twice daily (Riessland *et al.* 2010). For control experiments, mice were dosed with Dimethyl sulfoxide (DMSO) alone. As previously reported (Riessland *et al.* 2010), SAHA treatment significantly increased SMN protein expression levels in the *gastrocnemius* (figure 3.9). I confirm here that SMN levels were increased two fold in SMA mice treated with SAHA compared to SMA mice treated with DMSO alone (figure 3.11; N=5 SMA mice, N=4 SMA + SAHA; *P>0.05, ANOVA with Tukey's *post hoc* test). Importantly, SAHA treatment significantly ameliorated SMN-induced changes in levels of VDAC2 and parvalbumin. VDAC2 showed a 1.25 fold decrease after treatment with SAHA as compared to DMSO treated SMA mice. The SAHA treated SMA mice showed similar levels of VDAC2 when compared with control mice (figure 3.11C; N=5 control mice, N=5 SMA mice, N=4 SMA + SAHA; *P>0.05, **P>0.01, ANOVA with Tukey's *post hoc* test). Parvalbumin levels were increased two fold in SMA mice after treatment with SAHA as compared to DMSO treated SMA mice (figure

3.11D; N=5 control mice, N=5 SMA mice, N=4 SMA + SAHA; **P>0.01, ***P>0.001, ANOVA with Tukey's *post hoc* test). Interestingly, as well as rescue of VDAC2 and parvalbumin, SAHA treatment also significantly decreased the level of the cell death marker H2AX, to similar levels observed in control mice (figure 3.11E; N=5 control mice, N=5 SMA mice, N=4 SMA + SAHA; ***P>0.001, ANOVA with Tukey's *post hoc* test). These results suggest a potential treatment with SAHA to rescue muscle pathology in SMA mice.

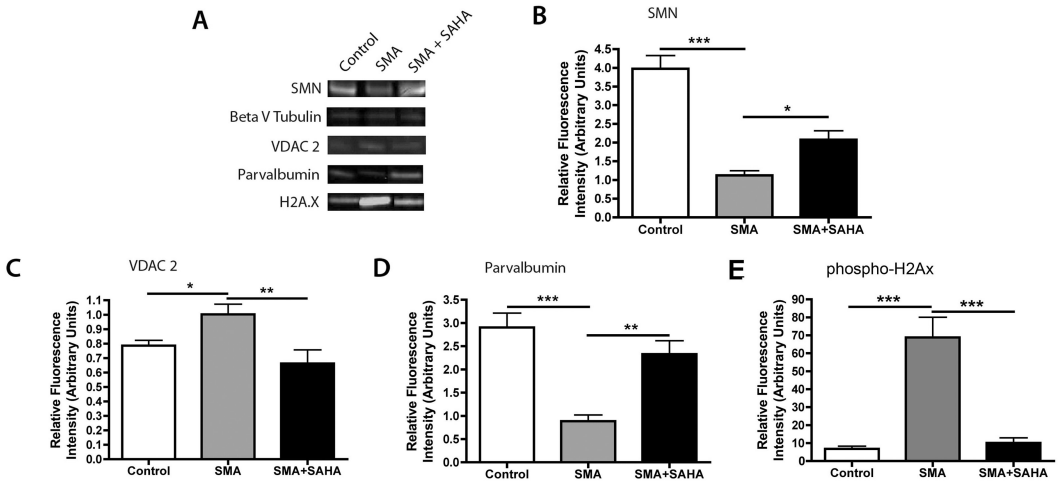

Figure 3.11 Reversal of SMA-induced molecular pathology of skeletal muscle by treatment with the histone deacetylase inhibitor (HDACi) SAHA. (A) Representative fluorescent western blots on *gastrocnemius* muscle from Taiwanese SMA mice (SMA), littermate controls (Control) and SAHA-treated Taiwanese SMA mice (SMA + SAHA) at P10 showing levels of SMN, beta-V-tubulin (loading control), VDAC2, parvalbumin and H2AX. **(B-E)** Bar charts (mean ± SEM) showing expression levels of SMN, VDAC2, parvalbumin and H2AX. **(B)** SMN levels were significantly decreased in Taiwanese SMA mice compared with controls (***P< 0.001; ANOVA with Tukey's post hoc test) and were significantly increased in SMA mice treated with SAHA (*P< 0.05). **(C)** VDAC2 levels were significantly increased in SMA mice (*P< 0.05) and decreased with SAHA treatment (**P< 0.01), returning to levels observed in littermate controls. **(D)** Parvalbumin levels were significantly decreased in SMA mice (***P< 0.001) but were increased with SAHA treatment (**P< 0.01), restoring them to 75% of those found in healthy control muscle. **(E)** H2AX levels were significantly increased in SMA mice (***P< 0.001) but were decreased with SAHA treatment (***P< 0.001), restoring them to those found in healthy control muscle. n=19 independent measurements from N=5 mice (Control), n=17, N=5 (SMA), n=11, N=4 (SMA + SAHA).

3.3 Discussion

3.3.1 Overview of results

In this chapter molecular pathology of skeletal muscle has been identified and characterised with the use of a label-free proteomic technique in an established mouse model of severe SMA. The protein changes that were identified were present during the earliest stages of disease (at P1) and occurred in the absence of any detectable degeneration of lower motor neurons. The expression levels of two proteins, VDAC2 and parvalbumin, identified with the proteomic screen were validated in a different mouse model of SMA and in a different muscle and showed the same robust up-regulation of VDAC2 and down-regulation of parvalbumin. In addition, changed expression levels were also confirmed in human muscle biopsies. Interestingly, molecular pathology of skeletal muscle was ameliorated in mice treated with the FDA-approved HDAC inhibitor SAHA. These findings therefore provide significant experimental support for the hypothesis that SMN-induced changes in skeletal muscle cannot solely be attributed to motor neuron degeneration. In addition, the molecular changes that were identified in SMA muscle were distinct from those reported in chronically or acutely denervated muscle.

3.3.2 Muscle is an important pathological target in SMA

Several other studies have supported the proposal that muscle is affected and may contribute to SMA pathogenesis. For example, a recent study has shown that satellite cells (muscle stem cells) located between the sarcolemma and the basal lamina, are accumulated in hind limbs of severe SMA mice and undergo premature differentiation. This led to reduced myofiber number and average size of the muscle

fibers (Hayhurst *et al.* 2012). In addition, cultured satellite cells from SMA mice fail to form multinucleated myotubes efficiently (Hayhurst *et al.* 2012). Other *in vitro* studies support this data and have shown that muscle cells derived from SMA patients can inhibit neuronal outgrowth and development when co-cultured with wild-type healthy motor neurons (Henderson *et al.* 1987; Braun *et al.* 1995; Guettier-Sigrist *et al.* 2002). In addition, a study showed that myotubes from human SMA fetuses also revealed a delay in growth and maturation *in vitro* (Martinez-Hernandez *et al.* 2009). Moreover, fibroblast growth factor (FGF) signalling in muscle can ameliorate SMN-associated abnormalities at the neuromuscular junction in Drosophila (Sen *et al.* 2011) and increased levels of insulin-like growth factor (IGF-1) in muscle modulates SMA phenotype in mice (Bosch-Marce *et al.* 2011). In addition, studies of SMN protein expression and localization have identified the SMN complex in muscle from both mice and Drosophila, as well as in C2C12 cells *in vitro* (Shafey *et al.* 2005; Rajendra *et al.* 2007; Walker *et al.* 2008). Taken together, these findings suggest that SMN levels are critical for the establishment and maintenance of molecular homeostasis in skeletal muscle. The findings in this chapter fit in with these earlier studies and add valuable additional insights as it is the first *in vivo* study on the role of muscle in SMA with the ability to rule out denervation-induced changes. In addition, the experimental design used in this study generated a reliable list of proteins that could lead to other hypothesis in the role for muscle in SMA. To summarize, direct disruption of muscle resulting from low levels of SMN is likely to be a significant contributor to SMA pathogenesis, alongside pathological changes in motor neurons.

3.3.3 Proteins identified are known to be involved in other neuromuscular diseases

Interestingly, many of the proteins identified by the proteomic screen as being altered in skeletal muscle during SMA have previously been implicated in other neuromuscular diseases where intrinsic muscle pathology occurs. For example, decorin is associated with modified proliferation and differentiation of myogenic cells in x-linked muscular dystrophy (Abe *et al.* 2009) and reticulocalbin 1 expression is altered in dystrophic muscles (Zhang *et al.* 2006). Galectin 1 has been implicated in myoblast differentiation, skeletal muscle development and muscle regeneration (Svensson and Tagerud 2009; Grossi *et al.* 2011). Similarly, proteins such as serpin H1 (a.k.a. HSP47) and vinculin, through its interaction with dysferlin, have been implicated in muscle fiber repair and maintenance of the muscle membrane respectively (Higuchi *et al.* 2007; de Morree *et al.* 2010). Thus, the proteins that are identified as having altered expression profiles in SMA muscle are consistent with those that might be expected to regulate intrinsic muscular pathology based on findings from other neuromuscular disorders.

3.3.4 Widespread protein changes in muscles of SMA mouse models and SMA patients

Two proteins of particular interest in the context of this study were VDAC2 and parvalbumin. Both showed modified expression levels in skeletal muscle across two different mouse models of SMA as well as in muscle biopsies from SMA patients, and both proteins responded significantly to SAHA treatment. This confirms that the changes identified in the rostral band of LAL are not specific changes in this

particular muscle but are widespread changes in muscles of SMA mouse models and very interestingly also in human muscle.

VDAC2 is a mitochondrial protein associated with formation of channels in the mitochondrial outer membrane, responsible for regulating cell death pathways and calcium signalling (Cheng *et al.* 2003; Roy *et al.* 2009; Subedi *et al.* 2011). It is also a core component of the muscle response to aging (O'Connell and Ohlendieck 2009) and has been implicated in early pathogenic events occurring in the mdx mouse model of muscular dystrophy (Massa *et al.* 2000). Parvalbumin is a cytosolic calcium buffer in muscle, breakdown of which similarly contributes to muscular dystrophy (Gailly 2002; Rome 2006).

Since both VDAC2 and parvalbumin are involved in calcium signalling, a disruption in calcium homeostasis might play a role in muscle pathology in SMA mice. Abnormal calcium homeostasis has been suggested to play an important role in skeletal muscle degeneration in muscular dystrophy (Shin *et al.* 2013). Mechanisms suggested by which elevated level of calcium causes muscle wasting in muscular dystrophy could be either through activation of calcium-dependent proteases such as calpains which eventually lead to the degradation of muscle proteins and necrosis (Goll *et al.* 2003), or by modulating the activity of calcineurin/nuclear factor of activated T-cells (NFAT) pathway (Hogan *et al.* 2003), or by acting as important secondary messengers that trigger intracellular responses such as excitation-contraction (E‑C) coupling and activation of various signalling pathways (Gailly 2002).

3.3.5 Evidence of increased levels of cell death in muscle of SMA mice

The observation of increased levels of the cell death marker H2AX is confirming earlier studies. Studies have suggested that cell death may be increased in muscle during SMA. DNA fragmentation with DNA strand breaks and up-regulated levels of Bax were observed in muscle of SMA patients (Tews and Goebel 1996; Tews and Goebel 1997). However, those observations could not rule out that cell death in muscle was occurring as a secondary effect of the degenerating motor neurons. In this chapter it has been ruled out that cell death in muscle is a secondary effect of motor neuron pathology, since the muscle I used has been confirmed to have normal innervation and no motor neuron degeneration.

3.3.6 HDAC inhibitors revers altered molecular composition of skeletal muscle in SMA

Finally, the finding that the altered molecular composition of skeletal muscle in SMA is reversible using the HDACi SAHA highlights the potential to treat SMN-induced muscle changes using small molecules and drugs. SAHA has been shown to penetrate into a range of tissues following administration - including the nervous system and muscle (Hockly *et al.* 2003; Hahnen *et al.* 2006; Riessland *et al.* 2010) - and is approved for use in humans by the FDA in the US. SAHA is a second generation HDACi, so it is likely that future generations will have even higher specificity and potency, increasing their attractiveness for use in SMA patients. The findings here suggest that attempts to develop better HDACi that specifically target SMN levels in skeletal muscle would likely lead to effective therapeutic options for

SMA. Testing other currently available HDACi for the potential to rescue muscle pathology *in vivo* will also be an important next step.

The current data do not allow me to ascertain whether raised SMN levels in muscle induced by SAHA also have a secondary impact on pathological changes occurring in other cell types (e.g. motor neurons), due to systemic delivery of the HDACi (Riessland *et al.* 2010). Thus, the potential for a causal relationship between the rescue of pathological changes occurring in muscle in SAHA treated SMA mice and the reduction in pathology of motor neurons previously reported (Riessland *et al.* 2010) remains untested and warrants further investigation. Nevertheless, the findings in this chapter show that intrinsic pathological changes in muscle are a significant feature of SMA, regardless of their possible secondary impact on other cell types. Taken together, this study suggests that the most effective SMA therapeutics will probably need to be directed at both muscle and motor neurons.

Chapter 4

Biomarker identification in mouse models of SMA

4.1 Introduction

Disease progression, as well as symptom severity, can vary significantly between individual patients with SMA, largely dependent upon the copy number of the near-identical *SMN2* gene (Swoboda *et al.* 2005; Lorson *et al.* 2010). A higher copy number of *SMN2* correlates with a milder phenotype. Similarly, disease-modifying genes are known to exist that can influence the severity of a patient's condition (Oprea *et al.* 2008).

A clearer understanding of the underlying genetics of SMA has led to potentially exciting pre-clinical breakthroughs over the past few years, with several therapeutic approaches revealing significant benefits in animal models of the disease. For example, experiments using gene therapy approaches to restore *SMN1* expression have yielded impressive amelioration in neuromuscular dysfunction and large increases in the lifespan of mice with SMA (Bevan *et al.* 2010; Foust *et al.* 2010; Valori *et al.* 2010; Dominguez *et al.* 2011). Other approaches aimed at increasing the amount of SMN protein produced by the *SMN2* gene by promoter activation or reduction of alternative splicing of *SMN2* exon 7 have also shown therapeutic benefit

in animal models (Brichta *et al.* 2003; Oskoui and Kaufmann 2008; Thurmond *et al.* 2008). As a result, there is a growing desire to undertake clinical trials in human patient cohorts in order to evaluate the potential benefits of these therapeutic approaches. However, performing clinical trials in cohorts of young patients (and in the case of severe forms of SMA, neonatal patients) brings with it a range of technical problems (Swoboda *et al.* 2007).

In order to improve the reliability and effectiveness of SMA clinical trials, robust biomarkers are required. Firstly, biomarkers are needed to allow accurate monitoring of disease activity and to predict disease progression in human patients (Kobayashi *et al.* 2013). Secondly, biomarkers are required to provide more accurate measures of the responses of individual patients and groups of patients to a new treatment or therapeutic approach (Guest *et al.* 2013). Several different approaches have previously been employed in an attempt to identify biomarkers for SMA in both mouse models and patient cohorts, incorporating a range of physical, functional and molecular readouts (Crawford *et al.* 2012; El-Khodor *et al.* 2012; Finkel *et al.* 2012; Kobayashi *et al.* 2013). However, robust biomarkers for SMA have yet to be identified.

Since I showed in the previous chapter that muscle is intrinsically affected in SMA, I investigated here whether biomarkers could be identified in this tissue. Proteomics technologies have recently been highlighted as a potentially powerful tool for biomarker discovery (Guest *et al.* 2013). In this study, I have utilized a state-of-the-art, label-free proteomics approach to identify individual proteins in the

neuromuscular system of SMA mice that report directly on disease status. By comparing the protein composition of skeletal muscle in SMA mice at a pre-symptomatic time-point (data from chapter 3) with the muscle proteome at a late-symptomatic time-point, I identified increased expression of both stress protein-70 (GRP75/mortalin; hereafter referred to as GRP75) and calreticulin as robust indicators of disease progression in SMA mice. I show that these potential protein biomarkers were similarly modified across different mouse models of SMA, across multiple different skeletal muscles, and were also measurable from skin biopsies. Furthermore, initial investigation of GRP75 and calreticulin levels in human muscle biopsies suggested that they were detectable and measurable by western blot.

4.2 Results

4.2.1 Label-free proteomics analysis reveals a list of 23 putative biomarkers of disease status in skeletal muscle from severe SMA mice

In order to identify potential new protein biomarkers capable of reporting directly on the progress of disease in SMA, I utilized unbiased, label-free proteomics technologies to compare the proteome of a pathologically affected tissue in SMA (skeletal muscle) at early- and late-symptomatic stages of the disease. Given the difficulty in obtaining human muscle samples at different time points for such an experiment, these initial proteomic screens were performed in the *levator auris longus* (LAL) of an established mouse model of SMA (the severe SMA mouse; *Smn*$^{-/-}$*;SMN2* (Monani et al. 2000)). The mouse LAL muscle is composed of two distinct muscle bands that are differentially affected in SMA mice: a caudal band that undergoes severe neuromuscular denervation and a rostral band that has minimal denervation but intrinsic muscular pathology (for more details on this see chapter 3, section 3.2.1 and 3.2.2). In order to obtain a pathologically homogeneous tissue sample for proteomics analysis, I chose to selectively examine the larger rostral band of the muscle.

The rostral band of LAL muscle was dissected from severe SMA mice and littermate controls (*Smn*$^{+/+}$*;SMN2*) at postnatal day one (P1; pre/early-symptomatic) and postnatal day five (P5; post-symptomatic; N=9 mice per genotype, per time-point) and proteins were extracted for mass-spectrometry analysis. The raw mass-spectrometry data from both P1 and P5 comparisons was uploaded to Progenesis

label-free software for further analyses. The progenesis output data from P1 mice was previously analysed using the IPI mouse database and was published (Mutsaers *et al.* 2011). However, since then the IPI database does not update anymore and therefore I switched to using the Swiss-Prot database. For the current study, to allow direct comparison with the P5 data, the P1 raw data was re-analysed in parallel with the P5 data. For a detailed description of the proteomic analysis see results chapter 3 section 3.2.3. Data from P1 tissue were analysed separately from data obtained from P5 tissue, but were compared afterwards in excel.

I identified 540 proteins in the P5 dataset (figure 4.1, left column). A filtering protocol was then applied for subsequent stringent positive identification of proteins, with only those proteins identified by two or more unique peptides taken forward for further analysis. Proteins that were either up- or down-regulated >20% in SMA muscle compared to controls were considered to have an altered expression profile (figure 4.1, middle column). To be considered as a putative biomarker, I was looking to identify proteins whose expression levels were unchanged in SMA muscle at P1 (pre/early-symptomatic), but were significantly changed at P5 (late-symptomatic). I therefore took the list of all proteins with modified expression in SMA mice at P5 compared to controls, and searched for expression data for the same proteins in the P1 comparison dataset. Any proteins found to have altered expression at both P5 and P1 were considered to be unsuitable as a biomarker and were therefore removed from the candidate list (figure 4.1, right column). This filtering of data resulted in the identification of 14 candidate biomarker proteins that were up-regulated in severe SMA mouse muscle at P5 but not at P1 (table 4.1, figure 4.2A) and 9 proteins that

were down-regulated in severe SMA mouse muscle at P5 but not at P1 (table 4.2, figure 4.2B).

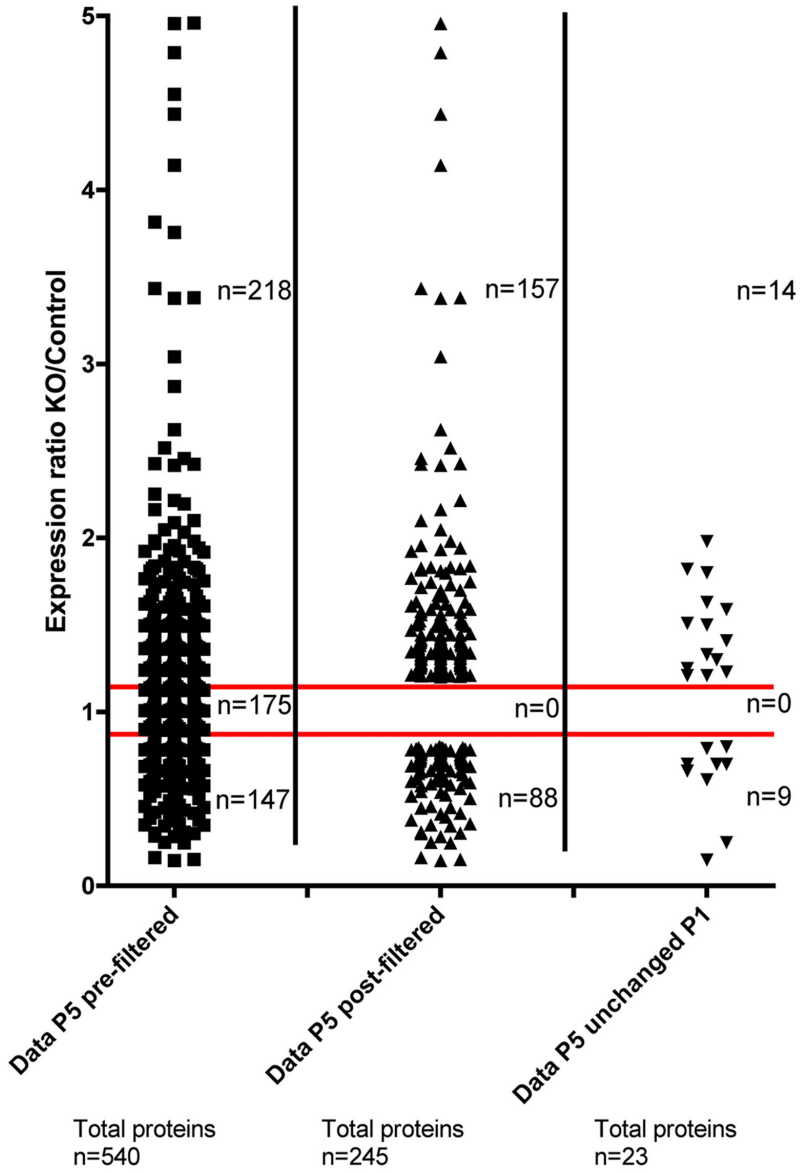

Figure 4.1 Filtering of proteomics data. The Scatter plot is showing the process of filtering undertaken on the raw proteomics data in order to generate a final list of 23 proteins modified in SMA mouse skeletal muscle at P5, but unchanged at P1. The left column shows all proteins identified by the Progenesis label-free proteomics software (n=540 proteins in total) in control and SMA (KO) mouse LAL muscle at P5, with the relative expression levels between samples represented as a ratio (KO/Control). The red bars indicate the 20% cut off threshold for being up-regulated or down-regulated in SMA mice compared to controls. The middle column shows the proteins remaining in the P5 dataset following filtering (e.g. that were either up- or down-regulated by > 20% and were identified by at least 2 peptides (n=245 proteins in total)). The right column shows those proteins that were identified as being changed in SMA mouse skeletal muscle at P5, but that were unchanged in comparable muscle samples at P1 (n=23 proteins in total).

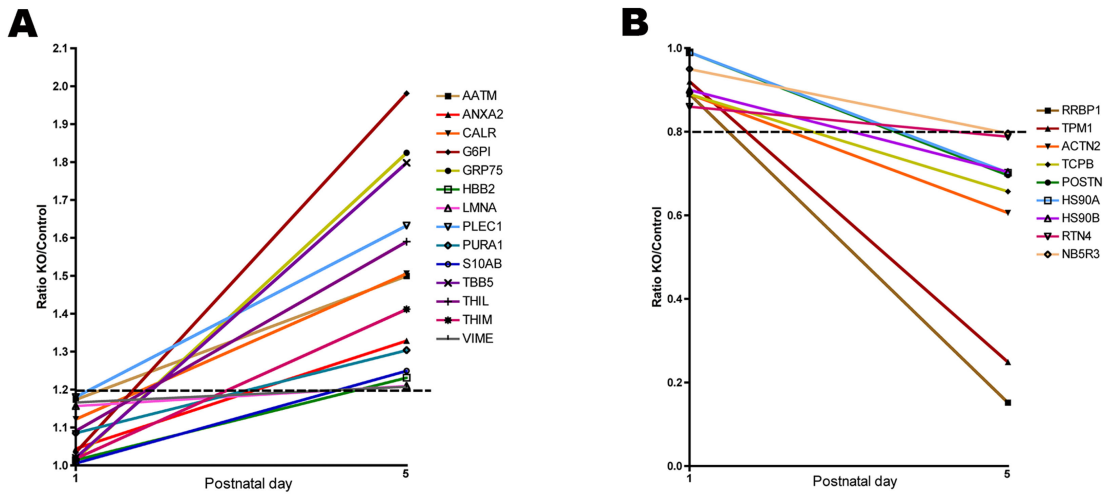

Figure 4.2 Identification of putative protein biomarkers for SMA in skeletal muscle from severe SMA mice. (A) Graph showing all 14 proteins that were unchanged at P1 in severe SMA mouse LAL muscle compared to littermate controls, but had increased levels >20% at P5. **(B)** Graph showing all 9 proteins that were unchanged at P1 in severe SMA mouse LAL muscle compared to littermate controls, but had decreased levels >20% at P5.

Table 4.1 Proteins unchanged at P1 but increased >20% at P5 in the rostral band of LAL muscle from SMA mice compared with littermate controls

Accession number	Protein name	Peptide count	Peptides used	Confidence score	Anova (p)*	Fold change at P1	Fold change at P5
G6PI_MOUSE	Glucose-6-phosphate isomerase	8	6	245.68	6.92E-06	1.03	1.98
GRP75_MOUSE	Stress-70 protein	5	3	170.83	5.59E-04	1.02	1.82
TBB5_MOUSE	Tubulin beta-5 chain	14	2	639.05	3.69E-05	1.02	1.80
PLEC1_MOUSE	Plectin-1	48	21	879.72	4.67E-06	1.18	1.63
THIL_MOUSE	Acetyl-CoA acetyltransferase	9	7	448.39	2.95E-04	1.09	1.59
CALR_MOUSE	Calreticulin	4	3	83.76	2.08E-03	1.12	1.51
AATM_MOUSE	Aspartate aminotransferase	12	7	443.54	1.50E-04	1.17	1.50
THIM_MOUSE	3-ketoacyl-CoA thiolase	16	12	473.14	1.16E-03	1.02	1.41
ANXA2_MOUSE	Annexin A2	12	10	729.11	1.28E-03	1.04	1.33
PURA1_MOUSE	Adenylosuccinate synthetase isozyme 1	7	5	247.24	1.19E-03	1.09	1.30
S10AB_MOUSE	Protein S100-A11	2	2	166.21	2.78E-02	1.01	1.25
HBB2_MOUSE	Hemoglobin subunit beta-2	12	6	702.27	1.51E-03	1.01	1.23
LMNA_MOUSE	Lamin-A/C	13	7	567.31	2.19E-04	1.16	1.21
VIME_MOUSE	Vimentin	20	12	776.2	3.50E-04	1.17	1.21

Table 4.2 Proteins unchanged at P1 but decreased >20% at P5 in the rostral band of LAL muscle from SMA mice compared with littermate controls

Accession	Protein name	Peptide count	Peptides used	Confidence score	Anova (p)*	Fold change at P1	Fold change at P5
RRBP1_MOUSE	Ribosome-binding protein 1	9	3	60.23	1.97E-05	1.12	-6.59
TPM1_MOUSE	Tropomyosin alpha-1 chain	17	6	652.67	6.87E-06	1.09	-4.02
ACTN2_MOUSE	Alpha-actinin-2	27	15	1413.57	1.82E-04	1.12	-1.65
TCPB_MOUSE	T-complex protein 1 subunit beta	8	3	162.09	2.07E-03	1.12	-1.52
POSTN_MOUSE	Periostin	5	3	142.66	7.55E-04	1.01	-1.44
HS90A_MOUSE	Heat shock protein HSP 90-alpha	10	3	326.05	7.71E-04	1.01	-1.42
HS90B_MOUSE	Heat shock protein HSP 90-beta	17	8	600.51	6.45E-05	1.11	-1.42
RTN4_MOUSE	Reticulon-4	8	5	123.82	1.69E-02	1.16	-1.27
NB5R3_MOUSE	NADH-cytochrome b5 reductase 3	4	3	65.43	3.90E-05	1.05	-1.26

4.2.2 Validation of putative protein biomarkers in the rostral band of levator auris longus

In order to validate the list of candidate biomarkers generated by this proteomics analysis, I obtained more tissue from SMA mice and littermate controls for western blot validation. I selected a subset of proteins for validation in the rostral band of LAL. I selected two proteins based on the magnitude of their expression change and the availability of suitable antibodies for western blotting as well as their expression pattern in different tissues (i.e. not muscle-specific, but widely expressed). Stress-protein 70 (GRP75) and calreticulin showed both an increased expression (1.8 and 1.5 fold respectively) in SMA mice.

Western blots performed on protein extracts from the rostral band of LAL showed an increased trend for both GRP75 and calreticulin expression (figure 4.3; N=2 mice per genotype). Because the severe SMA mice were only P5 when they were sacrificed and the rostral band of LAL is a very small muscle, not much protein could be extracted from it. Therefore I used the Taiwanese SMA mice for the rest of my experiments and also to determine whether similar changes in protein levels could be detected in a genetically distinct mouse model of SMA.

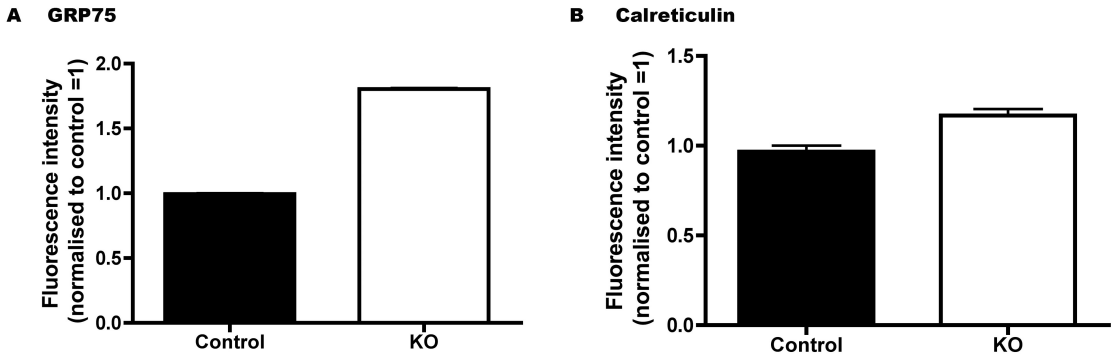

Figure 4.3 Validation of GRP75 and calreticulin in the rostral band of LAL of severe SMA mice compared to control. (A) Bar chart (mean ± SEM) showing a trend towards an increased expression of GRP75 in the rostral band of the LAL (N=2 mice per genotype). **(B)** Bar chart (mean ± SEM) showing a trend towards an increased expression of calreticulin.

4.2.3 Validation of putative protein biomarkers in the Taiwanese mouse model of SMA

For further validation I used a different skeletal muscle, the *gastrocnemius,* from the Taiwanese SMA mice to examine whether the changes were not specific to the rostral band of LAL. The *gastrocnemius* muscle is located in the hind limb of the mouse. I selected two more proteins for validation: T-complex protein 1 subunit beta (TCPB) which was decreased by 1.5 fold and ribosome-binding protein 1 (RRBP1), which was decreased by 6.6 fold in the proteomics data from severe SMA mice (table 4.2).

Levels of TCP1, GRP75 and Calreticulin were measured in the *gastrocnemius* muscle of Taiwanese SMA mice and littermate controls at a mid/late-symptomatic time-point (P9; figure 4.4A). Levels of TCPB were unchanged in the SMA mice compared to controls (figure 4.4B; N=3 mice per genotype; P>0.05, two-tailed,

unpaired *t*-test), thereby failing to validate the original proteomics data in the severe mouse model of SMA. However, in contrast, levels of both GRP75 and Calreticulin were significantly increased in the Taiwanese SMA mouse muscle, showing that the changes in these proteins were conserved between severe and Taiwanese SMA mice, as well as between the LAL and *gastrocnemius* muscle (figure 4.4B/C; **P<0.01, ***P<0.001 unpaired, two-tailed *t*-test). RRBP1 could not be detected with western blot. Both TCPB and RRBP1 were excluded from further experiments as these proteins failed to function as potential biomarkers.

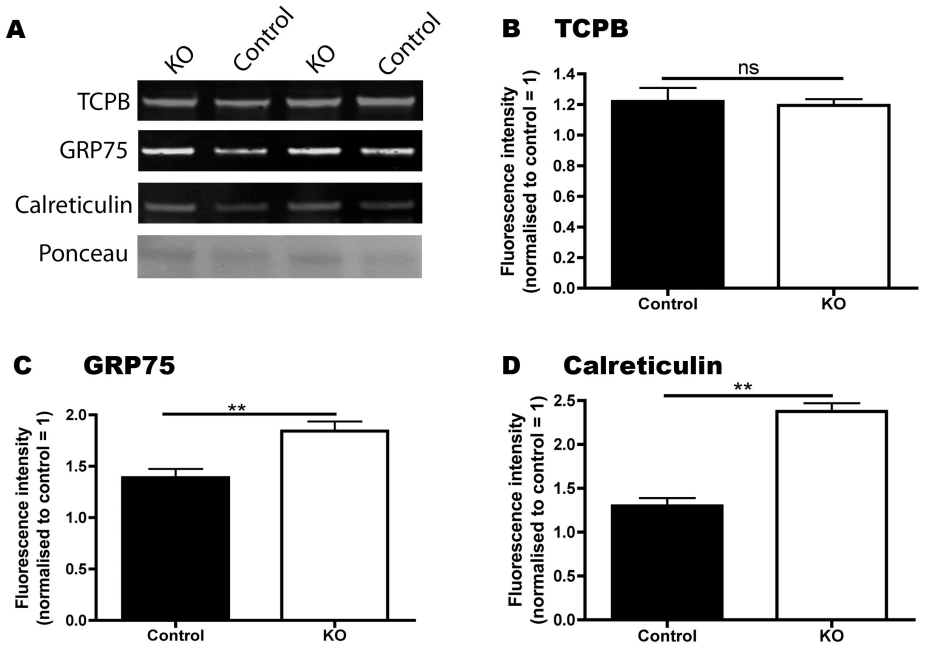

Figure 4.4 Validation of calreticulin and GRP75 as potential biomarkers in a different muscle from a genetically distinct SMA mouse model. (A) Representative fluorescent western blots on *gastrocnemius* muscle from Taiwanese SMA mice (KO) and littermate controls at P9 (mid/late-symptomatic) showing levels of TCPB, GRP75, calreticulin and Ponceau (loading control).**(B-D)** Bar charts (mean ± SEM) showing expression levels of TCPB, GRP75 and calreticulin in control and Taiwanese SMA mice (KO) at P9. **(B)** TCPB levels showed no difference in expression levels in SMA mice compared with controls (N=3 mice per genotype; P>0.05; unpaired, two-tailed t-test). **(C)** GRP75 levels were significantly increased in Taiwanese SMA mice compared with controls (**P<0.01; unpaired, two-tailed t-test). **(D)** Calreticulin levels were also significantly increased in Taiwanese SMA mice compared with controls (***P<0.001; unpaired, two-tailed t-test).

4.2.4 Preliminary investigation suggests that levels of GRP75 and calreticulin are increased in SMA patient muscle biopsies

Next, I wanted to establish whether the increased levels of GRP75 and calreticulin, observed to correlate with disease progression in SMA mouse models, were also measureable in skeletal muscle from SMA patients. Therefore, levels of GRP75 and calreticulin were examined using quantitative fluorescent western blotting on human muscle biopsy samples obtained through EuroBioBank (for more details see chapter 2 materials and methods). Biopsies were obtained from the *quadriceps femoris* (large muscle group covering the front and sides of the thigh) from three type II/III SMA patients (aged between 3 and 25 years old, for more details see table 2.1 and 2.2). All three patients had a genetic diagnosis of SMA confirmed by a homozygous deletion of the *SMN1* gene. Three roughly age-matched control samples (aged between 15 and 27 years old) were also obtained, genetically confirmed to have no mutations in the *SMN1* gene.

Levels of both GRP75 and calreticulin could be readily identified and showed a trend towards increased levels in SMA patients compared to controls (figure 4.5). GRP75 levels increased on average by 50% compared to controls, although the considerable variability between individuals and low sample size meant that this different did not reach statistical significance (figure 4.5B; N=3 samples per group; $P>0.05$, unpaired, two-tailed *t*-test). Calreticulin levels were significantly increased in the SMA patient biopsies, on average by 50% compared to controls (figure 4.5C; N=3 samples per group; $*P<0.05$, unpaired, two-tailed *t*-test), however there was still considerable variability between individuals. Whilst these experiments only represent an initial

attempt to measure GRP75 and calreticulin levels in patient muscle biopsies, and are limited by the very small sample size, these preliminary investigations suggest that both GRP75 and calreticulin may potentially represent accessible protein biomarkers in skeletal muscle conserved between mouse models and patients.

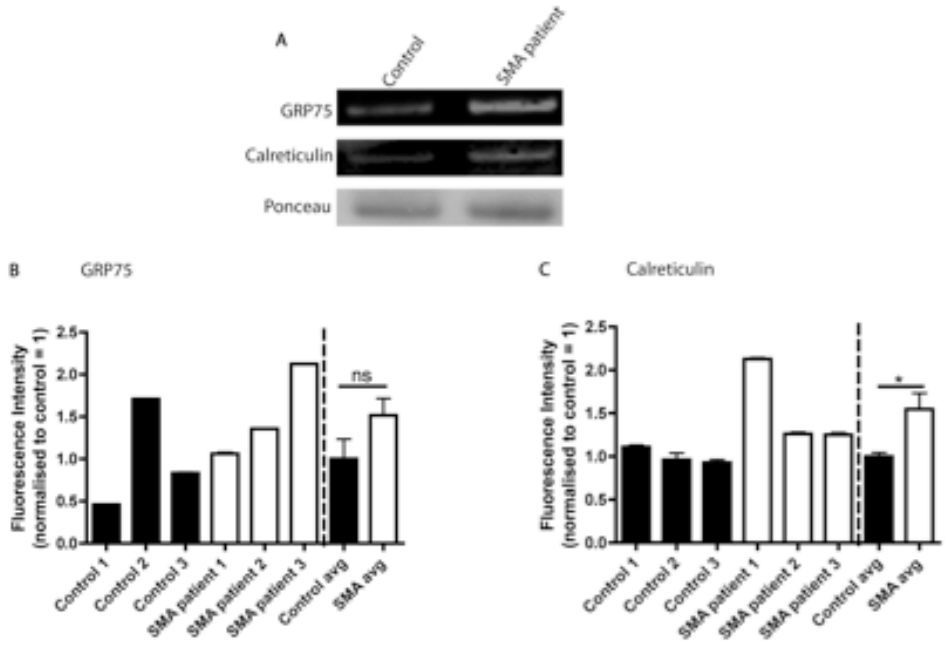

Figure 4.5 There is a trend towards increased expression levels of GRP75 and calreticulin in muscle biopsies from SMA patients. (A) Representative fluorescent western blots on *quadriceps femoris* muscle biopsy samples from an SMA patient (type II/III) and an age-matched non-SMA control showing levels of GRP75, calreticulin and Ponceau (loading control). **(B-C)** Bar charts showing expression levels of GRP75 and calreticulin in SMA patient muscle biopsies compared with controls. Data are shown for each individual patient (black and white bars to the left of the hashed line; error bars show variability between two independent measurements taken from that individual's biopsy) as well as a pooled mean for each group (right of the line; ± SEM; n=6 measurements for each group, two independent measurements from each patient biopsy). **(B)** GRP75 levels showed a trend towards increased expression in SMA patients, but this difference did not reach statistical significance ($P>0.05$; unpaired, two-tailed t-test). **(C)** Calreticulin levels were significantly increased in SMA patient muscle ($*P<0.05$; unpaired, two-tailed *t*-test).

4.2.5 Altered levels of GRP75 and calreticulin can be detected in skin biopsies from SMA mice

My analyses of GRP75 and calreticulin levels in skeletal muscle from SMA mouse models (supported by preliminary investigations of SMA patient tissue), suggested that these two proteins may potentially represent robust protein biomarkers for SMA. However, obtaining muscle biopsies from patients is an invasive procedure that is not ideal for repeated analyses of protein levels during a clinical trial, especially in small children. As a result, the availability of biomarker proteins in more peripherally accessible tissue (such as skin and/or blood) would make it much easier to obtain quick, repeated tissue samples for monitoring purposes.

Therefore, the next question to ask was whether GRP75 and calreticulin could be reliably identified and measured in skin and blood. Analysis of expression datasets (www.biogps.org) confirmed that both GRP75 and calreticulin are known to be expressed in skin and whole blood extracts. To establish whether these proteins were detectable in skin and blood samples from a mouse model, western blots were performed for both of these proteins on samples taken from Taiwanese SMA mice and littermate controls at P9. Only calreticulin could be detected in whole blood and showed a significant increase in expression levels in SMA mice (figure 4.6; N=3 mice per genotype; **P<0.01, unpaired, two-tailed *t*-test).

However, both proteins were expressed in skin samples, with their levels being significantly increased in SMA mice compared to controls (figure 4.7). Thus, both GRP75 and calreticulin were readily identifiable in skin biopsies, with the alterations

in their levels in skin closely matching alterations previously observed in skeletal muscle (figure 4.7B/C; N=3 mice per genotype; **P<0.01, ***P<0.001, unpaired, two-tailed *t*-test). Since only calreticulin could be detected in whole blood samples I decided to exclude blood samples for further examination and focused on the skin samples.

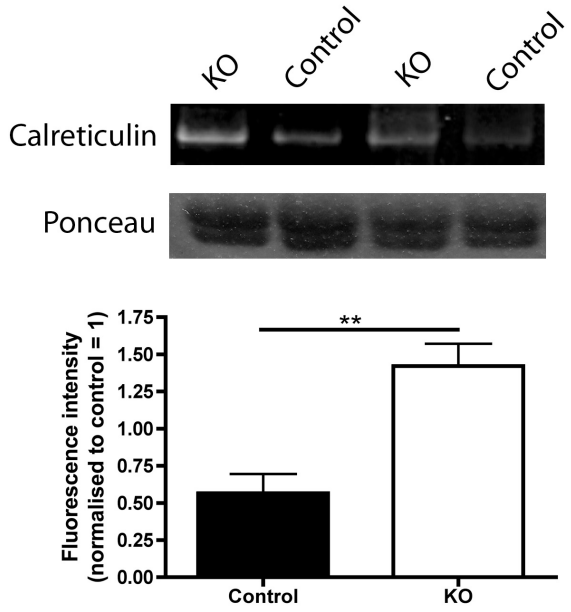

Figure 4.6 Validation of calreticulin levels in blood samples. Representative fluorescent western blots on blood samples from Taiwanese SMA mice (KO) and controls at P9 showing levels of calreticulin and Ponceau (N=3 mice per genotype). The bar chart (mean ± SEM) shows a significant increase in the levels of calreticulin in Taiwanese SMA mice (**P<0.01; unpaired, two-tailed *t*-test).

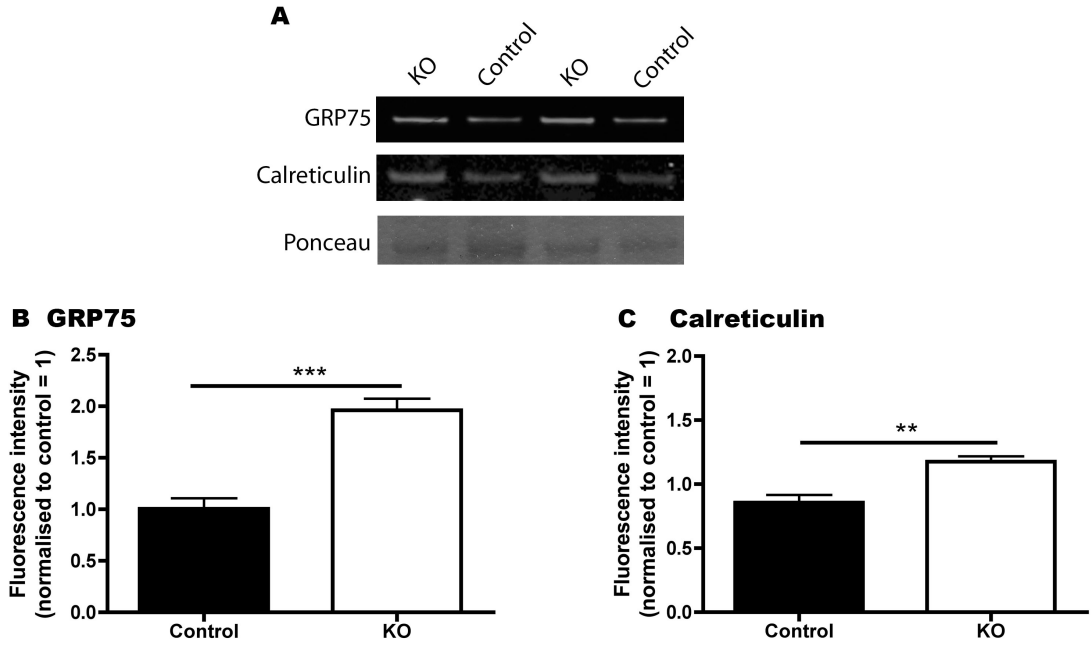

Figure 4.7 Validation of GRP75 and calreticulin in skin samples from Taiwanese SMA mice and controls. **(A)** Representative fluorescent western blots on skin tissue from Taiwanese SMA mice (KO) and littermate controls at P9 (mid/late-symptomatic) showing levels of GRP75, calreticulin and Ponceau (loading control). **(B/C)** Bar charts (mean ± SEM) showing expression levels of GRP75 and calreticulin in Taiwanese SMA mice (KO) and controls at P9 (N=3 mice per genotype). **(B)** GRP75 levels were significantly increased in Taiwanese SMA mice compared with controls (***P<0.001; unpaired, two-tailed *t*-test). **(C)** Calreticulin levels were significantly increased in Taiwanese SMA mice compared with controls (**P<0.01; unpaired, two-tailed *t*-test).

4.2.6 Levels of GRP75 and calreticulin in skin from Taiwanese SMA mice change over time

I wanted to establish whether GRP75 and calreticulin levels in skin matched the temporal profile that was originally identified in the muscle proteomics experiments. Therefore, I collected skin samples from Taiwanese SMA mice and littermate controls at four different time-points: P1 and P5 (pre-symptomatic), P7 (early-symptomatic), and P9 (mid/late-symptomatic). Temporal changes in the levels of GRP75 and calreticulin showed similar trends in SMA mouse skin, with no differences observed at pre/early-symptomatic time-points, but robust increases evident after onset of symptoms at postnatal day six (figure 4.8A/B). Thus, the temporal expression of GRP75 and calreticulin revealed a very similar profile in skin to that previously observed in skeletal muscle. Once again, the robust increases in expression correlated with disease progression, confirming that GRP75 and calreticulin may potentially represent peripherally accessible protein biomarkers capable of reporting on disease status in SMA.

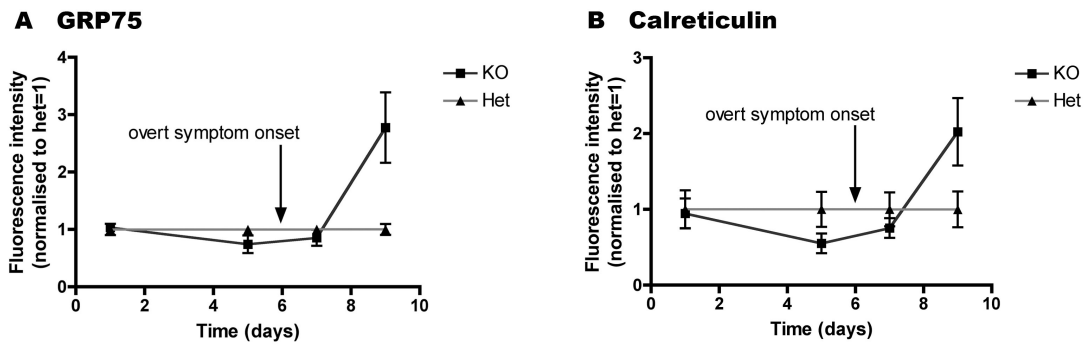

Figure 4.8 Increased levels of calreticulin and GRP75 in skin samples correlate with disease progression in SMA mice. (A/B) Time course of GRP75 and calreticulin expression in skin biopsies from Taiwanese SMA mice (KO) compared to controls (Het) (N=3 mice per genotype/time point). Tissue was analysed in mice at P1, P5 (both pre/early-symptomatic), P7 (early-symptomatic) and P9 (mid/late-symptomatic). **(A)** There was no increase in GRP75 levels in Taiwanese SMA mice until after overt disease onset (at P6). **(B)** Similarly, there was no increase in calreticulin levels in Taiwanese SMA mice until after overt disease onset.

4.2.7 GRP75 and calreticulin respond to treatment with the HDAC inhibitor, Trichostatin A

Finally, I investigated whether GRP75 and calreticulin would respond to treatment with the HDAC inhibitor, Trichostatin A (TSA) which has been shown to increase SMN levels and ameliorate disease severity in mice (Avila *et al.* 2007). Taiwanese mice were injected with Trichostatin A (TSA; 10 mg/kg) or DMSO alone from the day of birth (P1) until postnatal day eight (P8) once daily. Levels of GRP75 and calreticulin were measured in both skin and muscle tissue using western blot techniques. The SMA mice treated with TSA showed expression levels of GRP75 similar to levels in muscle tissue from control mice (figure 4.9A/B; N=6 Control mice, n=12 independent measurements; N=6 KO, n=12 independent measurements; N=5 KO + TSA, n=10 independent measurements, *P<0.05, **P<0.01; one-way ANOVA with Tukey's multiple comparison test). Calreticulin expression did not

respond to treatment with TSA (figure 4.9A/C). In skin tissue both GRP75 and calreticulin responded to the TSA treatment and showed expression levels similar to levels observed in the control mice (figure 4.10; N=6 Control mice, n=12 independent measurements; N=6 KO, n=12 independent measurements; N=5 KO + TSA, n=10 independent measurements, *P<0.05, **P<0.01, ***P<0.001; ANOVA with Tukey's post hoc test). These results suggest that expression levels of GRP75 and calreticulin reflect on the progression of disease severity and therefore provide further evidence that GRP75 and calreticulin (at least in skin samples) could be potential biomarkers for treatment in SMA.

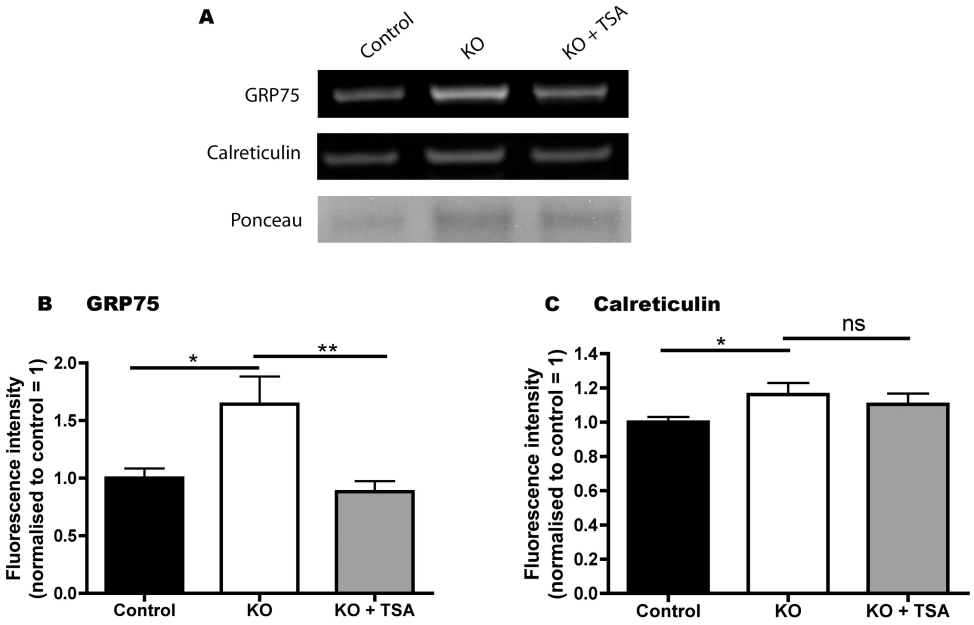

Figure 4.9 GRP75 respond to treatment with the HDAC inhibitor, Trichostatin A (TSA) in muscle samples from Taiwanese SMA mice. (A) Representative fluorescent western blots on muscle tissue from SMA mice (KO), SMA mice treated with TSA (KO +TSA) and littermate controls at P9 showing levels of GRP75, calreticulin and Ponceau (loading control). **(B)** Bar charts (mean ± SEM) showing expression levels for GRP75. Confirming increased levels in KO mice compared to control (N=6 Control mice, n=12 independent measurements; N=6 KO, n=12 independent measurements; N=5 KO + TSA, n=10 independent measurements, *P<0.05; one-way ANOVA with Tukey's multiple comparison test). In addition KO mice treated with TSA (KO + TSA) showed a response to treatment and levels were similar to control mice (**P<0.01). **(C)** Bar charts (mean ± SEM) showing expression levels for calreticulin. Confirming increased levels in KO mice compared to control (*P<0.05; one-way ANOVA with Tukey's multiple comparison test). However, calreticulin did not respond to treatment with TSA (P>0.05).

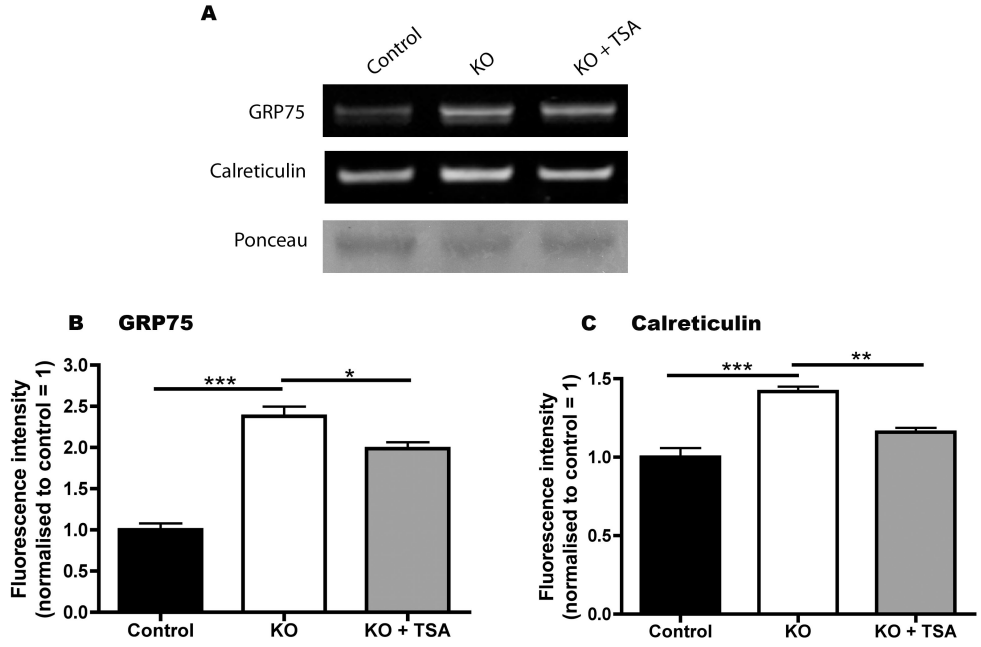

Figure 4.10 GRP75 and calreticulin respond to treatment with the HDAC inhibitor, Trichostatin A (TSA) in skin samples from Taiwanese SMA mice. (A) Representative fluorescent western blots on skin tissue from SMA mice (KO), SMA mice treated with TSA (KO +TSA) and littermate controls at P9 showing levels of GRP75, calreticulin and Ponceau (loading control). **(B)** Bar charts (mean ± SEM) showing expression levels for GRP75. Confirming increased levels in KO mice compared to control (N=6 Control mice, n=12 independent measurements; N=6 KO, n=12 independent measurements; N=5 KO + TSA, n=10 independent measurements, ***P<0.001; one-way ANOVA with Tukey's multiple comparison test). In addition KO mice treated with TSA (KO + TSA) showed a response to treatment and levels were similar to control mice (*P<0.05). **(C)** Bar charts (mean ± SEM) showing expression levels for calreticulin. Confirming increased levels in KO mice compared to control (***P<0.001; one-way ANOVA with Tukey's multiple comparison test). KO mice treated with TSA (KO + TSA) showed a response to treatment and levels were similar to control mice (**<P0.01).

4.3 Discussion

4.3.1 Overview of results

In this chapter, label-free proteomic technology was used to identify two proteins with the potential to act as biomarkers for SMA. The combination of proteomics technology with an established mouse model of SMA (where it is possible to accurately identify and isolate tissue from animals at different stages of disease) revealed that increased levels of GRP75 and calreticulin in skeletal muscle correlated with disease progression. Importantly, these potential protein biomarkers were also accessible in skin samples from SMA mice, suggesting that they can be monitored from easily harvested tissue in clinical trials. A preliminary study on patient muscle biopsies suggested that GRP75 and calreticulin were detectable and measurable in human tissue.

4.3.2 Proteomics technology could be a powerful tool for biomarker discovery

The use of label-free proteomics in this study provides further evidence that proteomics technologies represent a powerful tool for biomarker discovery (Guest *et al.* 2013). Indeed, proteomics technology has previously been used to screen for potential biomarkers in human SMA patients (Finkel *et al.* 2012; Kobayashi *et al.* 2013). Previous studies combining proteomics with animal models of SMA have mainly utilized the technology to uncover molecular pathways disrupted downstream of SMN (Fuller *et al.* 2010; Wishart *et al.* 2010; Mutsaers *et al.* 2011; Wu *et al.* 2011), but the current study demonstrates that similar approaches can be used to identify potential protein biomarkers, potentially suitable for future use in the human clinical context. In addition, the ability to identify potential protein biomarkers

conserved between different mouse models of SMA and SMA patients suggests that common biomarkers can be utilized in both pre-clinical testing of new treatments in animal models as well as in human clinical trials.

4.3.3 Advantages of SMA mouse models in biomarker identification

Recently, the first clinical trials have published data on biomarker identification using samples from SMA patients and controls. Patients were asked for one visit to the clinic and blood and urine samples were collected for proteomics, metabolomics and transcriptomics (Crawford *et al.* 2012; Finkel *et al.* 2012; Mano *et al.* 2012; Kobayashi *et al.* 2013). The studies revealed a list of protein changes in plasma, however these changes are likely to be downstream from the original disease perturbation in SMA, since blood shows normal levels of SMN protein (Finkel *et al.* 2012).

One of the key features of a useful biomarker is that it can be tracked over the time course of disease. Using a mouse model of SMA gives the opportunity to easily collect samples at different time points and monitor the changes in expression levels over this time. In this chapter, muscle tissue was used for the initial proteomic screen. As this tissue is pathological in SMA it is more likely to show changes that are dependent on the loss of SMN, than for example blood. Taking muscle biopsies at different time points is difficult to achieve in a patient cohort. In addition all mice have an identical background and healthy littermates can be used as controls, which eliminates confounding factors. Since many factors can influence the expression levels of biomarkers (for example the time of day of the biopsy and differences in

diet), it is essential to minimize these confounding factors. After initial screening for biomarkers in a mouse model of SMA, these proteins need to be tested in patients to validate whether the expression levels are similar.

4.3.4 GRP75 and/or calreticulin as a potential biomarker for SMA

GRP75 is a member of the Hsp70 family of chaperones, with roles including the regulation of energy generation, stress responses, muscle activity, mitochondrial activity, and cellular viability (Bhattacharyya *et al.* 1995; Ornatsky *et al.* 1995; Takahashi *et al.* 1998). GRP75 has been previously been identified as a possible biomarker for cancer and cardiovascular diseases (Deocaris *et al.* 2009) as well as being a potential prognostic factor for neuroblastoma (Hsu *et al.* 2008). GRP75 (also known as HSPA9) has also been implicated in the pathogenesis of other neurodegenerative conditions, including Parkinson's disease (De Mena *et al.* 2009) and Alzheimer's disease (Osorio *et al.* 2007) suggesting that it may contribute directly to SMA pathogenesis. Nevertheless, it is important to note that biomarkers do not need to actively contribute to disease pathogenesis in order to be effective. What is critical is that the levels of a biomarker must alter in a temporally traceable and predictable manner as an accurate measure of the molecular and physiological processes of disease progression.

Calreticulin is a multifunctional protein that has previously been identified as a potential biomarker for other diseases. For example, serum levels of calreticulin have been shown to increase in patients with rheumatoid arthritis (Ni *et al.* 2013) and increased levels of calreticulin have been reported in breast cancer (Gromov *et al.*

2010; Song *et al.* 2012), gastric cancer (Chen *et al.* 2009), and lung cancer (Liu *et al.* 2012). Calreticulin has also been identified as a prognostic factor for neuroblastoma (Hsu *et al.* 2005). However, calreticulin has not previously been linked to SMA, and whether it is actively involved in disease pathogenesis or not remains unclear. Interestingly, calreticulin has been implicated in regulating motor neuron pathology in a related motor neuron disease (ALS; (Bernard-Marissal *et al.* 2012)), suggesting that further investigations into its possible contribution to the pathogenesis of SMA are warranted.

4.3.5 Preliminary observations in human biopsies

My preliminary investigation of GRP75 and calreticulin levels in human skeletal muscle suggests that these proteins may potentially represent viable biomarkers in SMA patients. However, this preliminary investigation represent nothing more than an initial demonstration of the ability to detect and measure these proteins in human tissue and was hampered by a lack of detailed information from the Biobank regarding the actual stage of disease progression each patient was at when the muscle biopsy was harvested as well as the very small sample size. As a result, further, large-scale studies on patient cohorts will now be required to validate GRP75 and calreticulin as robust protein biomarkers for SMA in humans.

4.3.5 Future investigations

The demonstration in mouse models that increased levels of these proteins correlated with increasing disease severity suggests that a study in patients is now warranted. Moreover, the finding that these proteins can be tracked in skin samples suggests that

the use of skin biopsies might be of more practical use for these studies, reducing the need for repeated invasive muscle biopsies. In light of clinical trial design the results showing that GRP75 and likely also calreticulin respond to treatment with TSA in a mouse model of SMA are very interesting since it suggests that GRP75 and calreticulin could be capable of reporting on responsiveness to treatment in individuals. Further work is now required to validate these potential protein biomarkers in cohorts of SMA patients.

Chapter 5

Disruption of ubiquitin homeostasis and β-catenin signalling in SMA

5.1 Introduction

Despite clear understanding of the genetic causes of SMA, the mechanisms linking low levels of SMN to disease pathogenesis remain unclear. SMN protein is known to play key roles in several core canonical cellular pathways, including snRNP biogenesis and pre-mRNA splicing (Burghes and Beattie 2009). However, attempts to link disruptions in RNA processing directly to SMA pathogenesis have proven controversial (Zhang *et al.* 2008; Baumer *et al.* 2009). The identification of SMN protein in neurite processes and neuronal growth cones *in vitro* (Fan and Simard 2002) might suggest that SMN fulfils additional roles downstream from, or outside of RNA processing pathways in the nucleus and cell body. In addition, mutations in genes encoding proteins that are not directly involved in RNA processing can cause similar disease phenotypes. Mutations in the *UBA1* gene have been identified to cause X-linked infantile spinal muscular atrophy (Ramser *et al.* 2008).

In many neurodegenerative diseases degeneration of the synapse and distal axonal compartments precede the death of the cell body (Raff *et al.* 2002; Wishart *et al.* 2006). Why these distal compartments are vulnerable is currently not known. In

spinal muscular atrophy, neuromuscular junctions (NMJs) are early pathological targets. Synaptic pathology at the NMJ is initiated before the onset of major clinical symptoms in a mouse model of SMA (*Smn*$^{-/-}$;*SMN2*) (Murray *et al.* 2008).

SMN protein is ubiquitously expressed and recent studies indicate that it is not only the neuromuscular system that is affected in SMA, also other parts of the nervous system tissues have been shown to be affected (for example low levels of SMN have been shown to affect the hippocampus (Wishart *et al.* 2010)) as well as organs, including heart (Shababi *et al.* 2010), vasculature (Somers *et al.* 2013), liver (Hua *et al.* 2011) and pancreas (Bowerman *et al.* 2012). This suggests that SMN deficiency causes perturbations across a wide range of cells and tissues in SMA, albeit with motor neurons being most vulnerable (Sleigh *et al.* 2011).

In this chapter, I began by investigating whether SMN protein was localized and/or altered in the synapse *in vivo* in the central nervous system of SMA mice compared to littermate controls. Secondly, after having confirmed SMN protein expression in the synapse and decreased levels in synapses of SMA mice, an iTRAQ proteomics screen was performed to investigate the effect of low levels of SMN on protein expression levels in the synapse. This led to the identification of other molecular pathways downstream of SMN that are targeted in SMA. By using different animal models (mouse and zebrafish) novel roles for SMN were revealed in regulating ubiquitin homeostasis and β-catenin (*CTNNB1*, will be referred to as β-catenin throughout this thesis) signalling, perturbations in which are likely to contribute to the pathogenesis of SMA.

5.2 Results

5.2.1 SMN protein is localized to axonal and synaptic compartments of neurons in vivo

Previous results from the lab showed that neuromuscular junctions are early pathological targets in SMA (Murray *et al.* 2008). Motor neuron degeneration was observed in SMA mice *($Smn^{-/-}$;SMN2)* at a pre-symptomatic time point (P2) where the mice did not show major clinical symptoms (no weight loss or tremor compared to littermate controls). Therefore the first purpose of experiments in this chapter was to determine whether SMN protein was present and functional in distal compartments of the neuron *in vivo*. In our lab, it was not possible to isolate neuromuscular junctions for biochemical studies, therefore synapses from the brain were isolated instead. I chose to isolate synapses from the hippocampus, as it has been shown that the hippocampus contains high levels of SMN in a healthy mouse brain. In SMA mice the levels are significantly reduced and this causes reduced levels of proliferation and neurogenesis as well as modified expression levels of proteins that regulate proliferation, migration and developmental processes (Wishart *et al.* 2010).

In order to investigate the presence and role of SMN protein at the synapse, I made synaptosomes, which are isolated nerve terminals containing the complete pre-synaptic terminal, including mitochondria and synaptic vesicles, along with the post-synaptic membrane and the post-synaptic density. In brief, the hippocampus from both sides of the mouse brain was homogenized in a sucrose solution using a

homogenizer to help pinching off the synapses from the rest of the cell. Several centrifugation steps were performed to obtain an enriched synaptic fraction and a non-synaptic fraction (containing nuclear proteins). To confirm that the synaptosomes were pure (no contamination of non-synaptic compartments) protein levels for histone H2B (nuclear protein) were checked and were only observed in the non-synaptic fraction. Synaptophysin was used as a marker of synaptic vesicles, and was confirmed in the synaptic fractions (figure 5.1).

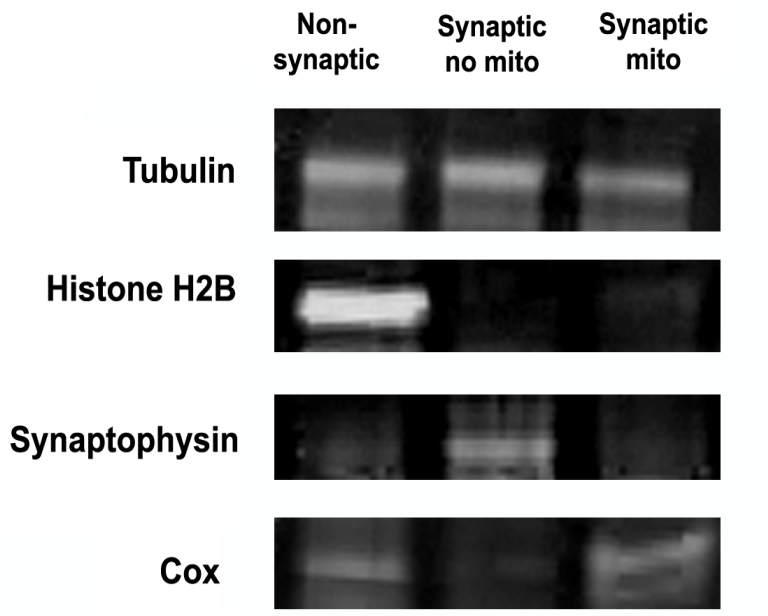

Figure 5.1 Representative fluorescent western blots showing the purity of synaptosome preparations from a wild-type mouse. The purity of the synaptosomes was demonstrated by the presence of a nuclear protein (Histone H2B) only in the non-synaptic fraction, with complete absence from the two synaptic fractions (synaptosomes without mitochondria and synaptic mitochondria). Synaptophysin was used as a marker of synaptic vesicles and COX IV was used as a marker of mitochondria. Tubulin is shown as a loading control.

Western blot experiments were performed on the synaptic fraction and confirmed that SMN protein was present in hippocampal synapses at postnatal day five (P5), with levels reduced in SMA mice (*Smn*$^{-/-}$*;SMN2,* N=3 mice) compared to littermate wild-type (*Smn*$^{+/+}$*;SMN2,* N=3 mice) and heterozygous (*Smn*$^{+/-}$*;SMN2,* N=3 mice) controls (figure 5.2). Note that SMN protein was hardly detectable in synapses isolated from SMA mice and was reduced by approximately 50 % in synapses from heterozygous littermate controls as compared to wild-type controls.

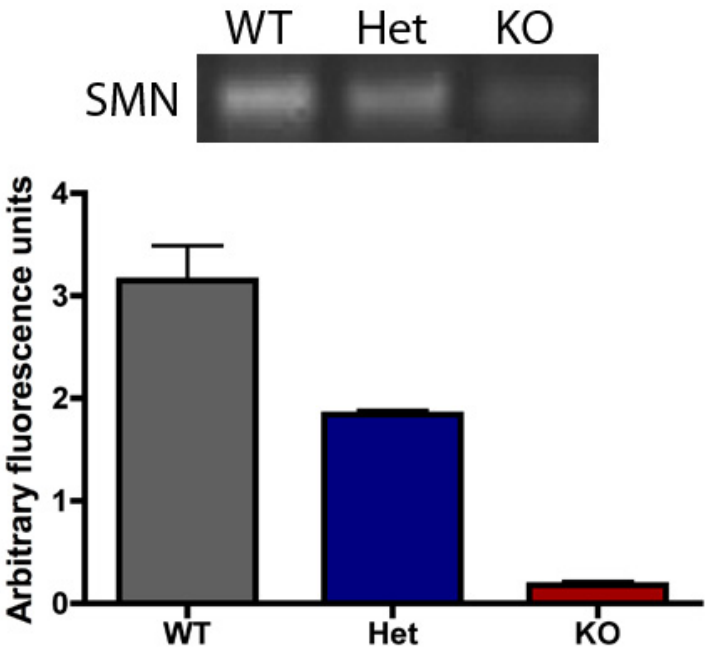

Figure 5.2 Relative expression levels of SMN protein in hippocampal synaptosomes. Synaptosomes were made from wild-type mice (WT; *Smn*$^{+/+}$*;SMN2*), heterozygous control mice (Het; *Smn*$^{+/-}$*;SMN2*) and SMA mice (KO; *Smn*$^{-/-}$*;SMN2*) at post-natal day five, quantified using fluorescent western blot (N=3 mice per genotype). Note that SMN protein was still present, albeit at very low levels, in homozygous SMA mouse synapses, as a result of expression from the human *SMN2* transgene.

Previous work has shown that mitochondria are dysfunctional in an SMA cell line (Acsadi *et al.* 2009). Therefore an extra centrifugation step was introduced to specifically isolate mitochondria from the synapses to investigate whether SMN protein was present there. Surprisingly, SMN protein was also present in fractions of synaptic mitochondria (figure 5.3; N=3 WT mice).

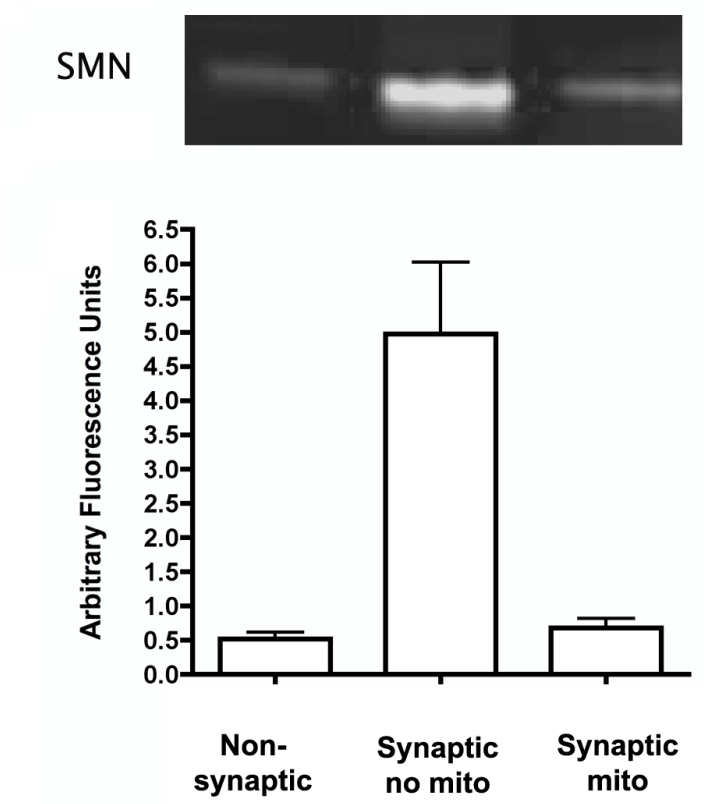

Figure 5.3 Quantification of SMN protein in subcellular fractions. Subcellular fractions were made from whole brain synaptosomes from wild-type mice (N=3 mice per fraction). SMN protein is present in both synaptosol as well as in synaptic mitochondria.

Next I investigated whether a binding partner and part of the SMN complex, Gemin5, was present in synapses from the hippocampus as well as cerebellum. I used a Gemin5 (GEM5C) antibody produced by Glenn Morris' Lab in Oswestry. In addition I compared a commercially available anti SMN antibody (BD SMN) and an anti SMN antibody produced by Glenn Morris' Lab (ManSMN). As shown in figure 5.4, both primary antibodies showed SMN expression levels in synapses from both the hippocampus and cerebellum of wild-type mice (N=2 mice) when quantified using fluorescent western blots. Although the antibodies showed differences in the reactivity, both recognized SMN protein in synapses from hippocampus and cerebellum. Gemin5 protein was also present in synapses of hippocampus and cerebellum (figure 5.4). After the observation that both SMN and Gemin5 were present at the synapse a co-immunoprecipitation was performed to investigate whether SMN and Gemin5 physically interact in the synapse. Whole synaptosome extracts were sent to Glenn Morris' Lab, where the co-immunoprecipitation was carried out. The synaptosome extracts were incubated with SMN, gemin5 or neurofilament (as a non-specific control) beads and bound proteins were eluted. The blot was developed with anti-SMN antibodies. Only the lanes with SMN or gemin5 beads show a band for SMN (appendix 1). This result shows that gemin5 retained the ability to physically interact with SMN in the synaptic proteome.

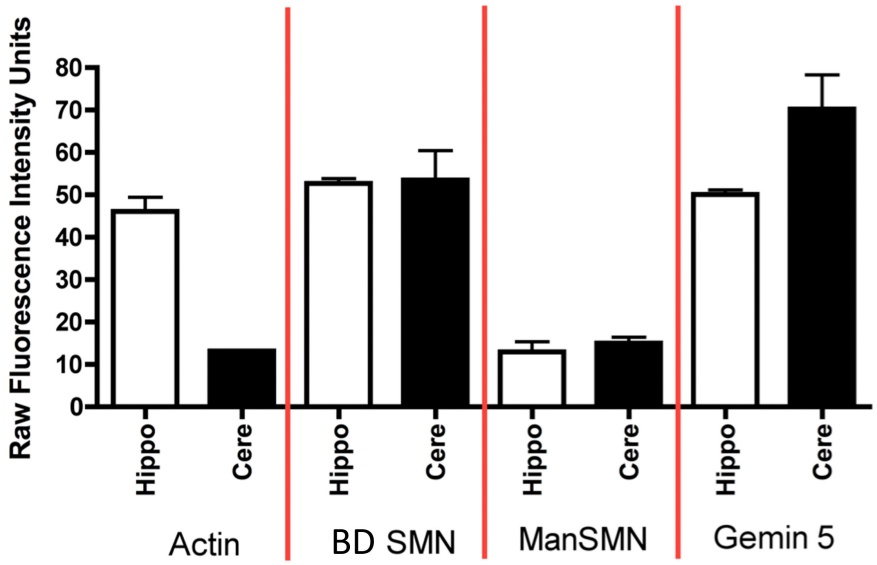

Figure 5.4 Gemin5, a binding partner of SMN is present in hippocampal and cerebellar synaptosomes. Bar charts (mean ± SEM) are showing protein levels of Actin, SMN and Gemin5 in hippocampal and cerebellar synaptosomes from WT mice (N=2). Note that two different SMN antibodies have been used, which show differences in the reactivity in the tissues.

5.2.2 Assessing the functional consequences of SMN expression in synaptic mitochondria

Given that SMN was found in synaptic mitochondria, and that mitochondrial stress has been implicated as a pathological mechanism in cell models of SMA (Acsadi *et al.* 2009), I tested whether mitochondria in synapses from SMA mice were more vulnerable to stress than those from control mice by investigating cytochrome C release from the mitochondria. Synaptosomes from whole brains of severe SMA mice (N=4 mice) and control littermate heterozygous mice (*Smn*$^{+/-}$*;SMN2*, N=8 mice) were prepared. I used whole brain synaptosomes in this case, to be able to obtain enough protein for analysis. The synaptosomes were resuspended in Krebs buffer supplemented with $Ca^{2+}Cl$ and left on a rocking platform in a 37 °C incubator to induce stress. At different time points (0, 0.5, 1, 2 and 3 hours) a sample was taken and RIPA buffer was used to break down the membranes of the synaptosomes and by spinning at 20 000 g all membrane bound proteins within the synaptosomes were formed into a pellet. The remaining supernatant contained all remaining soluble proteins from the synaptic cytosol (synaptosol). Synaptosolic fractionations were taken to measure cytochrome C levels using fluorescent quantitative western blotting.

Cytochrome C is a pro-apoptotic protein released by mitochondria into the cytosol in response to stress (Liu *et al.* 1996). The data shown in figure 5.5 revealed that there was no difference in the release of cytochrome C following heat-induced stress between SMA mice and control mice at any time point ($P>0.05$; Mann Whitney test for each time point). Cytochrome C release was expressed as a percentage of maximum release. Maximum release observed in this assay, was between three and

four hours. After this time point the levels of cytochrome C were variable and dropped, suggesting that the synaptosomes were probably dying. This assay suggests that mitochondria in synapses from SMA mice are not more vulnerable than mitochondria in control synapses.

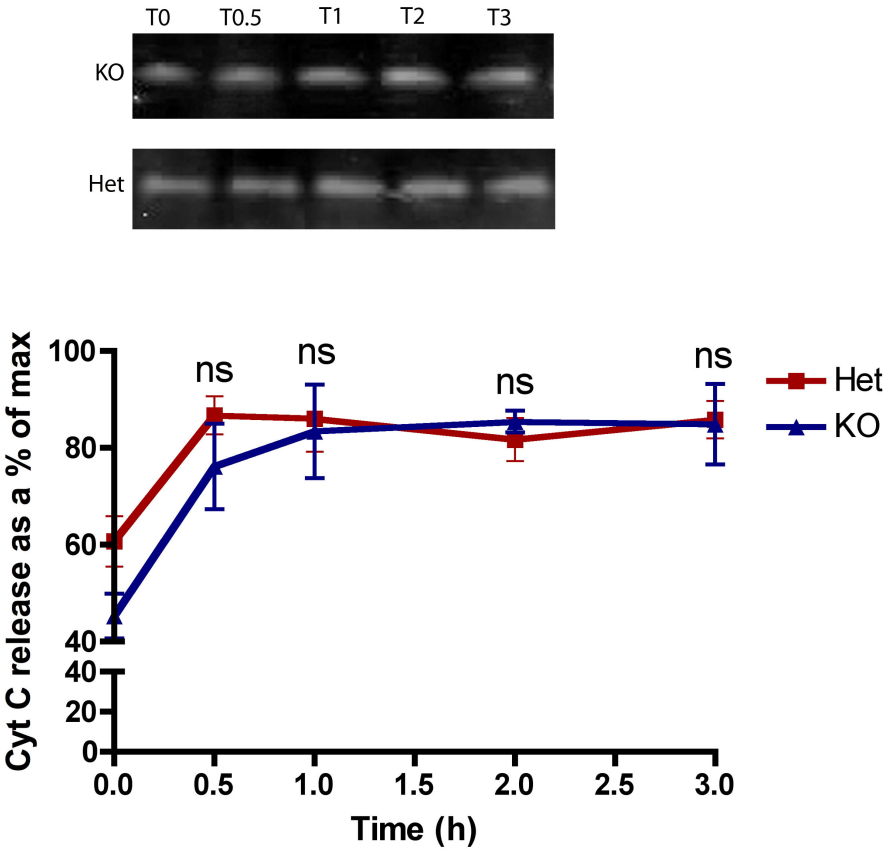

Figure 5.5 Ex vivo assay of cytochrome C release from synaptic mitochondria in whole brain synaptosomes. Whole brain synaptosomes from severe SMA mice (N=4 mice) and control heterozygous mice (*SMN*$^{+/-}$*;SMN2*, N=8) measured by quantitative fluorescent western blotting. The graph shows cytochrome C release as a percentage of the maximum release (±SEM) for both SMA and heterozygous control mice. There was no difference in synaptic mitochondrial vulnerability (P>0.05; Mann Whitney test for each time point).

5.2.3 SMN protein is required for normal accumulation of β-actin mRNA at the synapse

It has been proposed that SMN protein has a role in the transportation of β-actin mRNA to growth cones *in vitro* (Rossoll *et al.* 2003). Therefore I investigated whether SMN is involved in transportation of β-actin mRNA to the synapse in the synaptosomes *in vivo*. Brain synaptosomes from SMA and heterozygous control mice were made and RNA was extracted. The levels of mRNA in SMA mice and heterozygous control mice were compared to mRNA levels in wild-type synaptosomes. qRT-PCR was performed to test whether there was a difference in the amount of β-actin mRNA levels at the synapse in SMA mice and control littermates. I used two primer sets, which were designed against different parts of the β-actin RNA sequence (for sequences see material and methods chapter). To calculate the fold change I applied the equation $2^{-\Delta(\Delta CT)}$, where CT (cycle threshold) is defined as the number of cycles required for the fluorescent signal to cross the threshold (i.e. to exceed background level) (Livak and Schmittgen 2001). In this PCR I did not use a housekeeping gene, because most housekeeping genes (for example GAPDH) are changed in SMA. Instead, I decided to use the CT value of WT β-actin RNA levels as a control. ΔCT is calculated as CT_{target}-$CT_{control.}$ Therefore, in this study ΔCT_{SMA}= $CT_{\beta\text{-actinSMA}}$-$CT_{\beta\text{-actinWT}}$ and ΔCT_{Het} = $CT_{\beta\text{-actinHET}}$-$CT_{\beta\text{-actinWT}}$. The mean of CT_{WT} was calculated and subtracted to all ΔCT_{SMA} and ΔCT_{Het} values. The values were then named Δ(ΔCT). Then the fold change was calculated by applying the equation $2^{-\Delta(\Delta CT)}$. Figure 5.6 is showing that there was a clear trend towards a reduced level of β-actin mRNA at the synapse in SMA mice compared to the levels in heterozygous

control mice. In addition levels of β-actin mRNA were similar between wild-type and heterozygous mice.

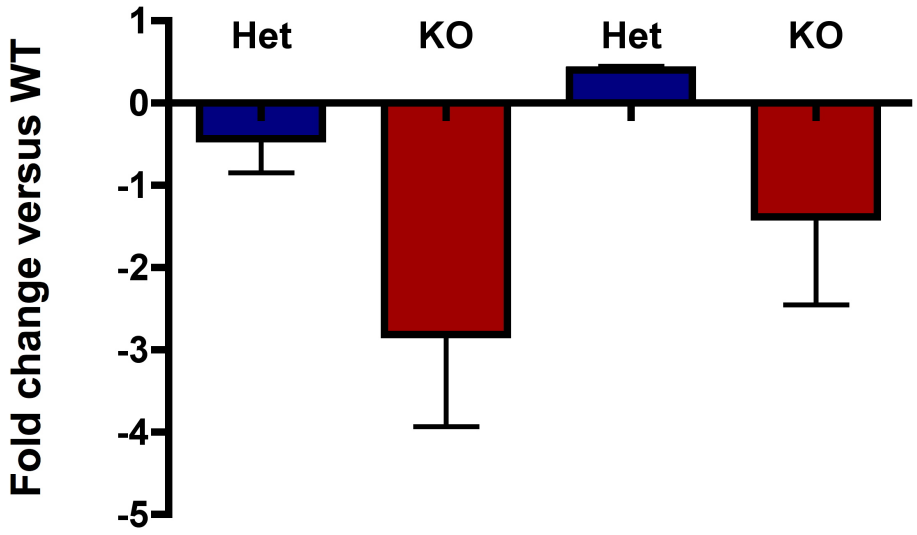

Figure 5.6 A reduction in β-actin mRNA levels in hippocampal synaptosomes. qRT-PCR using two different β-actin primer sets on hippocampal synaptosomes from SMA (N=3), heterozygous (N=2) and wild-type mice (N=1). This revealed a reduction in β-actin mRNA levels at the synapse in SMA mice. Bar chart shows fold change of β-actin mRNA in SMA mice and heterozygous mice as compared to wild-type mice (mean ± SEM).

5.2.4 iTRAQ proteomic screen reveals disruption in synaptic proteome of SMA mice

To gain more insights into the downstream effects of SMN depletion in synaptic compartments of the neurons, an unbiased iTRAQ proteomic screen was performed to quantify alterations in the molecular composition. P1 synaptosomes were prepared from hippocampi from severe SMA and wild-type littermate controls (N=9 mice per genotype) for iTRAQ analysis. This age was chosen as the hippocampus develops normally and morphological changes appear at late-symptomatic time (P5). Therefore changes in protein levels would be due to reduced levels of SMN and not

as a consequence of disease progression. Samples were run in duplicate using the 4-plex system (114 & 116 SMA mice and 115 & 117 control mice). After stringent filtering this screen identified 52 out of 150 (35%) unique proteins that had expression levels modified by more than 20 % in synapses from SMA mice compare to littermate controls (table 5.1 and 5.2). This indicates a robust disruption of the synaptic proteome as a consequence of low levels of SMN protein.

To identify specific molecular pathways and networks disrupted in the synapses of the hippocampus of SMA mice, an *in silico* pathway analysis was undertaken of the proteomics data set using Ingenuity Pathway Analysis software. For functional clustering analyses, the 52 proteins identified with the iTRAQ screen were uploaded in the software, and this revealed significant modifications in a range of pathways. The ubiquitination pathway, and UBA1 protein, (table 5.1 and 5.2; the red and purple marked proteins, table 5.3) were of special interest in the context of SMA because mutations in the gene coding for human UBA1 are sufficient to cause a genetically-distinct form of the disease, known as X-linked infantile spinal muscular atrophy (Ramser *et al.* 2008). Moreover, ubiquitination pathways are known to regulate axonal and synaptic stability (DiAntonio *et al.* 2001; Korhonen and Lindholm 2004) as well as the stability and degradation of SMN protein itself (Chang *et al.* 2004; Burnett *et al.* 2009; Hsu *et al.* 2010). Another interesting pathway that was identified using this software was the PI3K/AKT signalling pathway. AKT phosphorylates β-catenin, which increases its transcriptional activity and stimulates cell motility (Fang *et al.* 2007).

Table 5.1 Proteins with increased expression > 20 % in P1 synapses from SMA mice versus littermate controls

Protein ID	Protein name	Score	Mass	Peptide Matches	emPAI	Ratio SMA/WT
IPI00125899.1	**Ctnnb1 Catenin beta-1**	**208**	**89934**	**5**	**0.03**	**4.21**
IPI00341282.2	Atp5f1 ATP synthase subunit b, mitochondrial	70	32503	3	0.1	3.42
IPI00116279.3	Cct5 T-complex protein 1 subunit epsilon	65	66527	2	0.1	3.35
IPI00230427.5	Mif Macrophage migration inhibitory factor	77	13244	2	0.25	2.33
IPI00120457.1	Fdps Farnesyl pyrophosphate synthase	65	44789	2	0.07	2.21
IPI00117264.1	Park7 Protein DJ-1	91	22542	2	0.14	2.19
IPI00130280.1	Atp5a1 ATP synthase subunit alpha, mitochondrial	426	64441	9	0.21	2.09
IPI00132728.2	Cyc1 Isoform 1 of Cytochrome c1, heme protein, mitochondrial	144	37695	3	0.08	1.98
IPI00123494.3	**Psmd2 26S proteasome non-ATPase regulatory subunit 2**	**168**	**108430**	**3**	**0.03**	**1.93**
IPI00407692.3	Atp6v1a Isoform 1 of V-type proton ATPase catalytic subunit A	122	73812	3	0.04	1.77
IPI00323179.3	Gdi1 Rab GDP dissociation inhibitor alpha	396	55382	8	0.18	1.73
IPI00313962.3	**Uchl1 Ubiquitin carboxyl-terminal hydrolase isozyme L1**	**296**	**27614**	**11**	**0.24**	**1.67**
IPI00312527.4	Crmp1 Crmp1 protein	205	79818	7	0.12	1.65
IPI00555069.3	Pgk1 Phosphoglycerate kinase 1	112	50973	3	0.13	1.64
IPI00222430.5	Dbi acyl-CoA-binding protein isoform 1	122	17726	3	0.18	1.62
IPI00321190.1	Psap Sulfated glycoprotein 1	193	68883	5	0.09	1.60
IPI00221402.7	Aldoa Fructose-bisphosphate aldolase A	77	43678	2	0.07	1.59
IPI00117896.3	Mapre1 Microtubule-associated protein RP/EB family member 1	69	33627	2	0.09	1.59
IPI00407130.4	Pkm2 Isoform M2 of Pyruvate kinase isozymes M1/M2	158	63854	7	0.15	1.55
IPI00120030.1	Crym Mu-crystallin homolog	86	36123	2	0.09	1.54
IPI00127987.1	Arpc1a Actin-related protein 2/3 complex subunit 1A	76	45628	2	0.07	1.52
IPI00119113.3	Atp6v1b2 V-type proton ATPase subunit B, brain isoform	299	60171	6	0.05	1.47
IPI00462072.3	Eno1;Gm5506 Alpha-enolase	146	52497	5	0.26	1.46
IPI00118899.1	Actn4 Alpha-actinin-4	83	113581	3	0.06	1.46
IPI00230707.6	**Ywhag 14-3-3 protein gamma**	**925**	**31050**	**29**	**0.79**	**1.45**
IPI00129685.3	Tpt1 Translationally-controlled tumor protein	155	21725	4	0.15	1.42
IPI00133903.1	**Hspa9 Stress-70 protein, mitochondrial**	**82**	**81549**	**2**	**0.04**	**1.42**
IPI00113141.1	Cs Citrate synthase, mitochondrial	774	56023	20	0.18	1.42
IPI00281011.7	Marcksl1 MARCKS-related protein	176	22948	5	0.3	1.40
IPI00118821.2	Pafah1b2 Platelet-activating factor acetylhydrolase IB beta	136	27898	3	0.11	1.36
IPI00624192.3	Dpysl5 Dihydropyrimidinase-related protein 5	207	66659	8	0.15	1.34
IPI00119762.4	Dclk1 Doublecortin-like protein	150	65687	3	0.05	1.34
IPI00330804.4	**Hsp90aa1 Heat shock protein HSP 90-alpha**	**145**	**96806**	**4**	**0.07**	**1.32**
IPI00110684.1	Ppa1 Inorganic pyrophosphatase	91	37425	3	0.08	1.29
IPI00229080.7	**Hsp90ab1 Putative uncharacterized protein**	**134**	**94523**	**5**	**0.1**	**1.28**
IPI00110753.1	Tuba1a Tubulin alpha-1A chain	5994	53670	160	3.63	1.26
IPI00116283.1	Cct3 T-complex protein 1 subunit gamma	43	66349	2	0.1	1.25
IPI00117348.4	Tuba1b Tubulin alpha-1B chain	5770	53686	153	3.13	1.25
IPI00405986.3	Epb4.1l1 Erythrocyte protein band 4.1-like 1	81	127928	2	0.02	1.24
IPI00118986.1	Atp5o;LOC100047429 ATP synthase subunit O, mitochondrial	64	26576	2	0.12	1.22
IPI00330754.1	Bdh1 D-beta-hydroxybutyrate dehydrogenase, mitochondrial	51	42061	2	0.07	1.21

Table 5.2 Proteins with decreased expression > 20 % in P1 synapses from SMA mice versus littermate controls

Protein ID	Protein name	Score	Mass	Peptide Matches	emPAI	Ratio SMA/WT
IPI00123313.1	**Uba1 Ubiquitin-like modifier-activating enzyme 1**	**63**	**126857**	**2**	**0.02**	**0.43**
IPI00230194.5	Gng2 Guanine nucleotide-binding protein G(I)/G(S)/G(O) gamma-2	73	9112	2	0.37	0.54
IPI00121550.3	Atp1b1 Sodium/potassium-transporting ATPase subunit beta-1	66	40182	2	0.08	0.56
IPI00128973.1	Gap43 Neuromodulin	80	28200	2	0.24	0.65
IPI00120719.4	Cox5a Cytochrome c oxidase subunit 5A, mitochondrial	78	17472	3	0.4	0.67
IPI00554989.3	Ppia MCG121511, isoform CRA_b	336	20491	11	1.06	0.71
IPI00457898.3	Pgam1 Phosphoglycerate mutase 1	157	31666	5	0.1	0.75
IPI00128986.1	Tagln3 Transgelin-3	69	24645	2	0.13	0.76
IPI00307837.6	Eef1a1 Elongation factor 1-alpha 1	122	57341	5	0.11	0.79
IPI00115546.4	Gnao1 Isoform Alpha-2 of Guanine nucleotide-binding protein G(o) alpha	140	44847	4	0.23	0.80
IPI00308885.6	**Hspd1 Isoform 1 of 60 kDa heat shock protein, mitochondrial**	**750**	**69014**	**15**	**0.05**	**0.80**

Table 5.3 Clustering analysis of proteomic data revealing functional pathways modified in P1 SMA mouse synapses

Pathway	P Value	Individual Proteins
Oxidative Phosphorylation	1.61E-07	Atp5a1, Atp5f1, Atp6v1a, Cox5a, Cyc1, Ppa1
Protein Ubiquitination	8.59E-06	Hsp90aa1, Hsp90ab1, Hspa9, Hspd1, Psmd2, Uba1, Uchl1
Glycolysis/Gluconeugensis	1.14E-04	Aldoa, Pgam1, Pgk1, Pkm2
Purine Metabolism	1.15E-04	Atp1b1, Atp5a1, Atp5f1, Hsp90aa1, Hspd1, Pkm2
PI3K/AKT signaling	3.64E-04	Ctnnb1, Hsp90aa1, Hsp90ab1, Ywhag

5.2.5 UBA1 levels are also disrupted in the neuromuscular system

The proteomics screen was performed on tissue from the central nervous system. In order to establish whether ubiquitin-dependent pathways were also modified in tissues belonging to the neuromuscular system, UBA1 protein levels were examined in preparations of spinal cord and skeletal muscle from severe SMA mice at P5. UBA1 levels were reduced by 50 % in spinal cord (figure 5.7A) and > 60 % in *gastrocnemius* (figure 5.7B) from SMA mice compared to littermate controls (N=3 mice per genotype; ***P<0.001 and **P<0.01 unpaired, two-tailed *t*-test respectively). Beta V Tubulin was used as a loading control. This indicates a particular susceptibility of the neuromuscular system.

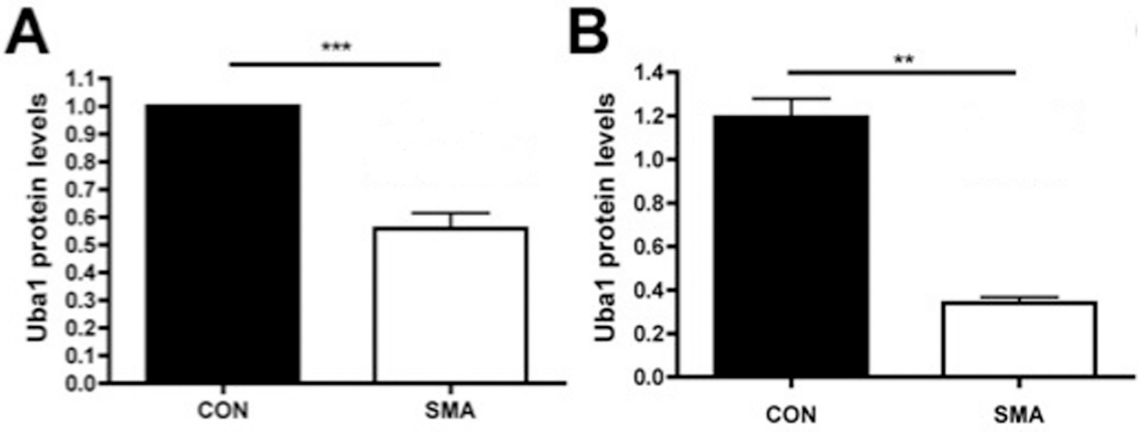

Figure 5.7 UBA1 levels are decreased in spinal cord and muscle tissue in SMA mice. Bar charts (mean ± SEM) showing significant reduction in levels of UBA1 in the spinal cord **(A)** and skeletal muscle **(B)** from severe SMA mice at P5, compared to littermate controls, quantified using fluorescent western blot (N=3 mice per genotype; **P<0.01 and ***P<0.001, unpaired two-tailed *t*-test).

5.2.6 Disruption of ubiquitin homeostasis directly correlates with SMN levels, and is reversible by treatment with Trichostatin A

Treatment with the histone deacetylase (HDAC) inhibitor trichostatin A (TSA) elevates SMN protein levels in the spinal cord and muscle, and ameliorates neuromuscular and central nervous system synaptic pathology in SMA mice (Avila *et al.* 2007; Ling *et al.* 2012). TSA treatment was therefore used to establish whether perturbations in UBA1 were directly correlated with SMN levels, and to test whether changes in UBA1 level was reversible by pharmacological intervention.

As a pilot experiment, SMA and littermate control pups were injected subcutaneously over the shoulders, into the loose skin over the neck with TSA (10 mg/kg) from the day of birth (P1) until P4. A second litter was injected with DMSO only. The mice were weighed daily. No difference was observed in the weight between TSA injected and DMSO only injected SMA mice (figure 5.8; N=9 Control mice, N= 1 SMA mice with DMSO, N= 3 SMA mice with TSA). This could be due to the fact that SMN levels were not increased in the TSA injected SMA mice (figure 5.9; N=9 Control mice, N= 1 SMA mice with DMSO, N= 3 SMA mice with TSA). Because subcutaneous injection did not increase the level of SMN protein, a second approach was undertaken.

SMA mice and littermate controls were treated with TSA intra-peritoneally (10 mg/kg daily) and compared with DMSO injected control mice. Again, mice were injected from the day of birth (P1) until P4 and were collected at P5. Previous trials with TSA were performed in the delta7 SMA mice (Avila *et al.* 2007; Mentis *et al.*

2011) because of their longer lifespan (14 days). Nevertheless, increased expression levels of SMN protein were observed in spinal cord of severe SMA mice treated with TSA compared to DMSO treated mice (figure 5.11A/B; N=5 Control mice, N=4 SMA mice with DMSO, N=3 SMA mice with TSA; *P<0.05, ***P<0.001, ANOVA with Tukey's post-hoc test). Also, levels of UBA1 were significantly increased in TSA-treated SMA mice, almost returning to levels found in littermate controls (figure 5.11A/C; N=6 Control mice, N=5 SMA mice with DMSO, N=4 SMA mice with TSA; **P<0.01, **P<0.01, ANOVA with Tukey's post-hoc test). SMA mice treated with DMSO showed a loss of weight at P5, this was not observed in the SMA mice treated with TSA (figure 5.10; N=6 Control mice, N=5 SMA mice with DMSO, N=4 SMA mice with TSA; P>0.05, ANOVA with Tukey's post-hoc test). This suggests that perturbations in UBA1 were both highly sensitive to SMN levels and amenable to pharmacological intervention.

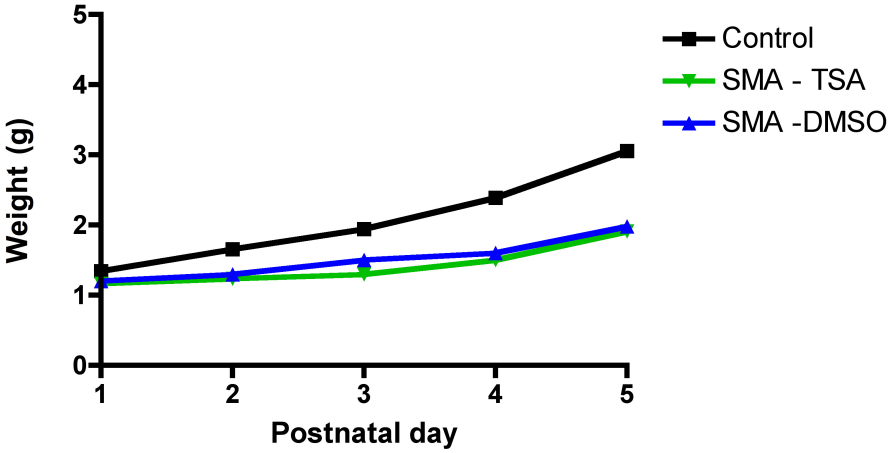

Figure 5.8 No weight gain in SMA mice after subcutaneous injection with TSA. Graph showing the weight curve of control mice (N=9), severe SMA mice treated with DMSO (N=1) and severe SMA mice treated with TSA subcutaneously (N=3). There is no improvement in weight after subcutaneous injection of TSA in SMA mice.

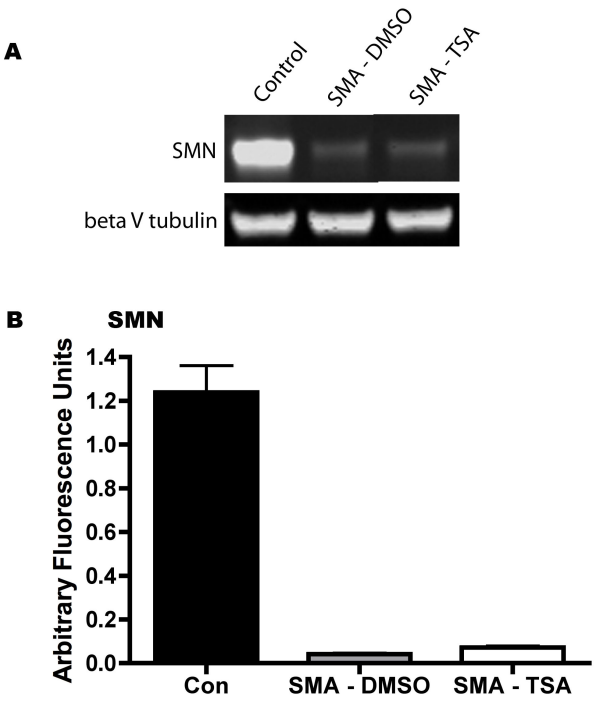

Figure 5.9 SMN levels are not increased after subcutaneous injections of TSA in severe SMA mice in spinal cord. (A) Representative fluorescent western blots showing levels of SMN in control mice, severe SMA mice treated with DMSO and severe SMA mice treated with TSA. Beta V tubulin was used as a loading control. **(B)** Bar charts (mean ± SEM) showing that SMN levels are dramatically decreased in SMA mice (N=1) as compared to littermate controls (N=9). Subcutaneous injection with TSA in SMA mice does not rescue the levels of SMN protein (N=3).

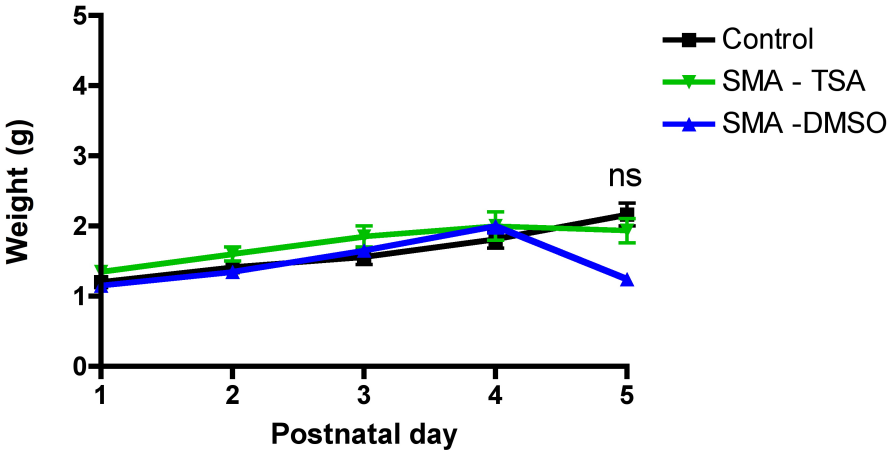

Figure 5.10 Modest increase in weight in SMA mice treated with TSA intra-peritoneally. Graph showing the weight curve of control mice (N=6), severe SMA mice treated with DMSO (N=5) and severe SMA mice treated with TSA (N=4) intra-peritoneally (P>0.05, ANOVA with Tukey's post-hoc test). Note that SMA mice treated with TSA show an increase in weight at P5 as compared to SMA treated with DMSO.

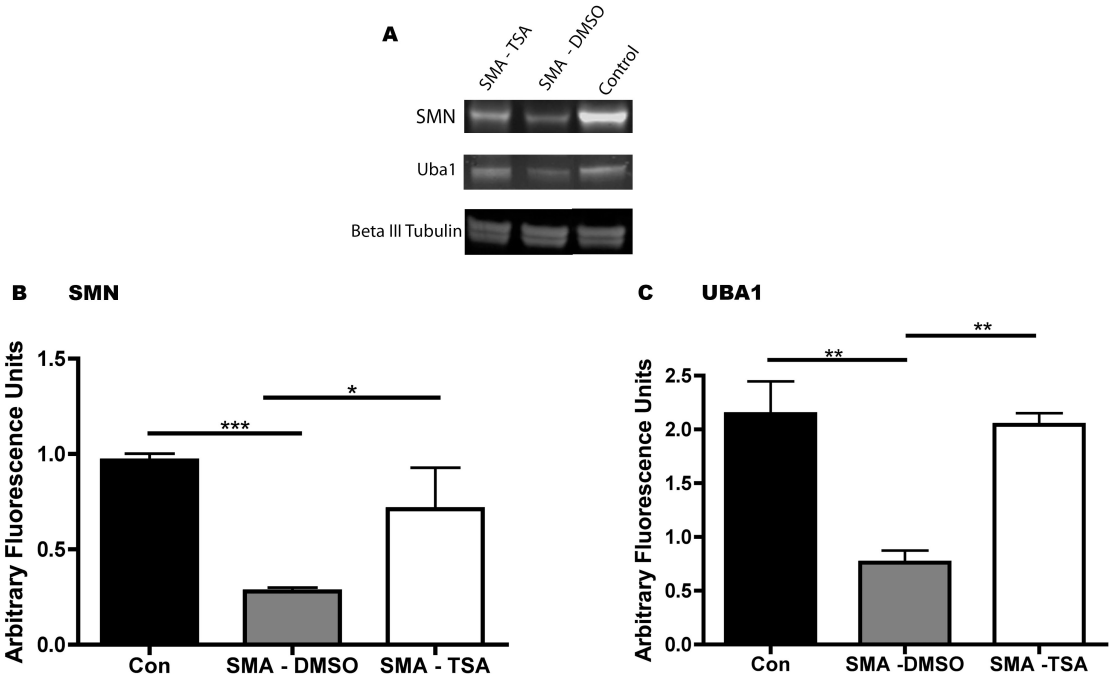

Figure 5.11 Intra-peritoneal injection of TSA in severe SMA mice rescues levels of SMN and UBA1 in spinal cord. (A) Representative fluorescent western blots showing levels of SMN and UBA1 in control mice, severe SMA mice treated with DMSO and severe SMA mice treated with TSA. **(B)** Bar charts (mean ± SEM) showing slightly increased levels of SMN in SMA mice after TSA injection (N=5 Control mice, N=4 SMA mice with DMSO, N=3 SMA mice with TSA; *P<0.05, ***P<0.001, ANOVA with Tukey's post-hoc test). **(C)** Bar charts (mean ± SEM) showing rescue of UBA1 levels in SMA mice after an intra-peritoneal injection with TSA (N=6 Control mice, N=5 SMA mice with DMSO, N=4 SMA mice with TSA; **P<0.01, **P<0.01, ANOVA with Tukey's post-hoc test). Note that levels are restored to almost the same levels as in control mice.

5.2.7 Deregulation of UBA1 protein levels leads to accumulation of β-catenin in vitro

UBA1 regulates the first stages of an enzymatic cascade in which ubiquitin molecules are ultimately conjugated to target proteins for proteasome degradation. Disruption of this cascade is often associated with a failure to degrade target proteins, resulting in their accumulation within the cell. Re-examination of the original proteomic dataset revealed one notable protein with such an accumulation: β-catenin levels were increased more than four fold in SMA mice compared to littermate controls (table 5.1).

B-catenin is a multifunctional protein; it is a central component of the cadherin cell adhesion complex (Aberle *et al.* 1994; Gumbiner 1997), regulating the control of cell adhesion and in addition it plays an essential role in various growth factor signal transduction pathways (Peifer 1995). One of these pathways is the PI3K/AKT signalling pathway (table 5.1 and 5.2; the blue and purple marked proteins, Table 5.3). PI3K/AKT is an intracellular pathway important in apoptosis. Phosphorylation of β-catenin by AKT results in relocation of β-catenin to the nucleus and increases its transcriptional activity (Fang *et al.* 2007).

Beta catenin is also a known target of the ubiquitin-proteasome system (Aberle *et al.* 1997). Phosphorylation of β-catenin by a multi-protein complex composed of tumor suppressor proteins adnomatous polyposis coli (APC), axin, and glycogen synthase kinase-3 (GSK3beta) is the trigger for its ubiquitination-dependent proteolysis (Peifer *et al.* 1994; Yost *et al.* 1996; Aberle *et al.* 1997; Orford *et al.* 1997).

To investigate whether accumulation of β-catenin levels in SMA occur as a result of low UBA1 levels, I treated cells with a cell-permeable UBA1 inhibitor called UBEI-41 (Balut *et al.* 2011) and measured the levels of β-catenin and beta III tubulin (used as a loading control). Primary rat hippocampal cultures and NSC-34 motor neuron-like cell line were treated with 50 μM of this inhibitor for two hours or with DMSO alone. Both the primary neurons as well as the NSC34 cells showed a significantly increased level of β-catenin when treated with the UBA1 inhibitor compared to cells treated with DMSO alone (figure 5.12; ***P<0.001, ANOVA with Tukey's post hoc test; N=12 coverslips DMSO, N=15 UBEI-41 for hippocampal neurons; N=19 DMSO, N=18 UBEI-41 for NSC-34 cells). Interestingly, a direct comparison of responses in the two cell lines revealed significantly higher levels of β-catenin in the NSC-34 cells, showing consistency with the enhanced vulnerability of motor neurons in SMA (**P<0.01, ANOVA with Tukey's post hoc test). These results suggest that UBA1 (or the whole ubiquitination pathway) is involved in maintaining normal levels of β-catenin in the cytoplasm *in vitro*.

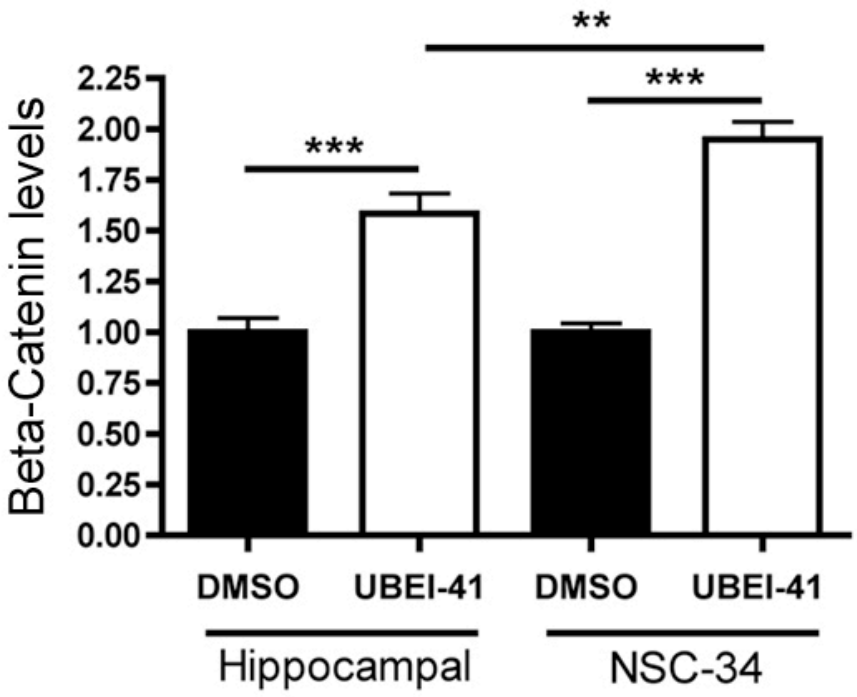

Figure 5.12 Cells show an increased level of β-catenin after treatment with a UBA1 inhibitor. Bar charts (mean ± SEM) showing that β-catenin levels are increased in primary cultures of rat hippocampal neurons and a motor neuron cell line (NSC-34) treated with 50 μM UBEI-41 for two hours (***P<0.001, ANOVA with Tukey's post hoc test; N=12 coverslips DMSO, N=15 UBEI-41 for hippocampal neurons; N=19 DMSO, N=18 UBEI-41 for NSC-34 cells). Motor neurons were significantly more susceptible than hippocampal neurons (**P<0.01).

5.2.8 Deregulation of UBA1 protein levels leads to accumulation of β-catenin in zebrafish and can be rescued by inhibition of β-catenin

Based on the in vitro data, UBEI-41 can be used as a tool to mimic UBA1 inhibition and its downstream consequences can be investigated. Therefore a collaboration was instigated with C. Becker's lab at the university of Edinburgh, to investigate whether UBA1 loss is directly contributing to disease pathogenesis and, in particular, motor neuron pathology *in vivo*. Zebrafish were treated with UBEI-41. At 10 μM UBEI-41, the majority of motor nerve abnormalities observed resulted from aberrant axonal branching. At 50 μM, however, only half of the motor nerve abnormalities observed

were a result of aberrant nerve branching, with the remainder of motor nerves revealing a more severe phenotype: short or missing motor axons (appendix 2). Importantly, these pathological events have been observed in motor axons in zebrafish models of SMA (McWhorter *et al.* 2003; Oprea *et al.* 2008). The study performed by McWhorter *et al.* injected zebrafish embryos with morpholino antisense oligonucleotide at the one to four-cell stage to decrease levels of SMN protein. After 36 hours there was a 61 % decrease in SMA protein levels and the embryos showed defects in motor axon outgrowth and pathfinding during the first three days of development (McWhorter *et al.* 2003) (appendix 3).

Since I showed that β-catenin levels were regulated by UBA1 *in vitro*, I designed an experiment to inhibit β-catenin in zebrafish treated with the UBA1 inhibitor. Zebrafish embryos were treated with the UBA1 inhibitor UBEI-41 and subsequently exposed to quercetin, a plant-derived flavonoid that robustly inhibits β-catenin signalling pathways by disrupting transcriptional activity of the β-catenin–Tcf complex (Park *et al.* 2005; Gelebart *et al.* 2008; Asuthkar *et al.* 2012). Treatment of zebrafish with motor neuron defects resulting from the addition of 50 μM UBEI-41 with 25 μM or 50 μM quercetin revealed a dose-dependent rescue of the motor axon branching phenotype (appendix 2). Strikingly, in the zebrafish treated with 50 μM quercetin, the number of abnormal motor nerves was reduced to that observed in control zebrafish not exposed to the UBA1 inhibitor. Motor nerve abnormalities induced by inhibition of *UBA1* in zebrafish were fully rescued by simultaneous inhibition of β-catenin signalling. In addition to the motor nerve disruptions observed, it was noted that exposure to UBEI-41 caused dose-dependent alteration of the gross

morphology of zebrafish embryos, manifesting as a bent body axis. These deficits were also corrected by treatment with quercetin (appendix 2).

5.2.9 Inhibition of β-catenin signalling ameliorates neuromuscular pathology, but not systemic pathology in Taiwanese SMA mice

Next I investigated whether pharmacological inhibition of β-catenin signalling with quercetin could have a similar effect on disease phenotype in SMA mice. For this drug trial I used the Taiwanese SMA mice (*Smn*$^{-/-}$;*SMN2*$^{tg/0}$ (Riessland *et al.* 2010)). These mice have a less severe phenotype and the mean survival is 10-11 days compared to 5-6 days in the severe SMA mice. Another advance of the Taiwanese SMA mice is that the breeding scheme allows 50% of the litter to be SMA mice (*Smn*$^{-/-}$;*SMN2*$^{tg/0}$) and 50 % to be control mice (*Smn*$^{-/+}$;*SMN2*$^{tg/0}$) (Riessland *et al.* 2010).

Quercetin was injected intra-peritoneal daily from the day of birth (P1). Mice were killed when they showed a decrease of 10 % in body-weight per day over two consecutive days or when the pups looked very ill (i.e. cold and dry skin and were not moving). A dose of 100 mg/kg, 50 mg/kg or 10 mg/kg were injected in the pups. I found that 100 mg/kg and 50 mg/kg was lethal, therefore I chose to continue with the 10 mg/kg dose. A parallel group of mice received injections of DMSO vehicle only (same volume as the mice received that were treated with quercetin). The treatment had no significant effect on neuromuscular function in SMA mice at pre-symptomatic ages (the righting test; figure 5.13; P3, N=30 Het DMSO; N=27 KO DMSO; N=21 KO quercetin; Kruskal Wallis test with Dunn's post hoc test). By

contrast, quercetin treatment significantly improved the performance of symptomatic (P6) SMA mice during this test (the righting test; figure 5.13; P6, N=31 Het DMSO; N=28 KO DMSO; N=27 KO quercetin; Kruskal Wallis test with Dunn's post hoc test). Although quercetin treated mice often appeared much healthier than their DMSO-treated counterparts at late symptomatic stages (P10; figure 5.14), treatment with quercetin did not increase survival (figure 5.15; N=10 mice DMSO; N=13 quercetin; P=0.9897 Chi-square test). In order to examine the possible causes of quercetin failing to ameliorate non-neuromuscular, systemic pathology, I quantified β-catenin levels in heart and liver from un-injected Taiwanese SMA mice. Surprisingly, β-catenin levels remained unchanged in heart and liver (figure 5.16A; N=3 mice per genotype; ***P< 0.001, ANOVA with Tukey's post-hoc test).

In contrast, reduced levels of UBA1 were present throughout all tissue and organ systems investigated (Figure 5.16B; N=3 mice per genotype; *P<0.05; **P<0.01; ***P<0.001, ANOVA with Tukey's post-hoc test). Thus, perturbations in β-catenin signalling pathways occurring downstream of disrupted ubiquitin homeostasis were restricted to the neuromuscular system, thereby revealing distinct mechanisms driving pathology in the neuromuscular system compared to other tissue and organ systems in SMA.

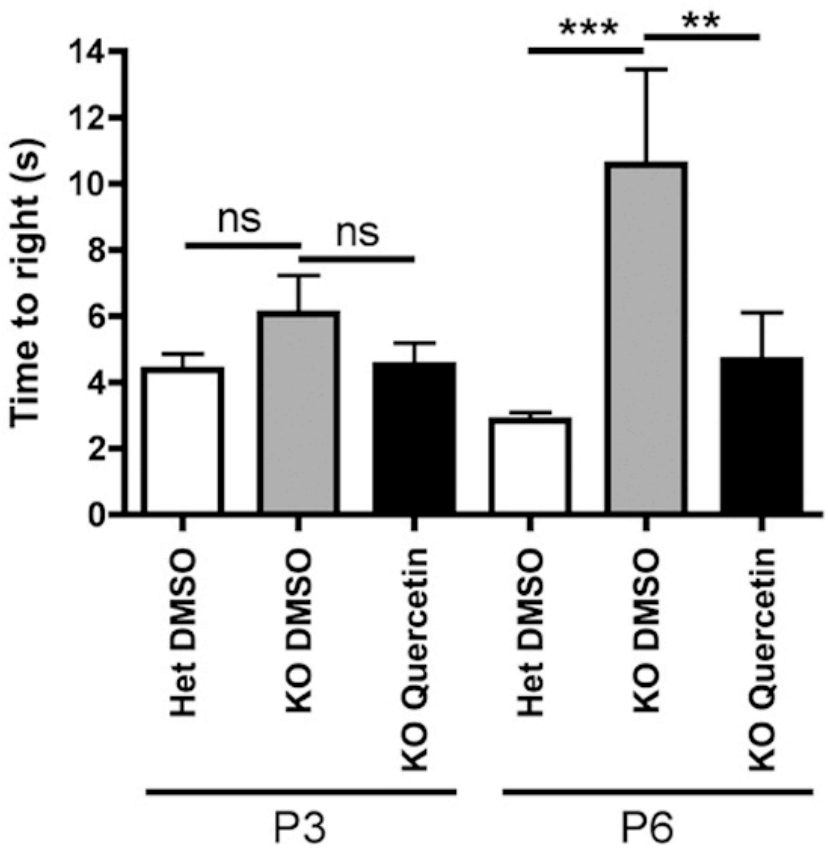

Figure 5.13 Significant improvement in neuromuscular function (righting test) in symptomatic (P6) Taiwanese SMA mice. At P6 Taiwanese SMA (KO) mice treated with 10 mg/kg quercetin from birth show an improvement in neuromuscular function. Quercetin treatment had no significant effect on basal neuromuscular function pre-symptomatically at P3 (Kruskal Wallis test with Dunn's post hoc test; P3, N=30 tests, Het DMSO; N=27 KO DMSO; N=21 KO quercetin; P6, N=31, Het DMSO; N=28 KO DMSO; N=27 KO quercetin).

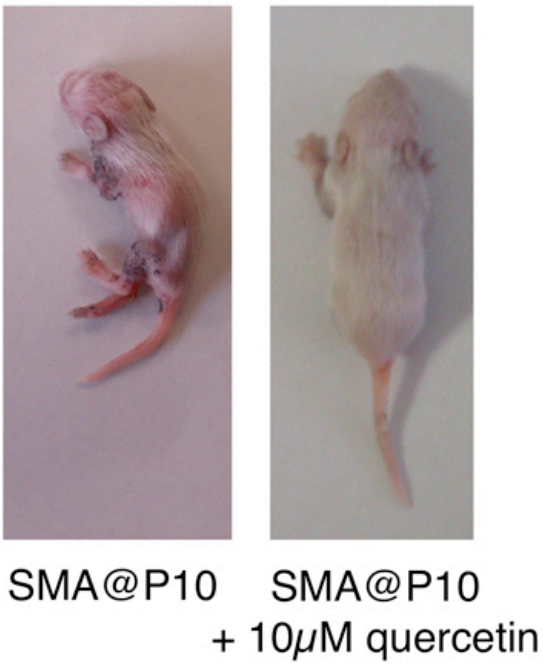

Figure 5.14 Quercetin treated Taiwanese SMA mice look healthier than Taiwanese SMA mice treated with DMSO. Taiwanese SMA mouse (left panel) and a quercetin-treated Taiwanese SMA mouse (right panel) at P10.

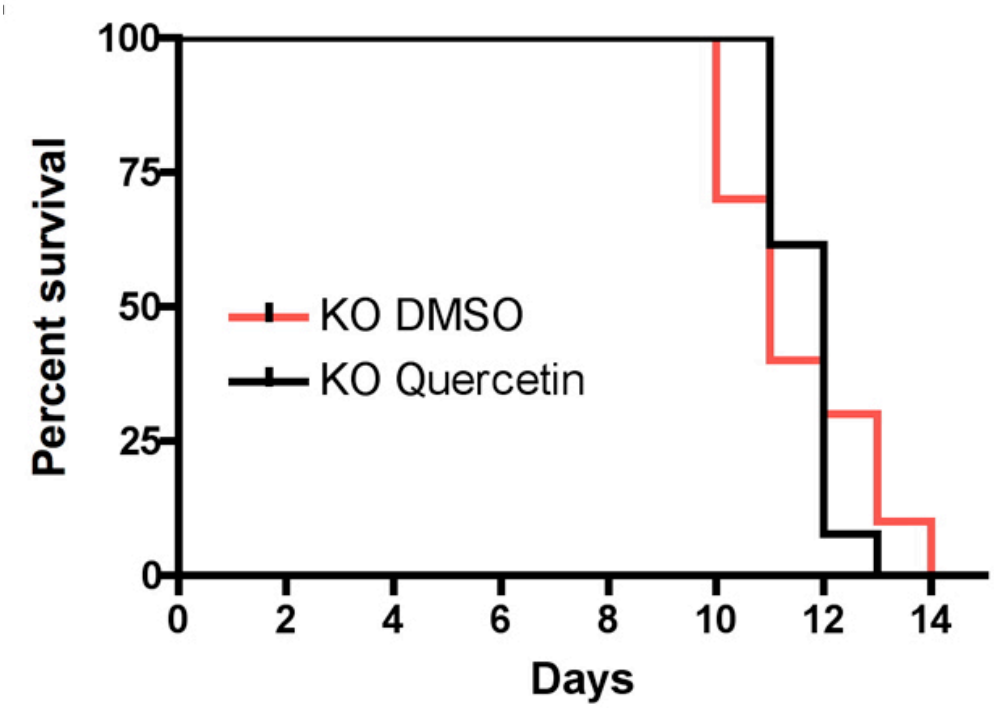

Figure 5.15 No improvement in survival after treatment with quercetin. Survival curve for Taiwanese SMA mice treated with 10 mg/kg quercetin (KO Quercetin) showing no significant difference compared to DMSO treated mice (P=0.9897 Chi-square test; N=10 mice DMSO; N=13 quercetin).

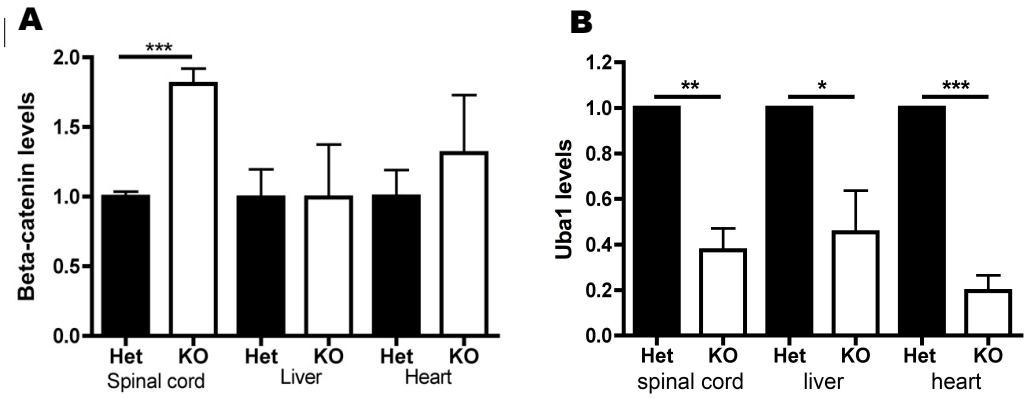

Figure 5.16 B-catenin and UBA1 levels in spinal cord, liver and heart. (A) Levels of β-catenin in spinal cord, liver and heart of Taiwanese SMA mice at P10 (KO) compared to littermate controls (Het), quantified using fluorescent western blot. B-catenin was significantly increased in the spinal cord, but not in the liver or heart (N=3 mice per genotype; ANOVA with Tukey's post-hoc test). **(B)** Levels of UBA1 protein in the spinal cord, liver and heart of Taiwanese SMA mice at P10 (KO) compared to littermate controls (Het; normalised to 1), quantified using fluorescent western blot (N=3 mice per genotype; *P<0.05; **P<0.01;***P<0.001).This figure was made with help of G. Hamilton and T. Wishart.

5.2.10 UCH-L1 enzyme regulates levels of β-catenin

Another component of the ubiquitination pathway that was significantly changed in the proteomic screen was UCH-L1. This enzyme was increased in SMA hippocampal synapses by 1.7 fold. To test whether the increased expression of this enzyme had an effect on β-catenin levels, I used an UCH-L1 inhibitor to treat rat hippocampal neurons in culture (7 days old) and NSC-34 cells and subsequently measured the levels of β-catenin and ubiquitin (as a positive control for the efficiency of the drug). I tested different concentrations and durations of drug treatment. For an optimal effect in the NSC-34 cells the best concentration was 10 μM and the best time for treatment was three hours. The scatter plots are shown as a percentage of the control (figure 5.17; N= 9 coverslips per time point, N= 6 coverslips per treatment; *P<0.05, **P<0.01, Kruskal-Wallis test with Dunn's post-hoc test). With these conditions β-catenin levels were significantly increased.

Ubiquitin levels showed an increased trend over time, with the highest expression at three hours, but this did not reach significance (figure 5.18; N= 9 coverslips per time point, P>0.05, Kruskal-Wallis test with Dunn's post-hoc test).

In the rat hippocampal neurons the optimal conditions were a concentration of 5 μM for 1 hour. Both β-catenin and ubiquitin levels were increased under these conditions (figure 5.19 and 5.20; N = 12 coverslips per time point, *P<0.05, Kruskal-Wallis test with Dunn's post-hoc test). These results suggest that UCH-L1 plays a role in maintaining the protein level of β-catenin in the cytoplasm.

UCH-L1 is a complex enzyme as it performs many functions in the ubiquitination pathway (Liu *et al.* 2002). UCH-L1 monomer has a deubiquitinating function, where it removes ubiquitin from target proteins and it also stabilizes mono ubiquitin (Larsen *et al.* 1998; Osaka *et al.* 2003). When it is in its dimer form it ligases ubiquitin molecules to each other or to the target protein (Liu *et al.* 2002; Setsuie and Wada 2007). It is therefore difficult to predict where an UCH-L1 inhibitor will act. In these experiments it seems that the ligase function was inhibited, because the ubiquitin levels (mono-ubiquitin levels were measured) were increased after treatment and so were β-catenin levels. Therefore it is possible that this specific inhibitor inhibits the dimerization of UCH-L1 *in vitro*.

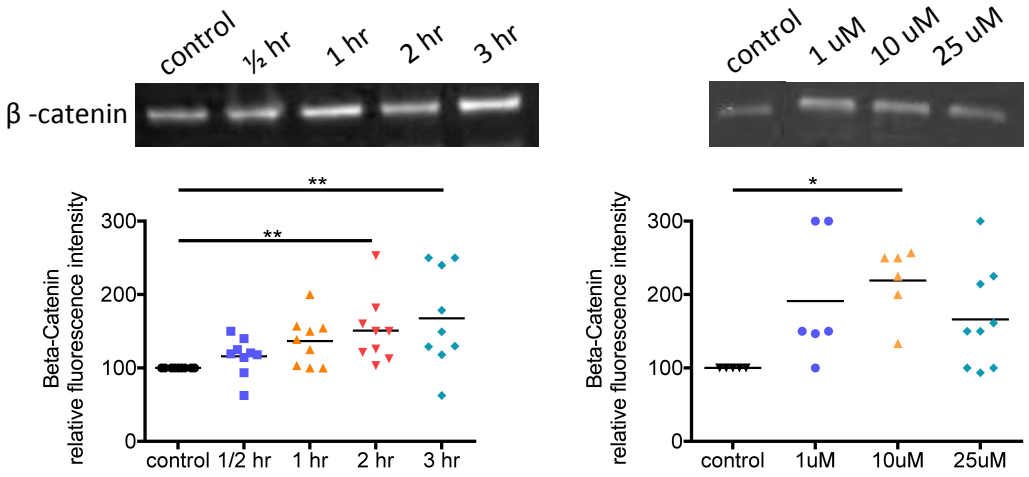

Figure 5.17 B-catenin levels in NSC-34 cells after treatment with UCH-L1 inhibitor. NSC-34 cells were treated with 10 μm of UCH-L1 inhibitor for 1/2h, 1h, 2h and 3h or with DMSO only (1h). There is a significant increase in β-catenin levels after 2h and 3h of treatment. The scatter plots are shown as a percentage of the control (N=9 coverslips per time point, **P<0.01, Kruskal-Wallis test with Dunn's post-hoc test). NSC34 cells were treated with different concentrations of UCH-L1 inhibitor (1 μM, 10 μM and 25 μM) for 1h. (*P<0.05; N=6 coverslips per treatment, Kruskal-Wallis test with Dunn's post-hoc test). Beta III tubulin was used as a loading control.

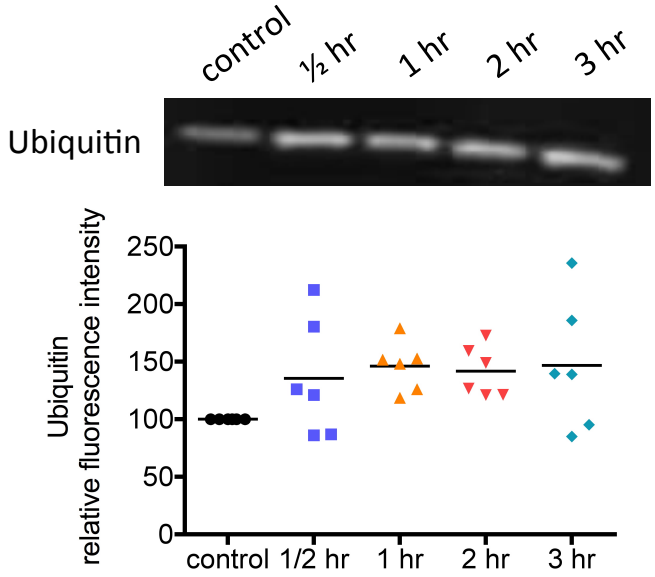

Figure 5.18 Ubiquitin levels in NSC-34 cells after treatment with UCH-L1 inhibitor. There is no significant increase in the levels of ubiquitin after 1/2h, 1h, 2h or 3h of treatment with 10 μM of UCH-L1 inhibitor. The scatter plots are shown as a percentage of the control (N=9 coverslips per time point, P>0.05, Kruskal-Wallis test with Dunn's post-hoc test).

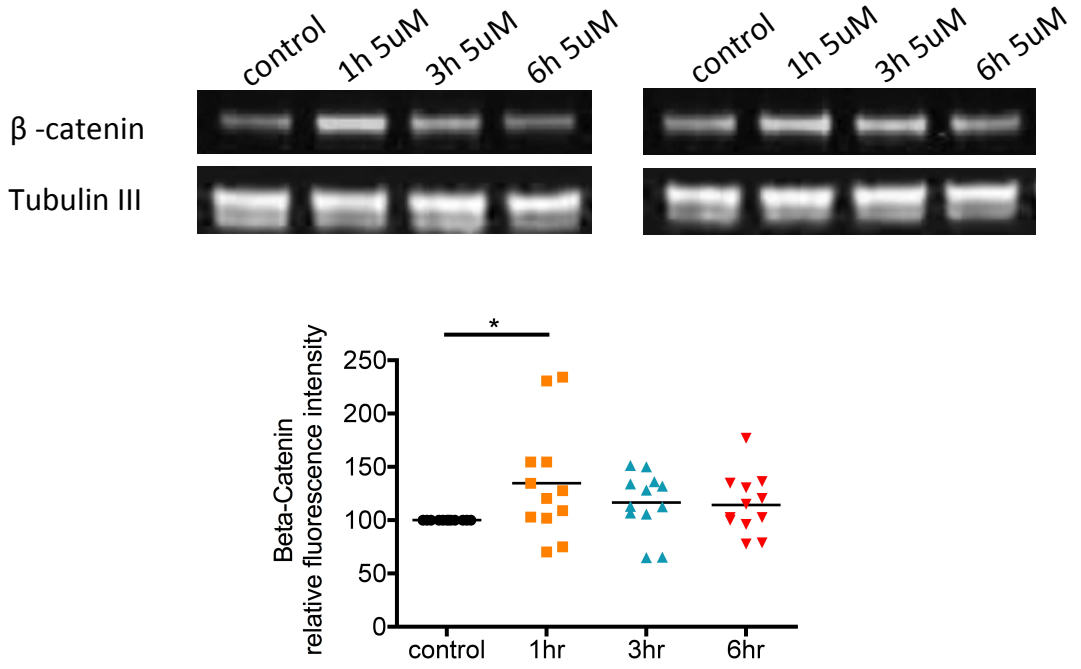

Figure 5.19 B-catenin levels in primary hippocampal rat neurons after treatment with UCH-L1 inhibitor. Cells were treated with 5 μM UCH-L1 inhibitor for 1h, 3h, 6h or with DMSO only for 1h. There is a significant increase in β-catenin levels after treatment for 1h, but not after 3h or 6h. The scatter plots are shown as a percentage of the control (N=12 coverslips per time point, *P<0.05, Kruskal-Wallis test with Dunn's post-hoc test).

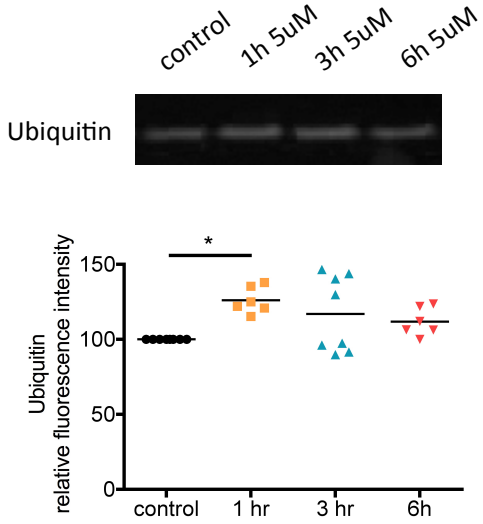

Figure 5.20 Ubiquitin levels in primary hippocampal rat neurons after treatment with UCH-L1 inhibitor. Cells were treated with 5 μM UCH-L1 inhibitor for 1h, 3h, 6h or with DMSO only for 1h. There is a significant increase in ubiquitin levels after treatment for 1h, but not after 3h or 6h. The scatter plots are shown as a percentage of the control (N=12 coverslips per time point, *P<0.05, Kruskal-Wallis test with Dunn's post-hoc test).

5.2.11 B-catenin protein levels are increased in muscle biopsies from SMA patients

Finally, levels of β-catenin and UBA1 were measured in muscle biopsies from SMA patients and non-SMA controls. I had three SMA patient biopsies. SMA patient 1 was four years of age and was diagnosed with type II SMA; SMA patient 2 was 25 years of age and diagnosed with type III SMA; SMA patient 3 was three years of age and diagnosed with type II SMA. The control group consisted of samples from individuals between 17 and 27 years of age. The controls were all tested for mutations or deletions in the *SMN1* gene. Although the levels of β-catenin varied among the SMA patients, overall there was a significant increase in the level of β-catenin (figure 5.21; N=3 per group, **P<0.01 two tailed, unpaired *t*-test). Levels of UBA1 varied between the three control samples (figure 5.22). For example there is an almost two fold difference in UBA1 levels between control 1 and control 3. Based on the control samples, I concluded that it was not possible to measure levels of UBA1 in SMA patients, as the control samples were so variable and it would therefore not be possible to compare the SMA samples to the control samples.

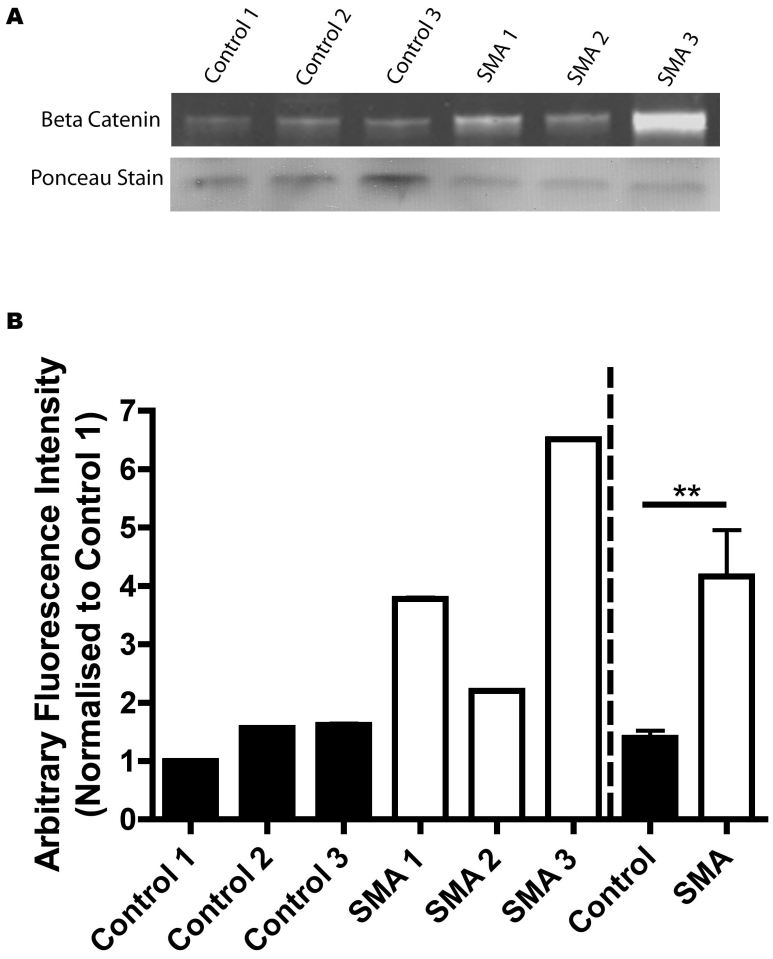

Figure 5.21 Beta-catenin levels are increased in muscle biopsies from SMA patients. (A) Representative western blots for β-catenin levels in three control muscle samples and three SMA patient samples. **(B)** Graph showing significantly increased levels of β-catenin in muscle biopsies from SMA patients (**P<0.01; two-tailed, unpaired *t*-test).

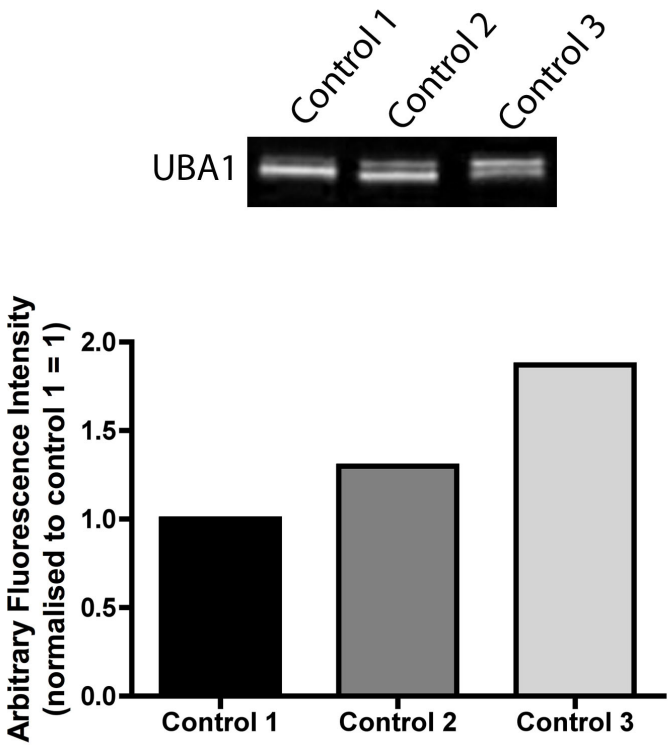

Figure 5.22 UBA1 levels are variable between human control samples. Graph is showing that there is variability in UBA1 levels between human control samples. Note that there is an almost two fold difference between control 1 and control 3.

5.3 Discussion

5.3.1 Overview of results

The experiments described here were initiated to identify pathways downstream of SMN that contribute to SMA pathogenesis and have revealed a novel role for SMN in regulating ubiquitin homeostasis, mediated largely via interactions with UBA1. In addition, this study has identified β-catenin as a downstream target of UBA1/ubiquitination pathways in the neuromuscular system, with disruption of β-catenin pathways in SMA. Pharmacological inhibition of β-catenin signalling using quercetin ameliorated neuromuscular pathology in zebrafish and in a mouse model of SMA. Whereas disruption of UBA1 was found to occur across a range of neuronal and non-neuronal organs in SMA mice, surprisingly, I found that downstream disruption of β-catenin was restricted to the neuromuscular system, and was not responsible for regulating SMN-dependent pathology in other tissues and organs. The findings here provide experimental evidence directly linking SMN protein to the regulation of ubiquitin homeostasis and β-catenin signalling in the neuromuscular system and also reveal fundamental molecular differences between pathways underlying neuromuscular and systemic pathology in SMA.

5.3.2 SMN protein is localized at the synapse and synaptic mitochondria

In the first part of this chapter it has been shown for the first time that SMN protein and one of its binding partners, Gemin5, were present at the synapse *in vivo*. In SMA mice the levels of SMN protein were significantly reduced. Gemin5 is a large tryptophan-asparticacid (WD) repeat protein and it binds directly to SMN in the

SMN complex (Gubitz *et al.* 2002; Gubitz *et al.* 2004). The presence of the multiple WD repeats (protein-protein interaction domains) implies that this protein is engaged in multiple protein interactions and might serve as a platform for the assembly of protein complexes (Gubitz *et al.* 2004). It has also been shown here that SMN and Gemin5 physically interact in the synaptosol. This indicates that the whole SMN complex might be present at the synapse and that SMN fulfils the same role as in the cell body in snRNP assembly, however it might have additional roles as well.

The data in this chapter supports earlier results where SMN protein was found in axons and growth cones *in vitro* (Fan and Simard 2002; Rossoll *et al.* 2003). In addition, to confirm the presents of SMN protein at the synapse *in vivo,* a study performed in *Drosophila,* using pan-neuronally driven dSMN-YFP, showed that SMN protein was present in pre-synaptic boutons at the NMJ in third instar larvae as well as in neuronal cytoplasm and in axons of motor neurons and photoreceptors. As a control experiment dSMN-YFP was driven in muscle and this resulted in no fluorescent signal in pre-synaptic boutons (this study was performed in collaboration with Philip Young at the Universities of Exeter and Plymouth).

Interestingly, SMN protein was also localized to synaptic mitochondria. The results from this chapter show that reduced levels of SMN do not have an effect on cytochrome C release from mitochondria. This means that synaptic mitochondrial mediated apoptosis cannot be a pathologic process in SMA. However, it cannot be ruled out that mitochondria have another role in pathology in SMA. Previous work has shown that mitochondria are dysfunctional in an SMA cell line (i.e. NSC-34 cells

that were transfected with siRNA to decrease SMN levels; showing 66 % decreased levels of SMN protein after 72 hours). In their study they found that ATP levels were decreased suggesting that ATP production is decreased. In addition SMN knock-down resulted in increased mitochondrial membrane potential and increased free radical production (Acsadi *et al.* 2009). Another study showed that the total active mitochondrial surface in the presynaptic terminals were reduced with approximately 50% in the TVA muscle of delta7 SMA mice (Torres-Benito *et al.* 2011). Contrary to the results detailed in this chapter, one other study found that SMN protein localizes to microsomes but not to mitochondria (La Bella *et al.* 2000).

5.3.3 B-actin accumulation in the synapse is disrupted in a mouse model of SMA in vivo

The results in this chapter suggest that low levels of SMN in the synapse cause disruption of the accumulation of β-actin mRNA. B-actin mRNA is transported from the nucleus, where it is synthesized in most cases, to distal compartments of the neuron. Actin is pre-dominantly localized in growth cones and plays a major role in growth cone movements and neurite growth (Bassell *et al.* 1998). Previous studies report that SMN protein interacts with hnRNP R instead of Gemin2 in the growth cone (Rossoll *et al.* 2002). hnRNP R can bind to β-actin mRNA full length and this suggest that SMN, via binding to hnRNP R could be involved in the transportation of specific mRNAs in motor axons (Rossoll *et al.* 2003). Therefore, the results in this chapter can not specifically say whether low levels of β-actin mRNA in the synapse of SMA mice were caused by transportation failure or translation failure at the synapse due to low levels of SMN.

Future work would have to be carried out to investigate this question. A co-immunoprecipitation on protein extracts from a peripheral nerve from SMA and control mice for SMN and hnRNP R would reveal whether there is a disruption in the binding of SMN to hnRNP R, which would disrupt the transportation of β-actin mRNA.

5.3.4 A role for the ubiquitin/proteasome pathway in SMA

The identification of changes in the synaptic proteome due to low levels of SMN led to the identification of changes in the Ubiquitin/proteasome pathway. Although it is known that SMN protein interacts with the ubiquitin-proteasome system in order to regulate its own stability (Chang *et al.* 2004; Burnett *et al.* 2009; Hsu *et al.* 2010), the results in this chapter significantly extends the understanding of the importance of these interactions to include a direct role for ubiquitin homeostasis in regulating SMA disease pathogenesis. When taken together with human genetic data showing that mutations in *UBA1* cause similar pathological changes to those found in SMN-dependent SMA (Ramser *et al.* 2008), the findings here suggest that perturbations in ubiquitin homeostasis, and UBA1 in particular, may represent a common molecular pathway underlying neuromuscular pathology across genetically-distinct forms of the disease. Moreover, the finding that perturbations in ubiquitin homeostasis in response to SMN deficiency, as well as dysregulation of β-catenin downstream of perturbations in UBA1, are evolutionarily conserved between mouse and zebrafish models, suggests that regulation of ubiquitin homeostasis represents a key biological role for SMN.

The identification of β-catenin as a key downstream target of ubiquitin pathways disrupted in SMA provides mechanistic insights into the pathways through which defects in ubiquitin homeostasis are transferred into pathological changes in the neuromuscular system. Although these pathways have not previously been linked to neuromuscular pathology in SMA, β-catenin signalling pathways are known to play an important role in regulating motor neuron differentiation and stability, including regulating synaptic structure and function (Murase *et al.* 2002; Li *et al.* 2008; Ojeda *et al.* 2011). Interestingly, Li *et al.* showed that motor neuron differentiation was regulated by retrograde signalling through β-catenin from skeletal muscle (Li *et al.* 2008). The demonstration of robust amelioration of neuromuscular pathology in zebrafish and mouse models of SMA treated with quercetin highlights the fact that β-catenin pathways in the neuromuscular system are amenable to pharmacological targeting *in vivo*. Thus, targeting β-catenin signalling pathways during the early stages of disease may represent an attractive therapeutic option for stabilizing the neuromuscular system in SMA, and possibly also related conditions.

The pathway analysis software identified modifications in the PI3K/AKT pathway with the most significant change in levels of β-catenin. There are several mechanisms that regulate the activation of β-catenin. B-catenin was originally identified as a component of cell-cell adhesion structures where it interacts with e-cadherin and links e-cadherin to α-catenin, which in turn mediates anchorage of the e-cadherin complex to the cortical actin cytoskeleton (Rimm *et al.* 1995). B-catenin functions also as a component of the canonical Wnt signalling pathway. Activation of the Wnt pathway inhibits the phosphorylation of β-catenin (Molenaar *et al.* 1996;

Liu *et al.* 2002). Stabilized hypophosphorylated β-catenin then translocates to the nucleus where it interacts with transcription factors of the TCF/LEF-1 family leading to the increased expression of genes, such as *MYC* and *CCND1* (He *et al.* 1998; Shtutman *et al.* 1999; Tetsu and McCormick 1999). When Wnt signalling is not active β-catenin is phosphorylated by GSK-3β, which leads to its degradation by the ubiquitin/proteasome system (Aberle *et al.* 1997). In addition β-catenin translocates to the nucleus in response to epidermal growth factor (EGF) stimulation (Hoschuetzky *et al.* 1994). AKT, which is activated downstream from EGF receptor signalling, phosphorylates β-catenin at Ser552 *in vitro* and *in vivo.* AKT can activate β-catenin-TCF/LEF-1 transcriptional activity both by indirect stabilization of β-catenin through inhibition of GSK-3β and direct phosphorylation of β-catenin, which enhances β-catenin nuclear accumulation and it translational activity (Fang *et al.* 2007).

Given that β-catenin is such a well-established target for the ubiquitin-proteasome system, and the magnitude of changes in β-catenin pathways observed in the neuromuscular system in SMA mice, it was surprising to find that quercetin treatment did not target systemic pathology in SMA. Our finding that β-catenin signalling pathways remained stable in tissues and organs outside the neuromuscular system explains the quercetin result, but also served to highlight an underappreciated complexity in molecular pathways underlying disease pathogenesis in SMA, implicating both β-catenin-dependent and β-catenin-independent pathways. These findings add significant additional support to the hypothesis that SMA is a multi-system disorder. The contribution of non-neuromuscular, systemic pathology,

affecting tissues and organs such as the heart, liver, lungs, intestine and vasculature, has only recently been fully appreciated in SMA animal models (Hamilton and Gillingwater 2013). As a result, several studies have demonstrated that a failure to target peripheral tissues and organs minimises the effectiveness of therapeutics (Hua *et al.* 2011; Schreml *et al.* 2013). Moreover, they further highlight the likely requirement to deliver therapeutics targeting either the *SMN1* or *SMN2* gene systemically in order to fully rescue SMA symptoms (Hua *et al.* 2011).

Chapter 6

A dopamine agonist does not ameliorate neuromuscular pathology in a mouse model of SMA

6.1 Introduction

In this final chapter I investigated a different potentially interesting drug for treatment of SMA. A recent study showed that dopamine released from the brain promoted generation of motor neurons in the developing spinal cord in zebrafish (Reimer *et al.* 2013). In addition, dopamine promotes generation of motor neurons in the lesioned spinal cord in adult zebrafish (Reimer *et al.* 2013). Earlier studies had already shown that dopamine was important for the development of different tissue. In *Drosophila,* depletion of dopamine during the second instar results in developmental abnormalities and lethality (Neckameyer 1996). I investigated whether a dopamine-agonist would have a beneficial effect on the disease severity in the Taiwanese SMA mice. Since motor neurons degenerate from a very early stage of the disease, a dopamine-agonist could have a beneficial effect.

R(-)-Propylnorapomorphine hydrochloride (NPA) is a potent and selective D_2 dopamine receptor agonist and has been shown to rescue motor neurons after reducing dopaminergic input from the brain by morpholino knock down of *th1* (rate limiting enzyme for dopamine synthesis; (Reimer *et al.* 2013)) in zebrafish. This

suggests that endogenous dopamine is important for the development of motor neurons and that it can be substituted by dopaminergic drugs.

I show here that a daily injection with 10 mg/kg of NPA does not ameliorate neuromuscular pathology in SMA, this includes number of axonal inputs and muscle fiber diameter.

6.2 Results

6.2.1 Treatment with NPA does not increase weight of SMA mice

R(-)-Propylnorapomorphine hydrochloride (NPA) was kept as a powder in the fridge. The drug was dissolved in a solution of sterile saline and 3% DMSO. Taiwanese SMA mice and littermate controls were injected with 10 mg/kg NPA from the day of birth (P1) until postnatal day 10 (P10). The mice were weighed daily. There was no difference observed in weight loss in the SMA mice treated with NPA compared to mice treated with DMSO (figure 6.1). Also the mice did not look healthier (i.e. same dry skin and were not moving as much as control littermates).

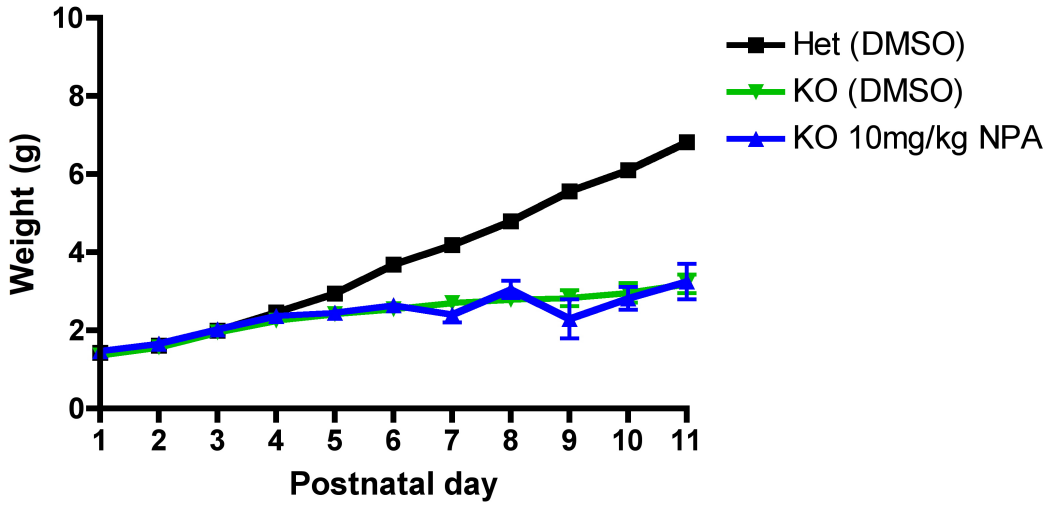

Figure 6.1 No increase in weight in SMA (KO NPA) mice treated with NPA compared to SMA mice treated with DMSO (KO DMSO).

6.2.2 No improvement of neuromuscular pathology in SMA mice treated with NPA

Since it has been shown that injecting dopaminergic drugs rescued motor neurons in zebrafish, I hypothesized that this would happen as well in a mouse model of SMA, where motor neurons start to degenerate soon after birth. To investigate this I studied the neuromuscular junctions (NMJs) from the *Levator auris longus* (LAL) and *transversus abdominus* (TVA) muscle from NPA treated SMA mice, DMSO treated SMA mice and control (Het) mice. If NPA rescues motor neurons this should be reflected in an amelioration of NMJ pathology. One way of measuring pathology is quantifying the number of axonal inputs on the endplate (figure 6.2A; axonal inputs are in green and the motor endplate is labelled in red). In Taiwanese SMA mice there is no widespread denervation as seen in the severe SMA mice (Murray *et al.* 2008), but instead these mice show an increased rate of axonal pruning.

An increased rate of axonal pruning was confirmed in the LAL of Taiwanese mice, as the number of axonal inputs was significantly decreased in SMA mice (KO) compared to littermate controls (Het) (figure 6.2A/B top panel; *P<0.05, **P<0.01, ANOVA with Tukey's post test). However, this pathology was not rescued by treatment with NPA (figure 6.2A/B). The TVA was less severely affected in the Taiwanese SMA mouse model. The number of axonal inputs in the TVA was not significantly different in Taiwanese SMA mice and control littermates, although there was a trend towards a smaller number of axonal inputs. As well as in the LAL, SMA mice treated with NPA did not show an improvement of axonal input numbers (figure 6.2A/B lower panel; P>0.05, ANOVA with Tukey's post test).

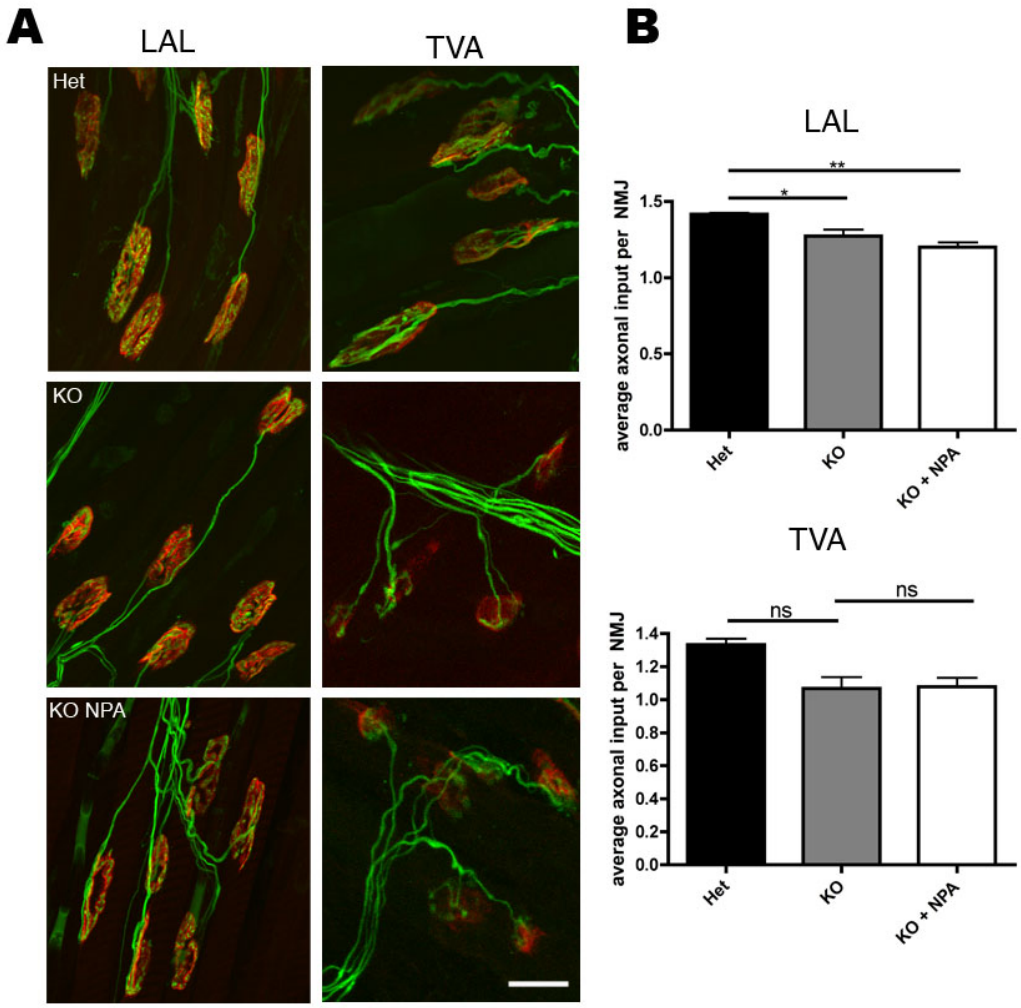

Figure 6.2 Neuromuscular pathology is not rescued by treatment with NPA. (A) Confocal micrographs showing axons (in green labelled neurofilament) innervating endplates on the muscle fiber (in red post-synaptic acetylcholine receptors labelled with TRITC-α-BTX) in the *Levator auris longus* (LAL) and *transversus abdominus* (TVA) of control het mice, SMA mice (KO) and SMA mice treated with NPA (KO NPA) at P9. Note that some endplates are innervated by more than one axon. **(B)** Bar charts showing a decreased average axonal input per NMJ in SMA (KO) mice compared to littermate controls (Het) in the LAL. This is not rescued by treating SMA mice with NPA (N=3 per genotype; *P<0.05, **P<0.01, ANOVA with Tukey's post test). In the TVA there is no difference in average axonal input per NMJ between SMA (KO) and control litters (Het) (N=3 per genotype; P>0.05, ANOVA with Tukey's post test). Scale bar = 15 μm.

In addition I investigated whether NPA had an effect on the development of the muscle fibers. The diameter of between 30 and 50 muscle fibers per mouse was measured in the LAL. I observed a decreased diameter in muscle fibers from SMA mice (KO) compared to littermate controls (Het). However, this was not rescued by treatment with NPA (figure 6.3A/B; P>0.05, *P<0.05, ANOVA with Tukey's post test).

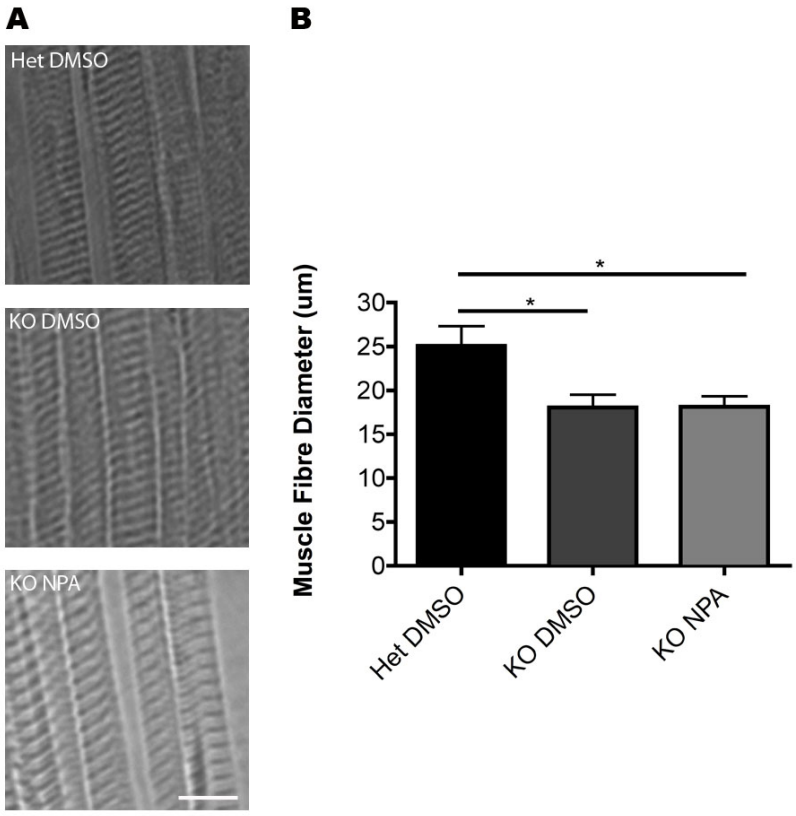

Figure 6.3 Treatment with NPA does not rescue muscle fiber diameter in SMA mice. (A) Micrographs showing muscle fibers from Control (Het), SMA (KO DMSO) and SMA mice treated with NPA (KO NPA). **(B)** Bar charts (± SEM) showing a decreased diameter in SMA (KO) mice compared to littermate control (Het). NPA did not rescue the muscle fiber diameter in SMA mice (KO NPA; N=3 mice per genotype; P>0.05, *P < 0.05; ANOVA with Tukey's post test). Scale bar = 30 µm.

6.3 Discussion

6.3.1 Overview of results

In this chapter I show that the potent and selective D_2 dopamine receptor agonist NPA does not rescue neuromuscular pathology, such as number of axonal inputs and muscle fiber size, in Taiwanese SMA mice. This suggests that dopamine has no effect on motor neuron rescue in SMA. However, it has to be noted that I did not have a readout that the agonist targeted the receptors and was active. Taken this result in a wider perspective, it shows that not all drugs that are given to the SMA mice are working. This is in favour of the quercetin trial confirming that what we see there is a real result.

6.3.2 Future work

Dopamine has been identified as a factor influencing neurogenesis in the developing brain and adult brain in mice (Popolo *et al.* 2004; Yang *et al.* 2008). It has been proposed that dopamine acts in part through activating the hedgehog pathway. This is the major signalling pathway involved in the developmental generation of motor neurons (Lewis and Eisen 2001). In addition it has been shown that the dopaminergic neurons that invade the spinal cord during neuronal differentiation are descending from the diencephalic dopaminergic neurons (McLean and Fetcho 2004). A recent study identified dopamine from the brain as a promoter of the generation of motor neurons in the developing spinal cord at the expense of V2 interneurons in zebrafish. This has been shown to be important for the motor performance of free-swimming larvae (Reimer *et al.* 2013). SMN protein is highly active during embryonic and

early postnatal development of the central nervous system (Gabanella *et al.* 2005). One explanation that I did not observe a rescue with the dopamine receptor agonist could be that the administration of the drug was too late. Motor neurons might have started degeneration and the rescue was too late.

In conclusion, the results that I show here are preliminary and further research is needed. The drug could be given to pregnant females to investigate whether the timing of the drug administration was too late. A treatment like this has shown to be effective in SMA mice where the pregnant female received water with the drug (sodium butyrate) ad libitum (Chang *et al.* 2001). This increased the survival of the pups. In addition it has to be noted that only one dose (10 mg/kg) of the drug was used, it might be that a higher dose of the drug is needed. This has not been tested.

Chapter 7

General discussion

7.1 Overview of results

In this thesis four questions have been addressed.

1. Is there a direct role for skeletal muscle in the pathogenesis of SMA?

   I show here for the first time that there are intrinsic molecular alterations *in vivo* in muscle tissue independent of denervation-induced changes. VDAC2 and parvalbumin were two proteins with changed expression identified in different muscles between two different mouse models of SMA. In addition the changed expression of VDAC2 and parvalbumin was also identified in muscle biopsies from SMA patients. Moreover, with the use of functional cluster analysis and H2AX labelling, I revealed increased activity of cell death pathways in SMA muscle. And finally, I show that the molecular alterations in muscle were rescued after treatment with the HDACi SAHA.

2. Can biomarkers be identified in skeletal muscle?

   GRP75 and calreticulin have been identified as potential biomarkers for SMA in skeletal muscle. The expression levels of these two proteins were unchanged at pre-symptomatic ages but were increased at late-symptomatic ages. In addition, GRP75 and calreticulin were also readily measurable in skin samples and showed the same change in expression in SMA mice compared to littermate controls. Moreover, levels of GRP75 and calreticulin responded to treatment with the

HDAC inhibitor TSA in both muscle and skin and showed expression levels similar to that in control mice. Preliminary results suggest that GRP75 and calreticulin are detectable and measurable in muscle samples from SMA patients and controls.

3. Can new pathways involved in disease pathogenesis be identified?

   I propose a new role for SMN protein in regulating the ubiquitination pathway, mediated largely via interactions with UBA1. In addition I show that β-catenin is a downstream target of the ubiquitination pathway in the neuromuscular system and that restoration of β-catenin levels does ameliorate neuromuscular pathology in zebrafish and in SMA mice. Interestingly, I found that β-catenin levels were not changed in non-neuronal tissue, suggesting that there are fundamental molecular differences between pathways underlying neuromuscular and systemic pathology in SMA.

4. Does a dopamine agonist ameliorate SMA phenotype in a mouse model of SMA?

   I show that increasing dopamine levels in the brain does not ameliorate neuromuscular pathology in SMA mice.

The work presented here has significantly contributed to the knowledge of disease pathogenesis in SMA.

7.2 The importance of a new role for SMN protein

Although the pathogenesis of SMA has been investigated extensively, and many new insights have been gained, the disease mechanism is still not fully understood. SMN protein is ubiquitously expressed and it is known to play key roles in generating small nuclear ribonucleoproteins (snRNPs) by combining small nuclear RNA (snRNA) molecules with Sm proteins, which leads to an impairment of pre-mRNA splicing (Liu *et al.* 1997). An additional role for SMN protein is in the stabilization and maturation of the neuromuscular junction. By moving along granules in the axons it plays an important role in the transportation of mRNAs in motor neurons (Fan and Simard 2002). B-actin mRNA depends on SMN to be transported to the growth cones (Rossoll *et al.* 2003). This is disrupted in SMA and therefore motor neurons have shorter axons and smaller growth cones (Rossoll *et al.* 2003). Even though these roles for SMN are known, it is still not know how low levels of SMN cause the neuromuscular system to degenerate in SMA. Therefore additional functions of SMN protein are expected. In addition it has becoming increasingly clear that other cell types and tissues are also vulnerable to low levels of SMN (Hamilton and Gillingwater 2013). The discovery of skeletal muscle pathology in this thesis supports the hypothesis that it is not only motor neurons that are affected. Importantly, the results in this thesis show muscle pathology independent of deneravation induced degeneration of the muscle. Despite the evidence provided in this thesis supporting a direct role for SMN in skeletal muscle, the extent to which intrinsic skeletal muscle pathology contributes to SMA pathogenesis is still not clear and will need further investigation.

In addition I identified SMN protein in mitochondria, which could imply that there are addition roles for SMN that are not yet discovered. Mitochondria are important for intracellular ATP, buffering of intracellular calcium, the generation of intracellular free radicals and involvement in the initiation of apoptotic cell death (Shaw 2005). Moreover, mitochondrial dysfunction has been suggested to contribute to motor neuron injury in an adult form of motor neuron disease, amyotrophic lateral sclerosis (ALS). In ALS patients, alterations in the morphology of mitochondria in muscle and motor neurons have been identified as well as increased mitochondrial volume and calcium levels within motor axon terminals in muscle biopsies (Siklos *et al.* 1996; Beal 2000).

Taken together the identification of new roles for SMN will lead to a better understanding of disease pathogenesis in SMA and subsequently to new targets for the treatment of SMA. In addition the identification of a new role for SMN in regulating the ubiquitination pathway and subsequent β-catenin levels is potentially important. The observation that the treatment with the β-catenin inhibitor ameliorated the neuromuscular pathology but did not increase the survival of the mice, suggested that non-neuronal tissues were not targeted by this treatment. This further suggests that not only the neuromuscular system should be targeted but also other tissues. Nevertheless, the identification of disruption of the ubiquitination pathway and β-catenin signalling pathways in SMA broadens the opportunity for new treatments.

7.3 Proteomics techniques in neuroscience research

The term proteome was first used in 1995 to describe the protein complement of a genome. The proteome is much more complex than either the genome or the transcriptome (figure 7.1). While it is estimated that the human genome comprises between 20 000 and 25 000 genes (number obtained from the international Human Genome Sequencing Consortium), the total number of proteins in the human proteome is estimated at over 1 million (Jensen 2004). This is because each protein can be chemically modified in different ways after translation (post-translation modification). A few examples of post-translation modification are phosphorylation, glycosylation, ubiquitination and methylation (Lebrilla and Mahal 2009).

Proteomics is the large-scale study of proteins, particularly their structures and functions. Proteomics is important because proteins represent the actual functional molecules in the cell. When mutations occur in the DNA, it is the proteins that are ultimately affected. In addition proteins do not act on their own but interact with other proteins and most drugs act on targeting proteins. Therefore I have been studying the proteome of different tissues from SMA mice. In chapters three, four and five, proteomic techniques were used to get an insight in the molecular changes in either muscle (chapter three and four) or synapses (chapter five) in SMA. Both are vulnerable tissues in SMA.

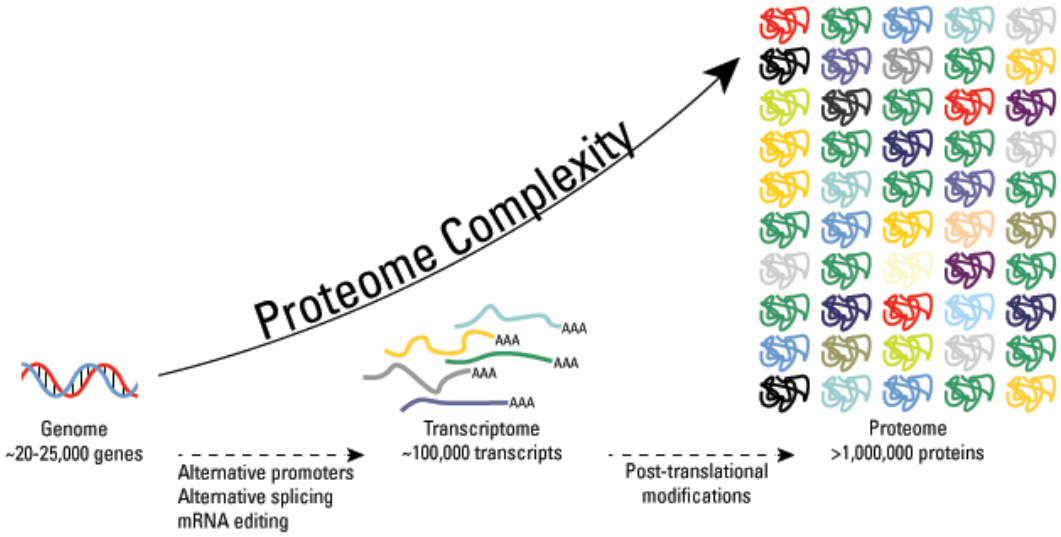

Figure 7.1 Proteome complexity. This figure illustrates the complexity of the proteome. This is mainly due to post-translational modifications. Proteins are the functional molecules of the cell and are the main targets for drug treatment. *Figure obtained from piercenet.com.*

Proteomics is a well-established technique in neuroscience research. There are two main quantitative methods: gel-based, two-dimensional gel electrophoresis (2-DE) and the more recently developed, non-gel-based liquid chromatography/mass spectrometry (LC/MS)-based profiling. 2-DE has been employed for protein separation since 1975 and it enables the separation of complex mixtures of proteins according to charge and molecular weight (Gorg *et al.* 2004). 2-DE gel-based methods are robust and reproducible but as a disadvantage labour-intensive. LC/MS techniques in contrast, have strength in analysing more complex protein samples and have a greater proteome coverage (Bantscheff *et al.* 2007). Quantitative results can be gained using stable isotope labels or label-free methods (Bantscheff *et al.* 2007; Patel *et al.* 2009). Isotope labels can be introduced as an internal standard into amino acids metabolically, chemically or enzymatically (Gygi *et al.* 1999). The common feature among these proteomic methods is that stable isotopes provide for

the quantitation (relative or absolute) of proteins, based upon a well-characterized increase in molecular mass in the protein or peptide of interest. For example iTRAQ (isobaric Tags for Relative and Absolute Quantitation) proteomics is based on covalent labelling of the N-terminus and side chain amines of peptides from protein digestions with tags of varying mass, which are then analysed by the mass spectrometer. In label-free methods two or more experiments are compared by direct mass spectrometric signal intensity for any given peptide (Bantscheff *et al.* 2007).

Proteomics allow for example to identify molecular difference in healthy versus disease tissue or how tissue response to a drug treatment. In SMA and also in other neuroscience research fields, proteomic techniques are now more frequently used. A few recent examples using iTRAQ proteomics are: a study investigating the possible side-effects of valproic acid (VPA) in SMA patient fibroblasts (Fuller *et al.* 2010) and Wishart *et al.* investigated changes in brain regions in SMA mice and identified molecular changes in the hippocampus (Wishart *et al.* 2010). In addition an *in vitro* study was performed on SMN-deficient embryonic stem cells from severe SMA mice and they identified activated cellular stress pathways that cause a dysregulation of energy metabolism, protein degradation and cytoskeleton stability (Wu *et al.* 2011). In other neuroscience fields, proteomic studies are used to answer similar questions. A proteomic study was performed to enable a greater understanding of alterations in the presynaptic molecular composition after induction of repeated morphine administration (Abul-Husn *et al.* 2011). This allowed the identification of potential therapeutic targets for opiate dependence and addiction. Another example is a comparative proteomic study where the researchers tried to establish global effects

of motor neuron disease on the proteome of skeletal muscle from the wobbler mouse (animal model for motor neuron disease (Staunton *et al.* 2011)).

In this thesis I have used proteomics to discover molecular alterations in muscle tissue from SMA mice, to identify biomarkers, and to identify new molecular pathways that are involved in SMA. This shows that proteomics is a very powerful tool and can be used to answer a wide range of questions.

7.4 Ubiquitin pathology in neurodegenerative disease

The ubiquitin-proteasome system is one of the routes of protein and organelle clearance in eukaryotic cell (Rubinsztein 2006). Disruptions in this system has been linked to several neurodegenerative diseases. Accumulation of ubiquitin conjugates and/or inclusion bodies associated with ubiquitin have been reported in for example neurofibriallary tangles of Alzheimer's disease, brainstem Lewy bodies in Parkinsons' disease and also in Bunina bodies in ALS (Alves-Rodrigues *et al.* 1998; Shaw 2005). In the SOD1 mouse (a mouse model for ALS; (Gurney *et al.* 1994) a mutated form of the SOD1 protein forms aggregates in the cytoplasm of motor neurons and sometimes in astrocytes. These aggregates seem to form before the onset of motor dysfunction (Shaw 2005). The identification of disruption in the ubiquitination pathway in SMA mice, might therefore add SMA to the list of neurodegenerative disease that involve problems in the clearance and accumulation of proteins. The disruption of the ubiquitin pathway resulted in increased levels of β-catenin in motor neurons and muscle in SMA mice. It is not known if the β-catenin

forms aggregates in the cytoplasm and via this way produces cellular toxicity leading to cell death. Further work on the effects of β-catenin accumulation is therefore required.

7.5 Conclusion

Taken together, I have shown here potentially new targets for treatment in spinal muscular atrophy. First of all, alterations in muscle have been identified independent of motor neuron denervation, suggesting that muscle is an important target in disease pathology. Secondly, I show that ubiquitin homeostasis and β-catenin signalling is disrupted due to low levels of SMN in the neuromuscular system. In addition ubiquitin homeostasis is also disrupted in other tissues. These new insights will hopefully lead to new discoveries for treatment. And last but not least I identified two potential biomarkers in muscle and skin from SMA mice. This will hopefully help with the improvement of drug trials/clinical trials for SMA.

References

Abbara C, Estournet B, Lacomblez L, Lelievre B, Ouslimani A, Lehmann B, Viollet L, Barois A and Diquet B (2011). "Riluzole pharmacokinetics in young patients with spinal muscular atrophy." *Br J Clin Pharmacol* **71**(3): 403-410.

Abe S, Hirose D, Kado S, Iwanuma O, Saka H, Yanagisawa N and Ide Y (2009). "Increased expression of decorin during the regeneration stage of mdx mouse." *Anat Sci Int* **84**(4): 305-311.

Aberle H, Bauer A, Stappert J, Kispert A and Kemler R (1997). "beta-catenin is a target for the ubiquitin-proteasome pathway." *EMBO J* **16**(13): 3797-3804.

Aberle H, Butz S, Stappert J, Weissig H, Kemler R and Hoschuetzky H (1994). "Assembly of the cadherin-catenin complex in vitro with recombinant proteins." *J Cell Sci* **107 (Pt 12)**: 3655-3663.

Abul-Husn NS, Annangudi SP, Ma'ayan A, Ramos-Ortolaza DL, Stockton SD, Jr., Gomes I, Sweedler JV and Devi LA (2011). "Chronic morphine alters the presynaptic protein profile: identification of novel molecular targets using proteomics and network analysis." *PLoS One* **6**(10): e25535.

Ackermann B, Krober S, Torres-Benito L, Borgmann A, Peters M, Hosseini Barkooie SM, Tejero R, Jakubik M, Schreml J, Milbradt J, Wunderlich TF, Riessland M, Tabares L and Wirth B (2013). "Plastin 3 ameliorates spinal muscular atrophy via delayed axon pruning and improves neuromuscular junction functionality." *Human molecular genetics* **22**(7): 1328-1347.

Acsadi G, Lee I, Li X, Khaidakov M, Pecinova A, Parker GC and Huttemann M (2009). "Mitochondrial dysfunction in a neural cell model of spinal muscular atrophy." *Journal of neuroscience research* **87**(12): 2748-2756.

Alves-Rodrigues A, Gregori L and Figueiredo-Pereira ME (1998). "Ubiquitin, cellular inclusions and their role in neurodegeneration." *Trends Neurosci* **21**(12): 516-520.

Anderson K, Potter A, Baban D and Davies KE (2003). "Protein expression changes in spinal muscular atrophy revealed with a novel antibody array technology." *Brain : a journal of neurology* **126**(Pt 9): 2052-2064.

Andreassi C, Angelozzi C, Tiziano FD, Vitali T, De Vincenzi E, Boninsegna A, Villanova M, Bertini E, Pini A, Neri G and Brahe C (2004). "Phenylbutyrate increases SMN expression in vitro: relevance for treatment of spinal muscular atrophy." *Eur J Hum Genet* **12**(1): 59-65.

Arkblad E, Tulinius M, Kroksmark AK, Henricsson M and Darin N (2009). "A population-based study of genotypic and phenotypic variability in children with spinal muscular atrophy." *Acta Paediatr* **98**(5): 865-872.

Arnold AS, Gueye M, Guettier-Sigrist S, Courdier-Fruh I, Coupin G, Poindron P and Gies JP (2004). "Reduced expression of nicotinic AChRs in myotubes from spinal muscular atrophy I patients." *Laboratory investigation; a journal of technical methods and pathology* **84**(10): 1271-1278.

Asuthkar S, Gondi CS, Nalla AK, Velpula KK, Gorantla B and Rao JS (2012). "Urokinase-type plasminogen activator receptor (uPAR)-mediated regulation of WNT/beta-catenin signaling is enhanced in irradiated medulloblastoma cells." *J Biol Chem* **287**(24): 20576-20589.

Avila AM, Burnett BG, Taye AA, Gabanella F, Knight MA, Hartenstein P, Cizman Z, Di Prospero NA, Pellizzoni L, Fischbeck KH and Sumner CJ (2007). "Trichostatin A increases SMN expression and survival in a mouse model of spinal muscular atrophy." *The Journal of clinical investigation* **117**(3): 659-671.

Azzouz M, Le T, Ralph GS, Walmsley L, Monani UR, Lee DC, Wilkes F, Mitrophanous KA, Kingsman SM, Burghes AH and Mazarakis ND (2004). "Lentivector-mediated SMN replacement in a mouse model of spinal muscular atrophy." *J Clin Invest* **114**(12): 1726-1731.

Balice-Gordon RJ and Lichtman JW (1993). "In vivo observations of pre- and postsynaptic changes during the transition from multiple to single innervation at developing neuromuscular junctions." *J Neurosci* **13**(2): 834-855.

Balut CM, Loch CM and Devor DC (2011). "Role of ubiquitylation and USP8-dependent deubiquitylation in the endocytosis and lysosomal targeting of plasma membrane KCa3.1." *FASEB J* **25**(11): 3938-3948.

Bantscheff M, Schirle M, Sweetman G, Rick J and Kuster B (2007). "Quantitative mass spectrometry in proteomics: a critical review." *Anal Bioanal Chem* **389**(4): 1017-1031.

Bassell GJ, Zhang H, Byrd AL, Femino AM, Singer RH, Taneja KL, Lifshitz LM, Herman IM and Kosik KS (1998). "Sorting of beta-actin mRNA and protein to neurites and growth cones in culture." *J Neurosci* **18**(1): 251-265.

Baumer D, Lee S, Nicholson G, Davies JL, Parkinson NJ, Murray LM, Gillingwater TH, Ansorge O, Davies KE and Talbot K (2009). "Alternative splicing events are a late feature of pathology in a mouse model of spinal muscular atrophy." *PLoS genetics* **5**(12): e1000773.

Beal MF (2000). "Mitochondria and the pathogenesis of ALS." *Brain* **123 (Pt 7)**: 1291-1292.

Beattie CE, Carrel TL and McWhorter ML (2007). "Fishing for a mechanism: using zebrafish to understand spinal muscular atrophy." *J Child Neurol* **22**(8): 995-1003.

Bebee TW, Dominguez CE and Chandler DS (2012). "Mouse models of SMA: tools for disease characterization and therapeutic development." *Human genetics*.

Berman SA, Moss D and Bursztajn S (1993). "Axonal branching and growth cone structure depend on target cells." *Dev Biol* **159**(1): 153-162.

Bernard-Marissal N, Moumen A, Sunyach C, Pellegrino C, Dudley K, Henderson CE, Raoul C and Pettmann B (2012). "Reduced calreticulin levels link endoplasmic reticulum stress and Fas-triggered cell death in motoneurons vulnerable to ALS." *J Neurosci* **32**(14): 4901-4912.

Bevan AK, Hutchinson KR, Foust KD, Braun L, McGovern VL, Schmelzer L, Ward JG, Petruska JC, Lucchesi PA, Burghes AH and Kaspar BK (2010). "Early

heart failure in the SMNDelta7 model of spinal muscular atrophy and correction by postnatal scAAV9-SMN delivery." *Hum Mol Genet* **19**(20): 3895-3905.

Bhattacharyya T, Karnezis AN, Murphy SP, Hoang T, Freeman BC, Phillips B and Morimoto RI (1995). "Cloning and subcellular localization of human mitochondrial hsp70." *J Biol Chem* **270**(4): 1705-1710.

Borycki AG and Emerson CP, Jr. (2000). "Multiple tissue interactions and signal transduction pathways control somite myogenesis." *Curr Top Dev Biol* **48**: 165-224.

Bosch-Marce M, Wee CD, Martinez TL, Lipkes CE, Choe DW, Kong L, Van Meerbeke JP, Musaro A and Sumner CJ (2011). "Increased IGF-1 in muscle modulates the phenotype of severe SMA mice." *Human molecular genetics* **20**(9): 1844-1853.

Bowerman M, Anderson CL, Beauvais A, Boyl PP, Witke W and Kothary R (2009). "SMN, profilin IIa and plastin 3: a link between the deregulation of actin dynamics and SMA pathogenesis." *Molecular and cellular neurosciences* **42**(1): 66-74.

Bowerman M, Swoboda KJ, Michalski JP, Wang GS, Reeks C, Beauvais A, Murphy K, Woulfe J, Screaton RA, Scott FW and Kothary R (2012). "Glucose metabolism and pancreatic defects in spinal muscular atrophy." *Ann Neurol* **72**(2): 256-268.

Brahe C, Vitali T, Tiziano FD, Angelozzi C, Pinto AM, Borgo F, Moscato U, Bertini E, Mercuri E and Neri G (2005). "Phenylbutyrate increases SMN gene expression in spinal muscular atrophy patients." *Eur J Hum Genet* **13**(2): 256-259.

Braun S, Croizat B, Lagrange MC, Poindron P and Warter JM (1997). "Degeneration of cocultures of spinal muscular atrophy muscle cells and rat spinal cord explants is not due to secreted factors and cannot be prevented by neurotrophins." *Muscle & nerve* **20**(8): 953-960.

Braun S, Croizat B, Lagrange MC, Warter JM and Poindron P (1995). "Constitutive muscular abnormalities in culture in spinal muscular atrophy." *Lancet* **345**(8951): 694-695.

Brichta L, Hofmann Y, Hahnen E, Siebzehnrubl FA, Raschke H, Blumcke I, Eyupoglu IY and Wirth B (2003). "Valproic acid increases the SMN2 protein level: a well-known drug as a potential therapy for spinal muscular atrophy." *Hum Mol Genet* **12**(19): 2481-2489.

Brichta L, Holker I, Haug K, Klockgether T and Wirth B (2006). "In vivo activation of SMN in spinal muscular atrophy carriers and patients treated with valproate." *Ann Neurol* **59**(6): 970-975.

Brzustowicz LM, Lehner T, Castilla LH, Penchaszadeh GK, Wilhelmsen KC, Daniels R, Davies KE, Leppert M, Ziter F, Wood D and et al. (1990). "Genetic mapping of chronic childhood-onset spinal muscular atrophy to chromosome 5q11.2-13.3." *Nature* **344**(6266): 540-541.

Burghes AH and Beattie CE (2009). "Spinal muscular atrophy: why do low levels of survival motor neuron protein make motor neurons sick?" *Nature reviews. Neuroscience* **10**(8): 597-609.

Burnett BG, Munoz E, Tandon A, Kwon DY, Sumner CJ and Fischbeck KH (2009). "Regulation of SMN protein stability." *Mol Cell Biol* **29**(5): 1107-1115.

Butchbach ME, Singh J, Thorsteinsdottir M, Saieva L, Slominski E, Thurmond J, Andresson T, Zhang J, Edwards JD, Simard LR, Pellizzoni L, Jarecki J, Burghes AH and Gurney ME (2010). "Effects of 2,4-diaminoquinazoline derivatives on SMN expression and phenotype in a mouse model for spinal muscular atrophy." *Hum Mol Genet* **19**(3): 454-467.

Chan YB, Miguel-Aliaga I, Franks C, Thomas N, Trulzsch B, Sattelle DB, Davies KE and van den Heuvel M (2003). "Neuromuscular defects in a Drosophila survival motor neuron gene mutant." *Human molecular genetics* **12**(12): 1367-1376.

Chang HC, Hung WC, Chuang YJ and Jong YJ (2004). "Degradation of survival motor neuron (SMN) protein is mediated via the ubiquitin/proteasome pathway." *Neurochem Int* **45**(7): 1107-1112.

Chang JG, Hsieh-Li HM, Jong YJ, Wang NM, Tsai CH and Li H (2001). "Treatment of spinal muscular atrophy by sodium butyrate." *Proc Natl Acad Sci U S A* **98**(17): 9808-9813.

Chen CN, Chang CC, Su TE, Hsu WM, Jeng YM, Ho MC, Hsieh FJ, Lee PH, Kuo ML, Lee H and Chang KJ (2009). "Identification of calreticulin as a prognosis marker and angiogenic regulator in human gastric cancer." *Ann Surg Oncol* **16**(2): 524-533.

Chen TH, Chang JG, Yang YH, Mai HH, Liang WC, Wu YC, Wang HY, Huang YB, Wu SM, Chen YC, Yang SN and Jong YJ (2010). "Randomized, double-blind, placebo-controlled trial of hydroxyurea in spinal muscular atrophy." *Neurology* **75**(24): 2190-2197.

Cheng EH, Sheiko TV, Fisher JK, Craigen WJ and Korsmeyer SJ (2003). "VDAC2 inhibits BAK activation and mitochondrial apoptosis." *Science* **301**(5632): 513-517.

Christ B and Ordahl CP (1995). "Early stages of chick somite development." *Anat Embryol (Berl)* **191**(5): 381-396.

Cifuentes-Diaz C, Frugier T, Tiziano FD, Lacene E, Roblot N, Joshi V, Moreau MH and Melki J (2001). "Deletion of murine SMN exon 7 directed to skeletal muscle leads to severe muscular dystrophy." *The Journal of cell biology* **152**(5): 1107-1114.

Cook JD, Iannaccone ST, Russman BS, Samaha F, Buncher RR, Ross D, Hare M, Smith C, Perkins B, Zimmerman L and et al. (1990). "A methodology to measure the strength of SMA patients. Dallas-Cincinnati-Newington Spinal Muscular Atrophy (DCN-SMA) Study Group." *Muscle Nerve* **13 Suppl**: S7-10.

Corti S, Locatelli F, Papadimitriou D, Del Bo R, Nizzardo M, Nardini M, Donadoni C, Salani S, Fortunato F, Strazzer S, Bresolin N and Comi GP (2007). "Neural stem cells LewisX+ CXCR4+ modify disease progression in an amyotrophic lateral sclerosis model." *Brain* **130**(Pt 5): 1289-1305.

Corti S, Nizzardo M, Nardini M, Donadoni C, Salani S, Ronchi D, Saladino F, Bordoni A, Fortunato F, Del Bo R, Papadimitriou D, Locatelli F, Menozzi G, Strazzer S, Bresolin N and Comi GP (2008). "Neural stem cell

transplantation can ameliorate the phenotype of a mouse model of spinal muscular atrophy." *J Clin Invest* **118**(10): 3316-3330.

Corti S, Nizzardo M, Nardini M, Donadoni C, Salani S, Ronchi D, Simone C, Falcone M, Papadimitriou D, Locatelli F, Mezzina N, Gianni F, Bresolin N and Comi GP (2010). "Embryonic stem cell-derived neural stem cells improve spinal muscular atrophy phenotype in mice." *Brain* **133**(Pt 2): 465-481.

Cossu G, Tajbakhsh S and Buckingham M (1996). "How is myogenesis initiated in the embryo?" *Trends Genet* **12**(6): 218-223.

Court FA, Gillingwater TH, Melrose S, Sherman DL, Greenshields KN, Morton AJ, Harris JB, Willison HJ and Ribchester RR (2008). "Identity, developmental restriction and reactivity of extralaminar cells capping mammalian neuromuscular junctions." *J Cell Sci* **121**(Pt 23): 3901-3911.

Cox B and Emili A (2006). "Tissue subcellular fractionation and protein extraction for use in mass-spectrometry-based proteomics." *Nat Protoc* **1**(4): 1872-1878.

Crawford TO, Paushkin SV, Kobayashi DT, Forrest SJ, Joyce CL, Finkel RS, Kaufmann P, Swoboda KJ, Tiziano D, Lomastro R, Li RH, Trachtenberg FL, Plasterer T and Chen KS (2012). "Evaluation of SMN protein, transcript, and copy number in the biomarkers for spinal muscular atrophy (BforSMA) clinical study." *PloS one* **7**(4): e33572.

Dachs E, Hereu M, Piedrafita L, Casanovas A, Caldero J and Esquerda JE (2011). "Defective neuromuscular junction organization and postnatal myogenesis in mice with severe spinal muscular atrophy." *J Neuropathol Exp Neurol* **70**(6): 444-461.

Darbar IA, Plaggert PG, Resende MB, Zanoteli E and Reed UC (2011). "Evaluation of muscle strength and motor abilities in children with type II and III spinal muscle atrophy treated with valproic acid." *BMC Neurol* **11**: 36.

De Mena L, Coto E, Sanchez-Ferrero E, Ribacoba R, Guisasola LM, Salvador C, Blazquez M and Alvarez V (2009). "Mutational screening of the mortalin gene (HSPA9) in Parkinson's disease." *J Neural Transm* **116**(10): 1289-1293.

de Morree A, Hensbergen PJ, van Haagen HH, Dragan I, Deelder AM, t Hoen PA, Frants RR and van der Maarel SM (2010). "Proteomic analysis of the dysferlin protein complex unveils its importance for sarcolemmal maintenance and integrity." *PLoS One* **5**(11): e13854.

de Ruijter AJ, van Gennip AH, Caron HN, Kemp S and van Kuilenburg AB (2003). "Histone deacetylases (HDACs): characterization of the classical HDAC family." *Biochem J* **370**(Pt 3): 737-749.

DeChiara TM, Bowen DC, Valenzuela DM, Simmons MV, Poueymirou WT, Thomas S, Kinetz E, Compton DL, Rojas E, Park JS, Smith C, DiStefano PS, Glass DJ, Burden SJ and Yancopoulos GD (1996). "The receptor tyrosine kinase MuSK is required for neuromuscular junction formation in vivo." *Cell* **85**(4): 501-512.

Deocaris CC, Kaul SC and Wadhwa R (2009). "The versatile stress protein mortalin as a chaperone therapeutic agent." *Protein Pept Lett* **16**(5): 517-529.

DiAntonio A, Haghighi AP, Portman SL, Lee JD, Amaranto AM and Goodman CS (2001). "Ubiquitination-dependent mechanisms regulate synaptic growth and function." *Nature* **412**(6845): 449-452.

Dietrich S, Abou-Rebyeh F, Brohmann H, Bladt F, Sonnenberg-Riethmacher E, Yamaai T, Lumsden A, Brand-Saberi B and Birchmeier C (1999). "The role of SF/HGF and c-Met in the development of skeletal muscle." *Development* **126**(8): 1621-1629.

Dominguez E, Marais T, Chatauret N, Benkhelifa-Ziyyat S, Duque S, Ravassard P, Carcenac R, Astord S, Pereira de Moura A, Voit T and Barkats M (2011). "Intravenous scAAV9 delivery of a codon-optimized SMN1 sequence rescues SMA mice." *Hum Mol Genet* **20**(4): 681-693.

El-Khodor BF, Cirillo K, Beltran JA, Mushlin R, Winberg ML, Charney R, Chomicova O, Marino T and Ramboz S (2012). "Prediction of death in the SMNDelta7 mouse model of spinal muscular atrophy: insight into disease stage and progression." *J Neurosci Methods* **209**(2): 259-268.

Evans AR, Euteneuer S, Chavez E, Mullen LM, Hui EE, Bhatia SN and Ryan AF (2007). "Laminin and fibronectin modulate inner ear spiral ganglion neurite outgrowth in an in vitro alternate choice assay." *Dev Neurobiol* **67**(13): 1721-1730.

Evans MC, Cherry JJ and Androphy EJ (2011). "Differential regulation of the SMN2 gene by individual HDAC proteins." *Biochem Biophys Res Commun* **414**(1): 25-30.

Fan L and Simard LR (2002). "Survival motor neuron (SMN) protein: role in neurite outgrowth and neuromuscular maturation during neuronal differentiation and development." *Hum Mol Genet* **11**(14): 1605-1614.

Fang D, Hawke D, Zheng Y, Xia Y, Meisenhelder J, Nika H, Mills GB, Kobayashi R, Hunter T and Lu Z (2007). "Phosphorylation of beta-catenin by AKT promotes beta-catenin transcriptional activity." *J Biol Chem* **282**(15): 11221-11229.

Farooq F, Molina FA, Hadwen J, MacKenzie D, Witherspoon L, Osmond M, Holcik M and MacKenzie A (2011). "Prolactin increases SMN expression and survival in a mouse model of severe spinal muscular atrophy via the STAT5 pathway." *The Journal of clinical investigation* **121**(8): 3042-3050.

Feldkotter M, Schwarzer V, Wirth R, Wienker TF and Wirth B (2002). "Quantitative analyses of SMN1 and SMN2 based on real-time lightCycler PCR: fast and highly reliable carrier testing and prediction of severity of spinal muscular atrophy." *Am J Hum Genet* **70**(2): 358-368.

Fidzianska A, Goebel HH and Warlo I (1990). "Acute infantile spinal muscular atrophy. Muscle apoptosis as a proposed pathogenetic mechanism." *Brain* **113 (Pt 2)**: 433-445.

Finkel RS, Crawford TO, Swoboda KJ, Kaufmann P, Juhasz P, Li X, Guo Y, Li RH, Trachtenberg F, Forrest SJ, Kobayashi DT, Chen KS, Joyce CL and Plasterer T (2012). "Candidate proteins, metabolites and transcripts in the Biomarkers for Spinal Muscular Atrophy (BforSMA) clinical study." *PloS one* **7**(4): e35462.

Foust KD, Wang X, McGovern VL, Braun L, Bevan AK, Haidet AM, Le TT, Morales PR, Rich MM, Burghes AH and Kaspar BK (2010). "Rescue of the spinal

muscular atrophy phenotype in a mouse model by early postnatal delivery of SMN." *Nat Biotechnol* **28**(3): 271-274.

Frugier T, Tiziano FD, Cifuentes-Diaz C, Miniou P, Roblot N, Dierich A, Le Meur M and Melki J (2000). "Nuclear targeting defect of SMN lacking the C-terminus in a mouse model of spinal muscular atrophy." *Hum Mol Genet* **9**(5): 849-858.

Fuller HR, Man NT, Lam le T, Shamanin VA, Androphy EJ and Morris GE (2010). "Valproate and bone loss: iTRAQ proteomics show that valproate reduces collagens and osteonectin in SMA cells." *J Proteome Res* **9**(8): 4228-4233.

Gabanella F, Carissimi C, Usiello A and Pellizzoni L (2005). "The activity of the spinal muscular atrophy protein is regulated during development and cellular differentiation." *Human molecular genetics* **14**(23): 3629-3642.

Gailly P (2002). "New aspects of calcium signaling in skeletal muscle cells: implications in Duchenne muscular dystrophy." *Biochim Biophys Acta* **1600**(1-2): 38-44.

Gall JG (2003). "The centennial of the Cajal body." *Nat Rev Mol Cell Biol* **4**(12): 975-980.

Garbes L, Riessland M, Holker I, Heller R, Hauke J, Trankle C, Coras R, Blumcke I, Hahnen E and Wirth B (2009). "LBH589 induces up to 10-fold SMN protein levels by several independent mechanisms and is effective even in cells from SMA patients non-responsive to valproate." *Hum Mol Genet* **18**(19): 3645-3658.

Gautam M, Noakes PG, Mudd J, Nichol M, Chu GC, Sanes JR and Merlie JP (1995). "Failure of postsynaptic specialization to develop at neuromuscular junctions of rapsyn-deficient mice." *Nature* **377**(6546): 232-236.

Gavrilina TO, McGovern VL, Workman E, Crawford TO, Gogliotti RG, DiDonato CJ, Monani UR, Morris GE and Burghes AH (2008). "Neuronal SMN expression corrects spinal muscular atrophy in severe SMA mice while muscle-specific SMN expression has no phenotypic effect." *Human molecular genetics* **17**(8): 1063-1075.

Gelebart P, Anand M, Armanious H, Peters AC, Dien Bard J, Amin HM and Lai R (2008). "Constitutive activation of the Wnt canonical pathway in mantle cell lymphoma." *Blood* **112**(13): 5171-5179.

Goll DE, Thompson VF, Li H, Wei W and Cong J (2003). "The calpain system." *Physiol Rev* **83**(3): 731-801.

Gorg A, Weiss W and Dunn MJ (2004). "Current two-dimensional electrophoresis technology for proteomics." *Proteomics* **4**(12): 3665-3685.

Greensmith L and Vrbova G (1997). "Disturbances of neuromuscular interaction may contribute to muscle weakness in spinal muscular atrophy." *Neuromuscular disorders : NMD* **7**(6-7): 369-372.

Grefte S, Kuijpers-Jagtman AM, Torensma R and Von den Hoff JW (2007). "Skeletal muscle development and regeneration." *Stem Cells Dev* **16**(5): 857-868.

Gromov P, Gromova I, Bunkenborg J, Cabezon T, Moreira JM, Timmermans-Wielenga V, Roepstorff P, Rank F and Celis JE (2010). "Up-regulated

proteins in the fluid bathing the tumour cell microenvironment as potential serological markers for early detection of cancer of the breast." *Mol Oncol* **4**(1): 65-89.

Gros J, Scaal M and Marcelle C (2004). "A two-step mechanism for myotome formation in chick." *Dev Cell* **6**(6): 875-882.

Grossi A, Lametsch R, Karlsson AH and Lawson MA (2011). "Mechanical stimuli on C2C12 myoblasts affect myoblast differentiation, focal adhesion kinase phosphorylation and galectin-1 expression: a proteomic approach." *Cell Biol Int* **35**(6): 579-586.

Grunstein M (1997). "Histone acetylation in chromatin structure and transcription." *Nature* **389**(6649): 349-352.

Grzeschik SM, Ganta M, Prior TW, Heavlin WD and Wang CH (2005). "Hydroxyurea enhances SMN2 gene expression in spinal muscular atrophy cells." *Ann Neurol* **58**(2): 194-202.

Gubitz AK, Feng W and Dreyfuss G (2004). "The SMN complex." *Experimental cell research* **296**(1): 51-56.

Gubitz AK, Mourelatos Z, Abel L, Rappsilber J, Mann M and Dreyfuss G (2002). "Gemin5, a novel WD repeat protein component of the SMN complex that binds Sm proteins." *J Biol Chem* **277**(7): 5631-5636.

Guest PC, Gottschalk MG and Bahn S (2013). "Proteomics: improving biomarker translation to modern medicine?" *Genome medicine* **5**(2): 17.

Guettier-Sigrist S, Coupin G, Braun S, Warter JM and Poindron P (1998). "Muscle could be the therapeutic target in SMA treatment." *Journal of neuroscience research* **53**(6): 663-669.

Guettier-Sigrist S, Hugel B, Coupin G, Freyssinet JM, Poindron P and Warter JM (2002). "Possible pathogenic role of muscle cell dysfunction in motor neuron death in spinal muscular atrophy." *Muscle Nerve* **25**(5): 700-708.

Gumbiner BM (1997). "Carcinogenesis: a balance between beta-catenin and APC." *Curr Biol* **7**(7): R443-446.

Gurney ME, Pu H, Chiu AY, Dal Canto MC, Polchow CY, Alexander DD, Caliendo J, Hentati A, Kwon YW, Deng HX and et al. (1994). "Motor neuron degeneration in mice that express a human Cu,Zn superoxide dismutase mutation." *Science* **264**(5166): 1772-1775.

Gygi SP, Rist B, Gerber SA, Turecek F, Gelb MH and Aebersold R (1999). "Quantitative analysis of complex protein mixtures using isotope-coded affinity tags." *Nat Biotechnol* **17**(10): 994-999.

Haddad H, Cifuentes-Diaz C, Miroglio A, Roblot N, Joshi V and Melki J (2003). "Riluzole attenuates spinal muscular atrophy disease progression in a mouse model." *Muscle Nerve* **28**(4): 432-437.

Hahnen E, Eyupoglu IY, Brichta L, Haastert K, Trankle C, Siebzehnrubl FA, Riessland M, Holker I, Claus P, Romstock J, Buslei R, Wirth B and Blumcke I (2006). "In vitro and ex vivo evaluation of second-generation histone deacetylase inhibitors for the treatment of spinal muscular atrophy." *Journal of neurochemistry* **98**(1): 193-202.

Hamilton G and Gillingwater TH (2013). "Spinal muscular atrophy: going beyond the motor neuron." *Trends Mol Med* **19**(1): 40-50.

Hastings ML, Berniac J, Liu YH, Abato P, Jodelka FM, Barthel L, Kumar S, Dudley C, Nelson M, Larson K, Edmonds J, Bowser T, Draper M, Higgins P and Krainer AR (2009). "Tetracyclines that promote SMN2 exon 7 splicing as therapeutics for spinal muscular atrophy." *Sci Transl Med* **1**(5): 5ra12.

Hayhurst M, Wagner AK, Cerletti M, Wagers AJ and Rubin LL (2012). "A cell-autonomous defect in skeletal muscle satellite cells expressing low levels of survival of motor neuron protein." *Dev Biol* **368**(2): 323-334.

He TC, Sparks AB, Rago C, Hermeking H, Zawel L, da Costa LT, Morin PJ, Vogelstein B and Kinzler KW (1998). "Identification of c-MYC as a target of the APC pathway." *Science* **281**(5382): 1509-1512.

Hegedus J, Putman CT and Gordon T (2007). "Time course of preferential motor unit loss in the SOD1 G93A mouse model of amyotrophic lateral sclerosis." *Neurobiol Dis* **28**(2): 154-164.

Heier CR and DiDonato CJ (2009). "Translational readthrough by the aminoglycoside geneticin (G418) modulates SMN stability in vitro and improves motor function in SMA mice in vivo." *Hum Mol Genet* **18**(7): 1310-1322.

Heier CR, Satta R, Lutz C and DiDonato CJ (2010). "Arrhythmia and cardiac defects are a feature of spinal muscular atrophy model mice." *Hum Mol Genet* **19**(20): 3906-3918.

Henderson CE, Hauser SL, Huchet M, Dessi F, Hentati F, Taguchi T, Changeux JP and Fardeau M (1987). "Extracts of muscle biopsies from patients with spinal muscular atrophies inhibit neurite outgrowth from spinal neurons." *Neurology* **37**(8): 1361-1364.

Higuchi I, Hashiguchi A, Matsuura E, Higashi K, Shiraishi T, Hirata N, Arimura K and Osame M (2007). "Different pattern of HSP47 expression in skeletal muscle of patients with neuromuscular diseases." *Neuromuscul Disord* **17**(3): 221-226.

Hockly E, Richon VM, Woodman B, Smith DL, Zhou X, Rosa E, Sathasivam K, Ghazi-Noori S, Mahal A, Lowden PA, Steffan JS, Marsh JL, Thompson LM, Lewis CM, Marks PA and Bates GP (2003). "Suberoylanilide hydroxamic acid, a histone deacetylase inhibitor, ameliorates motor deficits in a mouse model of Huntington's disease." *Proc Natl Acad Sci U S A* **100**(4): 2041-2046.

Hogan PG, Chen L, Nardone J and Rao A (2003). "Transcriptional regulation by calcium, calcineurin, and NFAT." *Genes Dev* **17**(18): 2205-2232.

Hoschuetzky H, Aberle H and Kemler R (1994). "Beta-catenin mediates the interaction of the cadherin-catenin complex with epidermal growth factor receptor." *J Cell Biol* **127**(5): 1375-1380.

Hsieh-Li HM, Chang JG, Jong YJ, Wu MH, Wang NM, Tsai CH and Li H (2000). "A mouse model for spinal muscular atrophy." *Nature genetics* **24**(1): 66-70.

Hsu SH, Lai MC, Er TK, Yang SN, Hung CH, Tsai HH, Lin YC, Chang JG, Lo YC and Jong YJ (2010). "Ubiquitin carboxyl-terminal hydrolase L1 (UCHL1) regulates the level of SMN expression through ubiquitination in primary spinal muscular atrophy fibroblasts." *Clinica chimica acta; international journal of clinical chemistry* **411**(23-24): 1920-1928.

Hsu WM, Hsieh FJ, Jeng YM, Kuo ML, Chen CN, Lai DM, Hsieh LJ, Wang BT, Tsao PN, Lee H, Lin MT, Lai HS and Chen WJ (2005). "Calreticulin expression in neuroblastoma--a novel independent prognostic factor." *Ann Oncol* **16**(2): 314-321.

Hsu WM, Lee H, Juan HF, Shih YY, Wang BJ, Pan CY, Jeng YM, Chang HH, Lu MY, Lin KH, Lai HS, Chen WJ, Tsay YG, Liao YF and Hsieh FJ (2008). "Identification of GRP75 as an independent favorable prognostic marker of neuroblastoma by a proteomics analysis." *Clin Cancer Res* **14**(19): 6237-6245.

Hua Y, Sahashi K, Hung G, Rigo F, Passini MA, Bennett CF and Krainer AR (2010). "Antisense correction of SMN2 splicing in the CNS rescues necrosis in a type III SMA mouse model." *Genes & development* **24**(15): 1634-1644.

Hua Y, Sahashi K, Rigo F, Hung G, Horev G, Bennett CF and Krainer AR (2011). "Peripheral SMN restoration is essential for long-term rescue of a severe spinal muscular atrophy mouse model." *Nature* **478**(7367): 123-126.

Jensen ON (2004). "Modification-specific proteomics: characterization of post-translational modifications by mass spectrometry." *Curr Opin Chem Biol* **8**(1): 33-41.

Kariya S, Park GH, Maeno-Hikichi Y, Leykekhman O, Lutz C, Arkovitz MS, Landmesser LT and Monani UR (2008). "Reduced SMN protein impairs maturation of the neuromuscular junctions in mouse models of spinal muscular atrophy." *Human molecular genetics* **17**(16): 2552-2569.

Kassar-Duchossoy L, Gayraud-Morel B, Gomes D, Rocancourt D, Buckingham M, Shinin V and Tajbakhsh S (2004). "Mrf4 determines skeletal muscle identity in Myf5:Myod double-mutant mice." *Nature* **431**(7007): 466-471.

Katoh-Semba R, Asano T, Ueda H, Morishita R, Takeuchi IK, Inaguma Y and Kato K (2002). "Riluzole enhances expression of brain-derived neurotrophic factor with consequent proliferation of granule precursor cells in the rat hippocampus." *FASEB J* **16**(10): 1328-1330.

Kaufmann P, McDermott MP, Darras BT, Finkel R, Kang P, Oskoui M, Constantinescu A, Sproule DM, Foley AR, Yang M, Tawil R, Chung W, Martens B, Montes J, O'Hagen J, Dunaway S, Flickinger JM, Quigley J, Riley S, Glanzman AM, Benton M, Ryan PA, Irvine C, Annis CL, Butler H, Caracciolo J, Montgomery M, Marra J, Koo B and De Vivo DC (2011). "Observational study of spinal muscular atrophy type 2 and 3: functional outcomes over 1 year." *Arch Neurol* **68**(6): 779-786.

Kim N, Stiegler AL, Cameron TO, Hallock PT, Gomez AM, Huang JH, Hubbard SR, Dustin ML and Burden SJ (2008). "Lrp4 is a receptor for Agrin and forms a complex with MuSK." *Cell* **135**(2): 334-342.

Kissel JT, Scott CB, Reyna SP, Crawford TO, Simard LR, Krosschell KJ, Acsadi G, Elsheik B, Schroth MK, D'Anjou G, LaSalle B, Prior TW, Sorenson S, Maczulski JA, Bromberg MB, Chan GM and Swoboda KJ (2011). "SMA CARNIVAL TRIAL PART II: a prospective, single-armed trial of L-carnitine and valproic acid in ambulatory children with spinal muscular atrophy." *PLoS One* **6**(7): e21296.

Kobayashi DT, Shi J, Stephen L, Ballard KL, Dewey R, Mapes J, Chung B, McCarthy K, Swoboda KJ, Crawford TO, Li R, Plasterer T, Joyce C, Chung WK,

Kaufmann P, Darras BT, Finkel RS, Sproule DM, Martens WB, McDermott MP, De Vivo DC, Walker MG and Chen KS (2013). "SMA-MAP: A Plasma Protein Panel for Spinal Muscular Atrophy." *PLoS One* **8**(4): e60113.

Kolb SJ, Gubitz AK, Olszewski RF, Jr., Ottinger E, Sumner CJ, Fischbeck KH and Dreyfuss G (2006). "A novel cell immunoassay to measure survival of motor neurons protein in blood cells." *BMC Neurol* **6**: 6.

Kong L, Wang X, Choe DW, Polley M, Burnett BG, Bosch-Marce M, Griffin JW, Rich MM and Sumner CJ (2009). "Impaired synaptic vesicle release and immaturity of neuromuscular junctions in spinal muscular atrophy mice." *The Journal of neuroscience : the official journal of the Society for Neuroscience* **29**(3): 842-851.

Korhonen L and Lindholm D (2004). "The ubiquitin proteasome system in synaptic and axonal degeneration: a new twist to an old cycle." *J Cell Biol* **165**(1): 27-30.

La Bella V, Kallenbach S and Pettmann B (2000). "Expression and subcellular localization of two isoforms of the survival motor neuron protein in different cell types." *J Neurosci Res* **62**(3): 346-356.

Larsen CN, Krantz BA and Wilkinson KD (1998). "Substrate specificity of deubiquitinating enzymes: ubiquitin C-terminal hydrolases." *Biochemistry* **37**(10): 3358-3368.

Le TT, Pham LT, Butchbach ME, Zhang HL, Monani UR, Coovert DD, Gavrilina TO, Xing L, Bassell GJ and Burghes AH (2005). "SMNDelta7, the major product of the centromeric survival motor neuron (SMN2) gene, extends survival in mice with spinal muscular atrophy and associates with full-length SMN." *Human molecular genetics* **14**(6): 845-857.

Lebrilla CB and Mahal LK (2009). "Post-translation modifications." *Curr Opin Chem Biol* **13**(4): 373-374.

Lefebvre S, Burglen L, Reboullet S, Clermont O, Burlet P, Viollet L, Benichou B, Cruaud C, Millasseau P, Zeviani M and et al. (1995). "Identification and characterization of a spinal muscular atrophy-determining gene." *Cell* **80**(1): 155-165.

Lewelt A, Krosschell KJ, Scott C, Sakonju A, Kissel JT, Crawford TO, Acsadi G, D'Anjou G, Elsheikh B, Reyna SP, Schroth MK, Maczulski JA, Stoddard GJ, Elovic E and Swoboda KJ (2010). "Compound muscle action potential and motor function in children with spinal muscular atrophy." *Muscle Nerve* **42**(5): 703-708.

Lewis KE and Eisen JS (2001). "Hedgehog signaling is required for primary motoneuron induction in zebrafish." *Development* **128**(18): 3485-3495.

Li XM, Dong XP, Luo SW, Zhang B, Lee DH, Ting AK, Neiswender H, Kim CH, Carpenter-Hyland E, Gao TM, Xiong WC and Mei L (2008). "Retrograde regulation of motoneuron differentiation by muscle beta-catenin." *Nat Neurosci* **11**(3): 262-268.

Li ZB, Lehar M, Samlan R and Flint PW (2005). "Proteomic analysis of rat laryngeal muscle following denervation." *Proteomics* **5**(18): 4764-4776.

Lichtman JW and Colman H (2000). "Synapse elimination and indelible memory." *Neuron* **25**(2): 269-278.

Lim SR and Hertel KJ (2001). "Modulation of survival motor neuron pre-mRNA splicing by inhibition of alternative 3' splice site pairing." *J Biol Chem* **276**(48): 45476-45483.

Lin W, Burgess RW, Dominguez B, Pfaff SL, Sanes JR and Lee KF (2001). "Distinct roles of nerve and muscle in postsynaptic differentiation of the neuromuscular synapse." *Nature* **410**(6832): 1057-1064.

Ling KK, Gibbs RM, Feng Z and Ko CP (2012). "Severe neuromuscular denervation of clinically relevant muscles in a mouse model of spinal muscular atrophy." *Human molecular genetics* **21**(1): 185-195.

Liu C, Li Y, Semenov M, Han C, Baeg GH, Tan Y, Zhang Z, Lin X and He X (2002). "Control of beta-catenin phosphorylation/degradation by a dual-kinase mechanism." *Cell* **108**(6): 837-847.

Liu Q and Dreyfuss G (1996). "A novel nuclear structure containing the survival of motor neurons protein." *The EMBO journal* **15**(14): 3555-3565.

Liu Q, Fischer U, Wang F and Dreyfuss G (1997). "The spinal muscular atrophy disease gene product, SMN, and its associated protein SIP1 are in a complex with spliceosomal snRNP proteins." *Cell* **90**(6): 1013-1021.

Liu R, Gong J, Chen J, Li Q, Song C, Zhang J, Li Y, Liu Z, Dong Y, Chen L and Jin B (2012). "Calreticulin as a potential diagnostic biomarker for lung cancer." *Cancer Immunol Immunother* **61**(6): 855-864.

Liu X, Kim CN, Yang J, Jemmerson R and Wang X (1996). "Induction of apoptotic program in cell-free extracts: requirement for dATP and cytochrome c." *Cell* **86**(1): 147-157.

Liu Y, Fallon L, Lashuel HA, Liu Z and Lansbury PT, Jr. (2002). "The UCH-L1 gene encodes two opposing enzymatic activities that affect alpha-synuclein degradation and Parkinson's disease susceptibility." *Cell* **111**(2): 209-218.

Livak KJ and Schmittgen TD (2001). "Analysis of relative gene expression data using real-time quantitative PCR and the 2(-Delta Delta C(T)) Method." *Methods* **25**(4): 402-408.

Lorson CL and Androphy EJ (2000). "An exonic enhancer is required for inclusion of an essential exon in the SMA-determining gene SMN." *Hum Mol Genet* **9**(2): 259-265.

Lorson CL, Hahnen E, Androphy EJ and Wirth B (1999). "A single nucleotide in the SMN gene regulates splicing and is responsible for spinal muscular atrophy." *Proc Natl Acad Sci U S A* **96**(11): 6307-6311.

Lorson CL, Rindt H and Shababi M (2010). "Spinal muscular atrophy: mechanisms and therapeutic strategies." *Human molecular genetics* **19**(R1): R111-118.

Lowery LA and Van Vactor D (2009). "The trip of the tip: understanding the growth cone machinery." *Nat Rev Mol Cell Biol* **10**(5): 332-343.

Lunn MR and Wang CH (2008). "Spinal muscular atrophy." *Lancet* **371**(9630): 2120-2133.

Mailman MD, Heinz JW, Papp AC, Snyder PJ, Sedra MS, Wirth B, Burghes AH and Prior TW (2002). "Molecular analysis of spinal muscular atrophy and modification of the phenotype by SMN2." *Genet Med* **4**(1): 20-26.

Main M, Kairon H, Mercuri E and Muntoni F (2003). "The Hammersmith functional motor scale for children with spinal muscular atrophy: a scale to test ability and monitor progress in children with limited ambulation." *Eur J Paediatr Neurol* **7**(4): 155-159.

Maness PF and Schachner M (2007). "Neural recognition molecules of the immunoglobulin superfamily: signaling transducers of axon guidance and neuronal migration." *Nat Neurosci* **10**(1): 19-26.

Mano T, Katsuno M, Banno H, Suzuki K, Suga N, Hashizume A, Tanaka F and Sobue G (2012). "Cross-sectional and longitudinal analysis of an oxidative stress biomarker for spinal and bulbar muscular atrophy." *Muscle Nerve* **46**(5): 692-697.

Markowitz JA, Tinkle MB and Fischbeck KH (2004). "Spinal muscular atrophy in the neonate." *J Obstet Gynecol Neonatal Nurs* **33**(1): 12-20.

Martinez TL, Kong L, Wang X, Osborne MA, Crowder ME, Van Meerbeke JP, Xu X, Davis C, Wooley J, Goldhamer DJ, Lutz CM, Rich MM and Sumner CJ (2012). "Survival motor neuron protein in motor neurons determines synaptic integrity in spinal muscular atrophy." *J Neurosci* **32**(25): 8703-8715.

Martinez-Hernandez R, Bernal S, Also-Rallo E, Alias L, Barcelo MJ, Hereu M, Esquerda JE and Tizzano EF (2013). "Synaptic defects in type I spinal muscular atrophy in human development." *J Pathol* **229**(1): 49-61.

Martinez-Hernandez R, Soler-Botija C, Also E, Alias L, Caselles L, Gich I, Bernal S and Tizzano EF (2009). "The developmental pattern of myotubes in spinal muscular atrophy indicates prenatal delay of muscle maturation." *J Neuropathol Exp Neurol* **68**(5): 474-481.

Martinou JC and Merlie JP (1991). "Nerve-dependent modulation of acetylcholine receptor epsilon-subunit gene expression." *J Neurosci* **11**(5): 1291-1299.

Massa R, Marliera LN, Martorana A, Cicconi S, Pierucci D, Giacomini P, De Pinto V and Castellani L (2000). "Intracellular localization and isoform expression of the voltage-dependent anion channel (VDAC) in normal and dystrophic skeletal muscle." *J Muscle Res Cell Motil* **21**(5): 433-442.

Mattis VB, Bowerman M, Kothary R and Lorson CL (2008). "A SMNDelta7 read-through product confers functionality to the SMNDelta7 protein." *Neurosci Lett* **442**(1): 54-58.

Mattis VB, Butchbach ME and Lorson CL (2008). "Detection of human survival motor neuron (SMN) protein in mice containing the SMN2 transgene: applicability to preclinical therapy development for spinal muscular atrophy." *J Neurosci Methods* **175**(1): 36-43.

Mattis VB, Ebert AD, Fosso MY, Chang CW and Lorson CL (2009). "Delivery of a read-through inducing compound, TC007, lessens the severity of a spinal muscular atrophy animal model." *Hum Mol Genet* **18**(20): 3906-3913.

McLean DL and Fetcho JR (2004). "Ontogeny and innervation patterns of dopaminergic, noradrenergic, and serotonergic neurons in larval zebrafish." *J Comp Neurol* **480**(1): 38-56.

McWhorter ML, Monani UR, Burghes AH and Beattie CE (2003). "Knockdown of the survival motor neuron (Smn) protein in zebrafish causes defects in motor axon outgrowth and pathfinding." *J Cell Biol* **162**(5): 919-931.

Melki J, Abdelhak S, Sheth P, Bachelot MF, Burlet P, Marcadet A, Aicardi J, Barois A, Carriere JP, Fardeau M and et al. (1990). "Gene for chronic proximal spinal muscular atrophies maps to chromosome 5q." *Nature* **344**(6268): 767-768.

Melki J, Lefebvre S, Burglen L, Burlet P, Clermont O, Millasseau P, Reboullet S, Benichou B, Zeviani M, Le Paslier D and et al. (1994). "De novo and inherited deletions of the 5q13 region in spinal muscular atrophies." *Science* **264**(5164): 1474-1477.

Mentis GZ, Blivis D, Liu W, Drobac E, Crowder ME, Kong L, Alvarez FJ, Sumner CJ and O'Donovan MJ (2011). "Early functional impairment of sensory-motor connectivity in a mouse model of spinal muscular atrophy." *Neuron* **69**(3): 453-467.

Mercuri E, Bertini E, Messina S, Solari A, D'Amico A, Angelozzi C, Battini R, Berardinelli A, Boffi P, Bruno C, Cini C, Colitto F, Kinali M, Minetti C, Mongini T, Morandi L, Neri G, Orcesi S, Pane M, Pelliccioni M, Pini A, Tiziano FD, Villanova M, Vita G and Brahe C (2007). "Randomized, double-blind, placebo-controlled trial of phenylbutyrate in spinal muscular atrophy." *Neurology* **68**(1): 51-55.

Molenaar M, van de Wetering M, Oosterwegel M, Peterson-Maduro J, Godsave S, Korinek V, Roose J, Destree O and Clevers H (1996). "XTcf-3 transcription factor mediates beta-catenin-induced axis formation in Xenopus embryos." *Cell* **86**(3): 391-399.

Monani UR, Sendtner M, Coovert DD, Parsons DW, Andreassi C, Le TT, Jablonka S, Schrank B, Rossoll W, Prior TW, Morris GE and Burghes AH (2000). "The human centromeric survival motor neuron gene (SMN2) rescues embryonic lethality in Smn(-/-) mice and results in a mouse with spinal muscular atrophy." *Hum Mol Genet* **9**(3): 333-339.

Murase S, Mosser E and Schuman EM (2002). "Depolarization drives beta-Catenin into neuronal spines promoting changes in synaptic structure and function." *Neuron* **35**(1): 91-105.

Murray LM, Comley LH, Thomson D, Parkinson N, Talbot K and Gillingwater TH (2008). "Selective vulnerability of motor neurons and dissociation of pre- and post-synaptic pathology at the neuromuscular junction in mouse models of spinal muscular atrophy." *Human molecular genetics* **17**(7): 949-962.

Murray LM, Gillingwater TH and Parson SH (2010). "Using mouse cranial muscles to investigate neuromuscular pathology in vivo." *Neuromuscular disorders : NMD* **20**(11): 740-743.

Murray LM, Lee S, Baumer D, Parson SH, Talbot K and Gillingwater TH (2010). "Pre-symptomatic development of lower motor neuron connectivity in a mouse model of severe spinal muscular atrophy." *Hum Mol Genet* **19**(3): 420-433.

Mutsaers CA, Wishart TM, Lamont DJ, Riessland M, Schreml J, Comley LH, Murray LM, Parson SH, Lochmuller H, Wirth B, Talbot K and Gillingwater

TH (2011). "Reversible molecular pathology of skeletal muscle in spinal muscular atrophy." *Human molecular genetics* **20**(22): 4334-4344.
Narver HL, Kong L, Burnett BG, Choe DW, Bosch-Marce M, Taye AA, Eckhaus MA and Sumner CJ (2008). "Sustained improvement of spinal muscular atrophy mice treated with trichostatin A plus nutrition." *Ann Neurol* **64**(4): 465-470.
Neckameyer WS (1996). "Multiple roles for dopamine in Drosophila development." *Dev Biol* **176**(2): 209-219.
Ni M, Wei W, Wang Y, Zhang N, Ding H, Shen C and Zheng F (2013). "Serum Levels of Calreticulin in Correlation with Disease Activity in Patients with Rheumatoid Arthritis." *J Clin Immunol*.
O'Connell K and Ohlendieck K (2009). "Proteomic DIGE analysis of the mitochondria-enriched fraction from aged rat skeletal muscle." *Proteomics* **9**(24): 5509-5524.
Ogg SC and Lamond AI (2002). "Cajal bodies and coilin--moving towards function." *J Cell Biol* **159**(1): 17-21.
Ojeda L, Gao J, Hooten KG, Wang E, Thonhoff JR, Dunn TJ, Gao T and Wu P (2011). "Critical role of PI3K/Akt/GSK3beta in motoneuron specification from human neural stem cells in response to FGF2 and EGF." *PLoS One* **6**(8): e23414.
Okada K, Inoue A, Okada M, Murata Y, Kakuta S, Jigami T, Kubo S, Shiraishi H, Eguchi K, Motomura M, Akiyama T, Iwakura Y, Higuchi O and Yamanashi Y (2006). "The muscle protein Dok-7 is essential for neuromuscular synaptogenesis." *Science* **312**(5781): 1802-1805.
Oprea GE, Krober S, McWhorter ML, Rossoll W, Muller S, Krawczak M, Bassell GJ, Beattie CE and Wirth B (2008). "Plastin 3 is a protective modifier of autosomal recessive spinal muscular atrophy." *Science* **320**(5875): 524-527.
Orford K, Crockett C, Jensen JP, Weissman AM and Byers SW (1997). "Serine phosphorylation-regulated ubiquitination and degradation of beta-catenin." *J Biol Chem* **272**(40): 24735-24738.
Ornatsky OI, Connor MK and Hood DA (1995). "Expression of stress proteins and mitochondrial chaperonins in chronically stimulated skeletal muscle." *Biochem J* **311 (Pt 1)**: 119-123.
Osaka H, Wang YL, Takada K, Takizawa S, Setsuie R, Li H, Sato Y, Nishikawa K, Sun YJ, Sakurai M, Harada T, Hara Y, Kimura I, Chiba S, Namikawa K, Kiyama H, Noda M, Aoki S and Wada K (2003). "Ubiquitin carboxy-terminal hydrolase L1 binds to and stabilizes monoubiquitin in neuron." *Hum Mol Genet* **12**(16): 1945-1958.
Oskoui M and Kaufmann P (2008). "Spinal muscular atrophy." *Neurotherapeutics* **5**(4): 499-506.
Osorio C, Sullivan PM, He DN, Mace BE, Ervin JF, Strittmatter WJ and Alzate O (2007). "Mortalin is regulated by APOE in hippocampus of AD patients and by human APOE in TR mice." *Neurobiol Aging* **28**(12): 1853-1862.
Park CH, Chang JY, Hahm ER, Park S, Kim HK and Yang CH (2005). "Quercetin, a potent inhibitor against beta-catenin/Tcf signaling in SW480 colon cancer cells." *Biochem Biophys Res Commun* **328**(1): 227-234.

Passini MA, Bu J, Richards AM, Kinnecom C, Sardi SP, Stanek LM, Hua Y, Rigo F, Matson J, Hung G, Kaye EM, Shihabuddin LS, Krainer AR, Bennett CF and Cheng SH (2011). "Antisense oligonucleotides delivered to the mouse CNS ameliorate symptoms of severe spinal muscular atrophy." *Sci Transl Med* **3**(72): 72ra18.

Passini MA, Bu J, Roskelley EM, Richards AM, Sardi SP, O'Riordan CR, Klinger KW, Shihabuddin LS and Cheng SH (2010). "CNS-targeted gene therapy improves survival and motor function in a mouse model of spinal muscular atrophy." *J Clin Invest* **120**(4): 1253-1264.

Patel VJ, Thalassinos K, Slade SE, Connolly JB, Crombie A, Murrell JC and Scrivens JH (2009). "A comparison of labeling and label-free mass spectrometry-based proteomics approaches." *J Proteome Res* **8**(7): 3752-3759.

Pearn J (1978). "Incidence, prevalence, and gene frequency studies of chronic childhood spinal muscular atrophy." *J Med Genet* **15**(6): 409-413.

Peifer M (1995). "Cell adhesion and signal transduction: the Armadillo connection." *Trends Cell Biol* **5**(6): 224-229.

Peifer M, Pai LM and Casey M (1994). "Phosphorylation of the Drosophila adherens junction protein Armadillo: roles for wingless signal and zeste-white 3 kinase." *Dev Biol* **166**(2): 543-556.

Plesca D, Mazumder S and Almasan A (2008). "DNA damage response and apoptosis." *Methods Enzymol* **446**: 107-122.

Popolo M, McCarthy DM and Bhide PG (2004). "Influence of dopamine on precursor cell proliferation and differentiation in the embryonic mouse telencephalon." *Dev Neurosci* **26**(2-4): 229-244.

Prior TW (2007). "Spinal muscular atrophy diagnostics." *J Child Neurol* **22**(8): 952-956.

Pun S, Sigrist M, Santos AF, Ruegg MA, Sanes JR, Jessell TM, Arber S and Caroni P (2002). "An intrinsic distinction in neuromuscular junction assembly and maintenance in different skeletal muscles." *Neuron* **34**(3): 357-370.

Raff MC, Whitmore AV and Finn JT (2002). "Axonal self-destruction and neurodegeneration." *Science* **296**(5569): 868-871.

Rajendra TK, Gonsalvez GB, Walker MP, Shpargel KB, Salz HK and Matera AG (2007). "A Drosophila melanogaster model of spinal muscular atrophy reveals a function for SMN in striated muscle." *J Cell Biol* **176**(6): 831-841.

Ramser J, Ahearn ME, Lenski C, Yariz KO, Hellebrand H, von Rhein M, Clark RD, Schmutzler RK, Lichtner P, Hoffman EP, Meindl A and Baumbach-Reardon L (2008). "Rare missense and synonymous variants in UBE1 are associated with X-linked infantile spinal muscular atrophy." *Am J Hum Genet* **82**(1): 188-193.

Reimer MM, Norris A, Ohnmacht J, Patani R, Zhong Z, Dias TB, Kuscha V, Scott AL, Chen YC, Rozov S, Frazer SL, Wyatt C, Higashijima S, Patton EE, Panula P, Chandran S, Becker T and Becker CG (2013). "Dopamine from the brain promotes spinal motor neuron generation during development and adult regeneration." *Dev Cell* **25**(5): 478-491.

Rezania K and Roos RP (2013). "Spinal cord: motor neuron diseases." *Neurol Clin* **31**(1): 219-239.

Riessland M, Ackermann B, Forster A, Jakubik M, Hauke J, Garbes L, Fritzsche I, Mende Y, Blumcke I, Hahnen E and Wirth B (2010). "SAHA ameliorates the SMA phenotype in two mouse models for spinal muscular atrophy." *Human molecular genetics* **19**(8): 1492-1506.

Riessland M, Brichta L, Hahnen E and Wirth B (2006). "The benzamide M344, a novel histone deacetylase inhibitor, significantly increases SMN2 RNA/protein levels in spinal muscular atrophy cells." *Human genetics* **120**(1): 101-110.

Rimm DL, Koslov ER, Kebriaei P, Cianci CD and Morrow JS (1995). "Alpha 1(E)-catenin is an actin-binding and -bundling protein mediating the attachment of F-actin to the membrane adhesion complex." *Proc Natl Acad Sci U S A* **92**(19): 8813-8817.

Rindt H, Buckley DM, Vale SM, Krogman M, Rose FF, Jr., Garcia ML and Lorson CL (2012). "Transgenic inactivation of murine myostatin does not decrease the severity of disease in a model of Spinal Muscular Atrophy." *Neuromuscul Disord* **22**(3): 277-285.

Rome LC (2006). "Design and function of superfast muscles: new insights into the physiology of skeletal muscle." *Annu Rev Physiol* **68**: 193-221.

Rose FF, Jr., Mattis VB, Rindt H and Lorson CL (2009). "Delivery of recombinant follistatin lessens disease severity in a mouse model of spinal muscular atrophy." *Hum Mol Genet* **18**(6): 997-1005.

Rossoll W, Jablonka S, Andreassi C, Kroning AK, Karle K, Monani UR and Sendtner M (2003). "Smn, the spinal muscular atrophy-determining gene product, modulates axon growth and localization of beta-actin mRNA in growth cones of motoneurons." *J Cell Biol* **163**(4): 801-812.

Rossoll W, Kroning AK, Ohndorf UM, Steegborn C, Jablonka S and Sendtner M (2002). "Specific interaction of Smn, the spinal muscular atrophy determining gene product, with hnRNP-R and gry-rbp/hnRNP-Q: a role for Smn in RNA processing in motor axons?" *Hum Mol Genet* **11**(1): 93-105.

Roy SS, Ehrlich AM, Craigen WJ and Hajnoczky G (2009). "VDAC2 is required for truncated BID-induced mitochondrial apoptosis by recruiting BAK to the mitochondria." *EMBO Rep* **10**(12): 1341-1347.

Rubinsztein DC (2006). "The roles of intracellular protein-degradation pathways in neurodegeneration." *Nature* **443**(7113): 780-786.

Rudnicki MA, Schnegelsberg PN, Stead RH, Braun T, Arnold HH and Jaenisch R (1993). "MyoD or Myf-5 is required for the formation of skeletal muscle." *Cell* **75**(7): 1351-1359.

Rudnik-Schoneborn S, Heller R, Berg C, Betzler C, Grimm T, Eggermann T, Eggermann K, Wirth R, Wirth B and Zerres K (2008). "Congenital heart disease is a feature of severe infantile spinal muscular atrophy." *J Med Genet* **45**(10): 635-638.

Rudnik-Schoneborn S, Vogelgesang S, Armbrust S, Graul-Neumann L, Fusch C and Zerres K (2010). "Digital necroses and vascular thrombosis in severe spinal muscular atrophy." *Muscle Nerve* **42**(1): 144-147.

Ruiz R, Casanas JJ, Torres-Benito L, Cano R and Tabares L (2010). "Altered intracellular Ca2+ homeostasis in nerve terminals of severe spinal muscular atrophy mice." *J Neurosci* **30**(3): 849-857.

Samaha FJ, Buncher CR, Russman BS, White ML, Iannaccone ST, Barker L, Burhans K, Smith C, Perkins B and Zimmerman L (1994). "Pulmonary function in spinal muscular atrophy." *J Child Neurol* **9**(3): 326-329.

Sanes JR, Johnson YR, Kotzbauer PT, Mudd J, Hanley T, Martinou JC and Merlie JP (1991). "Selective expression of an acetylcholine receptor-lacZ transgene in synaptic nuclei of adult muscle fibers." *Development* **113**(4): 1181-1191.

Sanes JR and Lichtman JW (1999). "Development of the vertebrate neuromuscular junction." *Annu Rev Neurosci* **22**: 389-442.

Sanes JR and Lichtman JW (2001). "Induction, assembly, maturation and maintenance of a postsynaptic apparatus." *Nat Rev Neurosci* **2**(11): 791-805.

Sato Y, Shimizu M, Mizunoya W, Wariishi H, Tatsumi R, Buchman VL and Ikeuchi Y (2009). "Differential expression of sarcoplasmic and myofibrillar proteins of rat soleus muscle during denervation atrophy." *Biosci Biotechnol Biochem* **73**(8): 1748-1756.

Schaar BT and McConnell SK (2005). "Cytoskeletal coordination during neuronal migration." *Proc Natl Acad Sci U S A* **102**(38): 13652-13657.

Schreml J, Riessland M, Paterno M, Garbes L, Rossbach K, Ackermann B, Kramer J, Somers E, Parson SH, Heller R, Berkessel A, Sterner-Kock A and Wirth B (2013). "Severe SMA mice show organ impairment that cannot be rescued by therapy with the HDACi JNJ-26481585." *Eur J Hum Genet* **21**(6): 643-652.

Sen A, Yokokura T, Kankel MW, Dimlich DN, Manent J, Sanyal S and Artavanis-Tsakonas S (2011). "Modeling spinal muscular atrophy in Drosophila links Smn to FGF signaling." *J Cell Biol* **192**(3): 481-495.

Setsuie R and Wada K (2007). "The functions of UCH-L1 and its relation to neurodegenerative diseases." *Neurochem Int* **51**(2-4): 105-111.

Shababi M, Habibi J, Yang HT, Vale SM, Sewell WA and Lorson CL (2010). "Cardiac defects contribute to the pathology of spinal muscular atrophy models." *Hum Mol Genet* **19**(20): 4059-4071.

Shafey D, Cote PD and Kothary R (2005). "Hypomorphic Smn knockdown C2C12 myoblasts reveal intrinsic defects in myoblast fusion and myotube morphology." *Exp Cell Res* **311**(1): 49-61.

Shaw PJ (2005). "Molecular and cellular pathways of neurodegeneration in motor neurone disease." *J Neurol Neurosurg Psychiatry* **76**(8): 1046-1057.

Shin J, Tajrishi MM, Ogura Y and Kumar A (2013). "Wasting mechanisms in muscular dystrophy." *Int J Biochem Cell Biol*.

Shtutman M, Zhurinsky J, Simcha I, Albanese C, D'Amico M, Pestell R and Ben-Ze'ev A (1999). "The cyclin D1 gene is a target of the beta-catenin/LEF-1 pathway." *Proc Natl Acad Sci U S A* **96**(10): 5522-5527.

Siklos L, Engelhardt J, Harati Y, Smith RG, Joo F and Appel SH (1996). "Ultrastructural evidence for altered calcium in motor nerve terminals in amyotropic lateral sclerosis." *Ann Neurol* **39**(2): 203-216.

Sleigh JN, Gillingwater TH and Talbot K (2011). "The contribution of mouse models to understanding the pathogenesis of spinal muscular atrophy." *Dis Model Mech* **4**(4): 457-467.

Somers E, Riessland M, Schreml J, Wirth B, Gillingwater TH and Parson SH (2013). "Increasing SMN levels using the histone deacetylase inhibitor SAHA ameliorates defects in skeletal muscle microvasculature in a mouse model of severe spinal muscular atrophy." *Neuroscience letters*.

Somers E, Stencel Z, Wishart TM, Gillingwater TH and Parson SH (2012). "Density, calibre and ramification of muscle capillaries are altered in a mouse model of severe spinal muscular atrophy." *Neuromuscul Disord* **22**(5): 435-442.

Song MN, Moon PG, Lee JE, Na M, Kang W, Chae YS, Park JY, Park H and Baek MC (2012). "Proteomic analysis of breast cancer tissues to identify biomarker candidates by gel-assisted digestion and label-free quantification methods using LC-MS/MS." *Arch Pharm Res* **35**(10): 1839-1847.

Stathas D, Kalfakis N, Kararizou E and Manta P (2008). "Spinal muscular atrophy: DNA fragmentation and immaturity of muscle fibers." *Acta Histochem* **110**(1): 53-58.

Staunton L, Jockusch H and Ohlendieck K (2011). "Proteomic analysis of muscle affected by motor neuron degeneration: the wobbler mouse model of amyotrophic lateral sclerosis." *Biochem Biophys Res Commun* **406**(4): 595-600.

Strahl BD and Allis CD (2000). "The language of covalent histone modifications." *Nature* **403**(6765): 41-45.

Struhl K (1998). "Histone acetylation and transcriptional regulatory mechanisms." *Genes Dev* **12**(5): 599-606.

Subedi KP, Kim JC, Kang M, Son MJ, Kim YS and Woo SH (2011). "Voltage-dependent anion channel 2 modulates resting Ca(2)+ sparks, but not action potential-induced Ca(2)+ signaling in cardiac myocytes." *Cell Calcium* **49**(2): 136-143.

Sumner CJ, Huynh TN, Markowitz JA, Perhac JS, Hill B, Coovert DD, Schussler K, Chen X, Jarecki J, Burghes AH, Taylor JP and Fischbeck KH (2003). "Valproic acid increases SMN levels in spinal muscular atrophy patient cells." *Ann Neurol* **54**(5): 647-654.

Sumner CJ, Wee CD, Warsing LC, Choe DW, Ng AS, Lutz C and Wagner KR (2009). "Inhibition of myostatin does not ameliorate disease features of severe spinal muscular atrophy mice." *Hum Mol Genet* **18**(17): 3145-3152.

Sun H, Liu J, Ding F, Wang X, Liu M and Gu X (2006). "Investigation of differentially expressed proteins in rat gastrocnemius muscle during denervation-reinnervation." *J Muscle Res Cell Motil* **27**(3-4): 241-250.

Svensson A and Tagerud S (2009). "Galectin-1 expression in innervated and denervated skeletal muscle." *Cell Mol Biol Lett* **14**(1): 128-138.

Swoboda KJ, Kissel JT, Crawford TO, Bromberg MB, Acsadi G, D'Anjou G, Krosschell KJ, Reyna SP, Schroth MK, Scott CB and Simard LR (2007). "Perspectives on clinical trials in spinal muscular atrophy." *J Child Neurol* **22**(8): 957-966.

Swoboda KJ, Prior TW, Scott CB, McNaught TP, Wride MC, Reyna SP and Bromberg MB (2005). "Natural history of denervation in SMA: relation to age, SMN2 copy number, and function." *Ann Neurol* **57**(5): 704-712.

Swoboda KJ, Scott CB, Crawford TO, Simard LR, Reyna SP, Krosschell KJ, Acsadi G, Elsheik B, Schroth MK, D'Anjou G, LaSalle B, Prior TW, Sorenson SL, Maczulski JA, Bromberg MB, Chan GM and Kissel JT (2010). "SMA CARNIVAL trial part I: double-blind, randomized, placebo-controlled trial of L-carnitine and valproic acid in spinal muscular atrophy." *PLoS One* **5**(8): e12140.

Takahashi M, Chesley A, Freyssenet D and Hood DA (1998). "Contractile activity-induced adaptations in the mitochondrial protein import system." *Am J Physiol* **274**(5 Pt 1): C1380-1387.

Talbot K (1999). "Spinal muscular atrophy." *J Inherit Metab Dis* **22**(4): 545-554.

Tetsu O and McCormick F (1999). "Beta-catenin regulates expression of cyclin D1 in colon carcinoma cells." *Nature* **398**(6726): 422-426.

Tews DS and Goebel HH (1996). "DNA fragmentation and BCL-2 expression in infantile spinal muscular atrophy." *Neuromuscul Disord* **6**(4): 265-273.

Tews DS and Goebel HH (1997). "Apoptosis-related proteins in skeletal muscle fibers of spinal muscular atrophy." *J Neuropathol Exp Neurol* **56**(2): 150-156.

Thomson SR, Nahon JE, Mutsaers CA, Thomson D, Hamilton G, Parson SH and Gillingwater TH (2012). "Morphological characteristics of motor neurons do not determine their relative susceptibility to degeneration in a mouse model of severe spinal muscular atrophy." *PLoS One* **7**(12): e52605.

Thurmond J, Butchbach ME, Palomo M, Pease B, Rao M, Bedell L, Keyvan M, Pai G, Mishra R, Haraldsson M, Andresson T, Bragason G, Thosteinsdottir M, Bjornsson JM, Coovert DD, Burghes AH, Gurney ME and Singh J (2008). "Synthesis and biological evaluation of novel 2,4-diaminoquinazoline derivatives as SMN2 promoter activators for the potential treatment of spinal muscular atrophy." *J Med Chem* **51**(3): 449-469.

Tiziano FD, Lomastro R, Di Pietro L, Barbara Pasanisi M, Fiori S, Angelozzi C, Abiusi E, Angelini C, Soraru G, Gaiani A, Mongini T, Vercelli L, Vasco G, Vita G, Luca Vita G, Messina S, Politano L, Passamano L, Di Gregorio G, Montomoli C, Orsi C, Campanella A, Mantegazza R and Morandi L (2013). "Clinical and molecular cross-sectional study of a cohort of adult type III spinal muscular atrophy patients: clues from a biomarker study." *Eur J Hum Genet* **21**(6): 630-636.

Tiziano FD, Lomastro R, Pinto AM, Messina S, D'Amico A, Fiori S, Angelozzi C, Pane M, Mercuri E, Bertini E, Neri G and Brahe C (2010). "Salbutamol increases survival motor neuron (SMN) transcript levels in leucocytes of spinal muscular atrophy (SMA) patients: relevance for clinical trial design." *J Med Genet* **47**(12): 856-858.

Torres-Benito L, Neher MF, Cano R, Ruiz R and Tabares L (2011). "SMN requirement for synaptic vesicle, active zone and microtubule postnatal organization in motor nerve terminals." *PLoS One* **6**(10): e26164.

Tsai LK, Tsai MS, Ting CH and Li H (2008). "Multiple therapeutic effects of valproic acid in spinal muscular atrophy model mice." *J Mol Med (Berl)* **86**(11): 1243-1254.

Valenzuela DM, Stitt TN, DiStefano PS, Rojas E, Mattsson K, Compton DL, Nunez L, Park JS, Stark JL, Gies DR and et al. (1995). "Receptor tyrosine kinase specific for the skeletal muscle lineage: expression in embryonic muscle, at the neuromuscular junction, and after injury." *Neuron* **15**(3): 573-584.

Valori CF, Ning K, Wyles M, Mead RJ, Grierson AJ, Shaw PJ and Azzouz M (2010). "Systemic delivery of scAAV9 expressing SMN prolongs survival in a model of spinal muscular atrophy." *Sci Transl Med* **2**(35): 35ra42.

Vrbova G (2008). "Spinal muscular atrophy: motoneurone or muscle disease?" *Neuromuscul Disord* **18**(1): 81-82.

Walker MP, Rajendra TK, Saieva L, Fuentes JL, Pellizzoni L and Matera AG (2008). "SMN complex localizes to the sarcomeric Z-disc and is a proteolytic target of calpain." *Hum Mol Genet* **17**(21): 3399-3410.

Wang WC, Wynn LW, Rogers ZR, Scott JP, Lane PA and Ware RE (2001). "A two-year pilot trial of hydroxyurea in very young children with sickle-cell anemia." *J Pediatr* **139**(6): 790-796.

Wen W, Zhu F, Zhang J, Keum YS, Zykova T, Yao K, Peng C, Zheng D, Cho YY, Ma WY, Bode AM and Dong Z (2010). "MST1 promotes apoptosis through phosphorylation of histone H2AX." *J Biol Chem* **285**(50): 39108-39116.

Williams JH, Schray RC, Patterson CA, Ayitey SO, Tallent MK and Lutz GJ (2009). "Oligonucleotide-mediated survival of motor neuron protein expression in CNS improves phenotype in a mouse model of spinal muscular atrophy." *J Neurosci* **29**(24): 7633-7638.

Wirth B, Brichta L and Hahnen E (2006). "Spinal muscular atrophy and therapeutic prospects." *Prog Mol Subcell Biol* **44**: 109-132.

Wishart TM, Huang JP, Murray LM, Lamont DJ, Mutsaers CA, Ross J, Geldsetzer P, Ansorge O, Talbot K, Parson SH and Gillingwater TH (2010). "SMN deficiency disrupts brain development in a mouse model of severe spinal muscular atrophy." *Hum Mol Genet* **19**(21): 4216-4228.

Wishart TM, Parson SH and Gillingwater TH (2006). "Synaptic vulnerability in neurodegenerative disease." *J Neuropathol Exp Neurol* **65**(8): 733-739.

Wu CY, Whye D, Glazewski L, Choe L, Kerr D, Lee KH, Mason RW and Wang W (2011). "Proteomic assessment of a cell model of spinal muscular atrophy." *BMC neuroscience* **12**: 25.

Wu Y, Sun H, Yakar S and LeRoith D (2009). "Elevated levels of insulin-like growth factor (IGF)-I in serum rescue the severe growth retardation of IGF-I null mice." *Endocrinology* **150**(9): 4395-4403.

Wyatt TJ and Keirstead HS (2010). "Stem cell-derived neurotrophic support for the neuromuscular junction in spinal muscular atrophy." *Expert Opin Biol Ther* **10**(11): 1587-1594.

Yagoda N, von Rechenberg M, Zaganjor E, Bauer AJ, Yang WS, Fridman DJ, Wolpaw AJ, Smukste I, Peltier JM, Boniface JJ, Smith R, Lessnick SL, Sahasrabudhe S and Stockwell BR (2007). "RAS-RAF-MEK-dependent oxidative cell death involving voltage-dependent anion channels." *Nature* **447**(7146): 864-868.

Yamagata H, Shimizu S, Nishida Y, Watanabe Y, Craigen WJ and Tsujimoto Y (2009). "Requirement of voltage-dependent anion channel 2 for pro-apoptotic activity of Bax." *Oncogene* **28**(40): 3563-3572.

Yang P, Arnold SA, Habas A, Hetman M and Hagg T (2008). "Ciliary neurotrophic factor mediates dopamine D2 receptor-induced CNS neurogenesis in adult mice." *J Neurosci* **28**(9): 2231-2241.

Yost C, Torres M, Miller JR, Huang E, Kimelman D and Moon RT (1996). "The axis-inducing activity, stability, and subcellular distribution of beta-catenin is regulated in Xenopus embryos by glycogen synthase kinase 3." *Genes Dev* **10**(12): 1443-1454.

Yusuf F and Brand-Saberi B (2012). "Myogenesis and muscle regeneration." *Histochem Cell Biol* **138**(2): 187-199.

Zerres K, Rudnik-Schoneborn S, Forkert R and Wirth B (1995). "Genetic basis of adult-onset spinal muscular atrophy." *Lancet* **346**(8983): 1162.

Zhang Y, Ye J, Chen D, Zhao X, Xiao X, Tai S, Yang W and Zhu D (2006). "Differential expression profiling between the relative normal and dystrophic muscle tissues from the same LGMD patient." *J Transl Med* **4**: 53.

Zhang Z, Lotti F, Dittmar K, Younis I, Wan L, Kasim M and Dreyfuss G (2008). "SMN deficiency causes tissue-specific perturbations in the repertoire of snRNAs and widespread defects in splicing." *Cell* **133**(4): 585-600.

Appendices

Appendix 1

Co-immunoprecipitation of Gemin5 and SMN

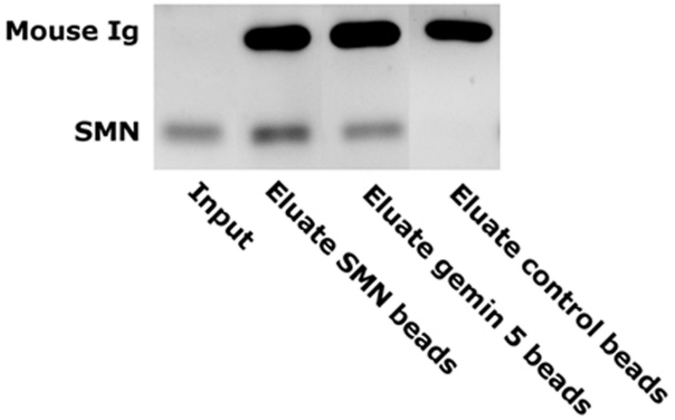

Gemin5 and SMN maintain the ability to physically interact in the synapse. Representative bands from an immunoprecipitation experiment where whole synaptosome extracts were incubated with SMN, gemin5 or neurofilament (as a non-specific control) beads and bound proteins were eluted, subject to separation by SDS-PAGE and transferred to nitrocellulose by western blotting. The blot was developed with anti-SMN antibodies. All lanes loaded with SDS extracts of beads contain a 50 kDa band of mouse Ig heavy chain which reacts with the HRP anti-mouse Ig used to develop the blot. Only the lanes with SMN or gemin5 beads bound SMN, showing that gemin5 and SMN retained the ability to physically interact in the synaptic proteome.

Appendix 2

Deregulation of UBA1 protein levels leads to accumulation of β-catenin in zebrafish and can be rescued by inhibition of β-catenin

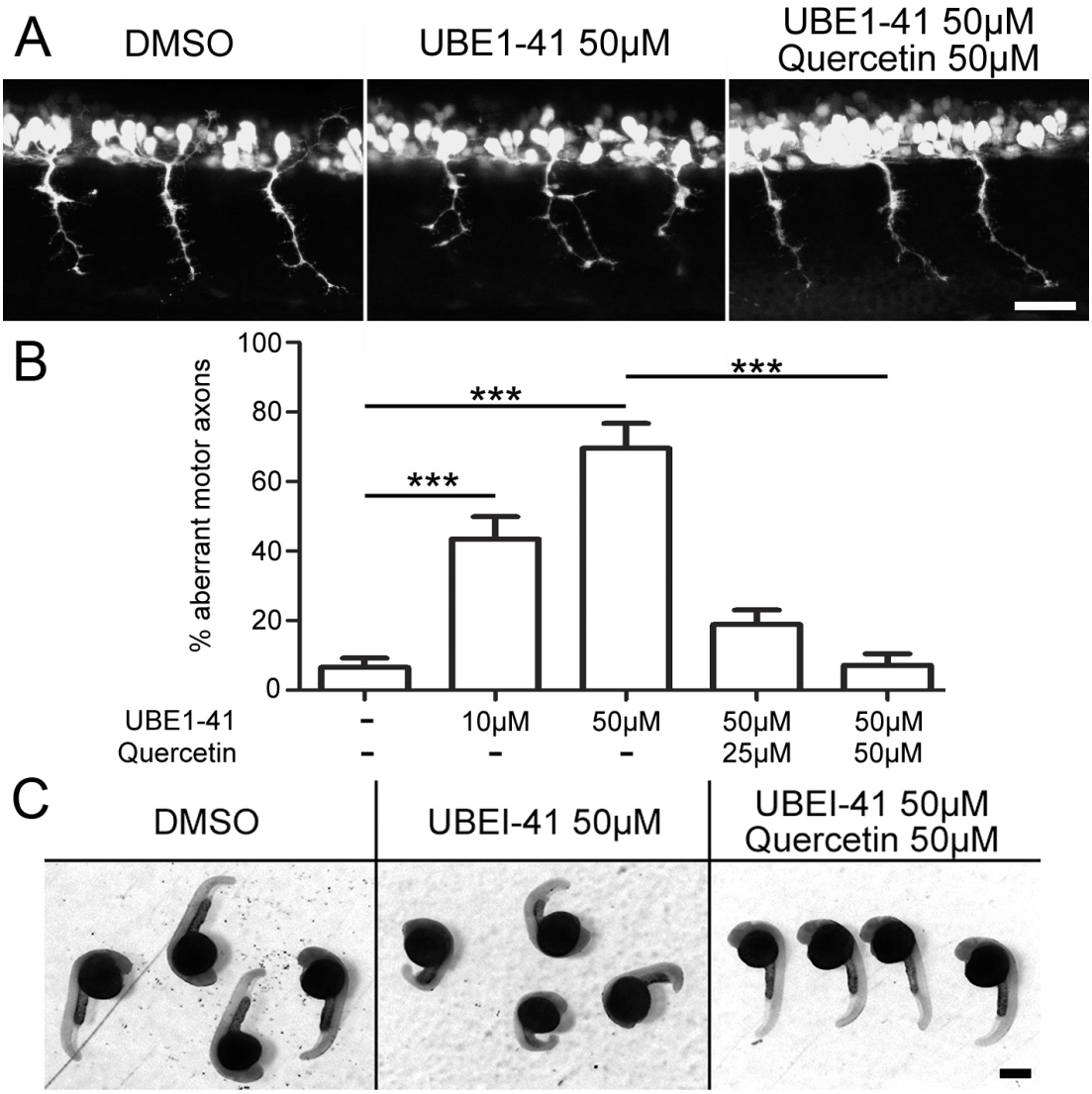

Rescue of UBA1-dependent motor axon defects in zebrafish by pharmacological inhibition of β-catenin signalling. (A) Representative confocal micrographs showing three segments of Tg(hb9:gfp) zebrafish embryos from the trunk region. Note the severe branching phenotype of the motor nerves in the UBEI-41 treated animal. This phenotype was rescued by quercetin treatment. Scale bar = 30 μm. **(B)** Dose-dependent increase in numbers of aberrant motor axons in the UBEI-41-treated group compared to DMSO controls. This phenotype was rescued by quercetin in a dose-dependent manner (DMSO controls n=331 nerves, N=14 animals; 10 μM UBEI-41 n=258, N=11; 50 μM UBEI-41 n=280, N=12; 50 μM UBEI-41 + 25 μM Quercetin n=143, N=6; 50 μM UBEI-41 + 50 μM Quercetin n=168, N=7;

Kruskal Wallis test with Dunn's post hoc test). **(C)** Representative overview images showing body axis defects in zebrafish embryos after UBEI-41 treatment compared to DMSO control. Note the rescue of this gross phenotype following application of 50 µM quercetin.

Appendix 3

Motor axons/nerves are abnormal in zebrafish embryos that are treated with smn morpholinos

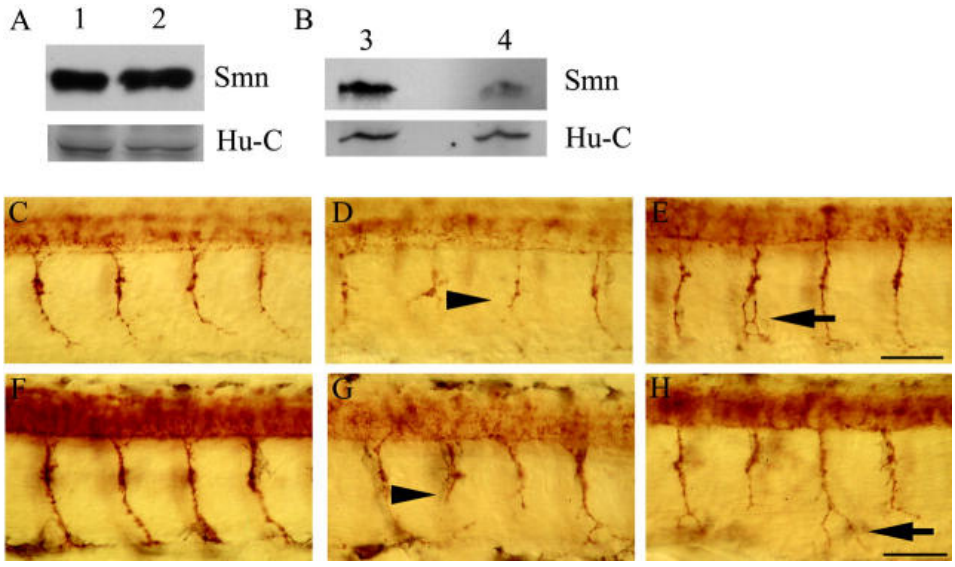

Motor axons/nerves are abnormal in embryos injected with 9 ng of smn MO. *Figure taken from (McWhorter et al. 2003) to show the comparision with UBA1 deficient zebrafish.* **(A/B)** Western blot analysis of WT uninjected (lanes 1 and 3), control MO–injected (lane 2), and smn MO–injected (9 ng) (lane 4) embryos at 36 h. Hu-C, a neuronal marker, is shown as a loading control. Lateral views of whole-mount embryos labelled with znp1 mAb at 27 **(C–E)** and 36 h **(F–H)** in embryos injected with control MO **(C and F)** or smn MO **(D, E, G, and H)**. Truncated motor axons/nerves (**D and G**; black arrowheads) and branched motor axons/nerves (**E and H**; black arrows) occur when Smn protein levels are further reduced. Bars: (**C–E**) 25 µm; (**F–H**) 30 µm.

Appendix 4

Papers published and under review

Wishart TM*, **Mutsaers CA***, Riessland M*, Reimer M*, Hamilton G, Hannam M, Eaton S, Fuller H, Roche S, Somers E, Morse R, Young P, Lamont D, Hammerschmidt M, Morris G, Parson S, Skehel P, Becker T, Robinson I, Becker C, Wirth B, Gillingwater TH. Dysregulation of ubiquitin homeostasis and β-catenin signalling promote spinal muscular atrophy (accepted at the Journal of Clincial Investigations) *equal contribution

Mutsaers CA, Lamont DJ, Hunter G, Wishart TM, Gillingwater TH. Label-free proteomics identifies Calreticulin and GRP75/Mortalin as peripherally accessible protein biomarkers for spinal muscular atrophy. Genome Med. 2013 Oct 18;5(10):95.

Thomson SR, Nahon JE, **Mutsaers CA**, Thomson D, Hamilton G, Parson SH, Gillingwater TH. Morphological characteristics of motor neurons do not determine their relative susceptibility to degeneration in a mouse model of severe spinal muscular atrophy. Plos One. 2012 Dec 7(12).

Mutsaers CA, Wishart TM, Lamont DJ, Riessland M, Schreml J, Comley LH, Murray LM, Parson SH, Lochmüller H, Wirth B, Talbot K, Gillingwater TH. Reversible molecular pathology of skeletal muscle in spinal muscular atrophy. Hum Mol Genet. 2011 Nov 15;20(22):4334-44.

Comley LH, Fuller HR, Wishart TM, **Mutsaers CA**, Thomson D, Wright AK, Ribchester RR, Morris GE, Parson SH, Horsburgh K, Gillingwater TH. ApoE isoform-specific regulation of regeneration in the peripheral nervous system. Hum Mol Genet. 2011 Jun 15;20(12):2406-21.

Wishart TM, Huang JP, Murray LM, Lamont DJ, **Mutsaers CA**, Ross J, Geldsetzer P, Ansorge O, Talbot K, Parson SH, Gillingwater TH. SMN deficiency disrupts brain development in a mouse model of severe spinal muscular atrophy. Hum Mol Genet. 2010 Nov 1;19(21):4216-28.

Xu W, Berger SP, Trouw LA, de Boer HC, Schlagwein N, **Mutsaers C**, Daha MR, van Kooten C. Properdin binds to late apoptotic and necrotic cells independently of C3b and regulates alternative pathway complement activation. J Immunol. 2008 Jun 1;180(11):7613-21.

Little D, Valori CF*, **Mutsaers CA*,** Bennett EJ, Wyles M, Shaw PJ, Gillingwater TH, Azzouz M, Ning K. PTEN Depletion Decreases Disease Severity and Prolongs Survival in a Mouse Model of Spinal Muscular Atrophy (under review) *equal contribution.

Powis RA, **Mutsaers CA**, Wishart TM, Hunter G, Wirth B, Gillingwater TH. Pharmacological inhibition of UCHL1 is not a valid therapeutic approach for the treatment of spinal muscular atrophy. (submitted)